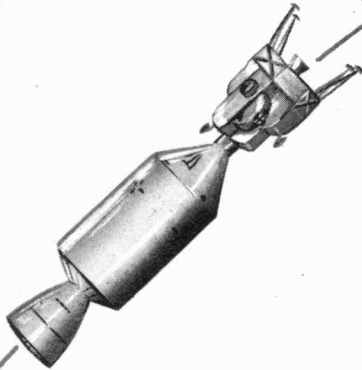
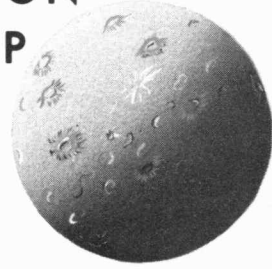


KSC/G. SILVER

# APOLLO NAVIGATION WORKING GROUP

TECHNICAL REPORT  
NO. AN - 1.3



# APOLLO MISSIONS AND NAVIGATION SYSTEMS CHARACTERISTICS

DECEMBER 15, 1967

RECEIVED

MIT/IL

JAN 8 '68

8-31

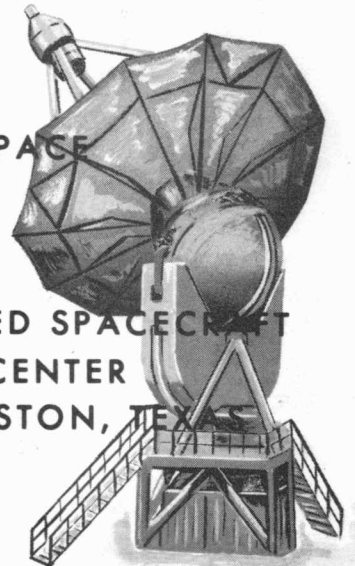


AMR FIELD STATION

NATIONAL AERONAUTICS AND SPACE  
ADMINISTRATION

GODDARD SPACE FLIGHT  
CENTER  
GREENBELT, MARYLAND

MANNED SPACECRAFT  
CENTER  
HOUSTON, TEXAS



APOLLO NAVIGATION  
WORKING GROUP  
TECHNICAL REPORT  
NO. AN - 1.3



*F. O. Vonbun*

F. O. Vonbun  
Chief, Mission Analysis Office  
Goddard Space Flight Center  
Greenbelt, Maryland

*John P. Mayer*

John P. Mayer  
Chief, Mission Planning  
and Analysis Division  
Manned Spacecraft Center  
Houston, Texas

## CONTRIBUTORS

### APOLLO MISSIONS

P. T. Pixley, Chapter Chairman, MSC  
H. D. Beck, MSC  
W. J. Bennett, MSC  
D. D. DeAtkine, MSC  
E. G. Dupnick, MSC  
D. J. Griffith, MSC

### TRAJECTORY PREDICTION MODEL

Robert T. Savely, Chapter Chairman, MSC  
E. Schiesser, MSC

### NAVIGATION AND COMMUNICATION SYSTEMS CHARACTERISTICS

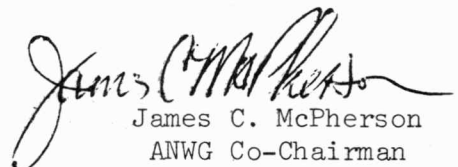
P. E. Schmidt, Chapter Chairman, GSFC  
B. Kruger, GSFC  
A. R. Chi, GSFC  
D. W. Curkendall, JPL  
H. Engel, Bissett-Berman Corp.  
H. Epstein, Bissett-Berman Corp.  
F. Kalil, GSFC  
T. James Blucker, MSC  
E. Schiesser, MSC  
C. Vegos, JPL

### NAVIGATION SOFTWARE CAPABILITIES

Howard G. deVezin, Chapter Chairman, MSC  
Michael J. Oles, MSC  
Robert T. Savely, MSC  
E. Schiesser, MSC  
George E. Wilson, MSC



Bodo Kruger  
ANWG Co-Chairman  
Goddard Space Flight Center  
Greenbelt, Maryland



James C. McPherson  
ANWG Co-Chairman  
Manned Spacecraft Center  
Houston, Texas

# CONTENTS

Section	Page
<b>TABLES</b> . . . . .	ix
<b>FIGURES</b> . . . . .	xi
<b>ABBREVIATIONS</b> . . . . .	xiii
<b>UNITS</b> . . . . .	xv
<b>1.0 INTRODUCTION</b> . . . . .	1-1
<b>2.0 CHANGES</b> . . . . .	2-1
<b>3.0 APOLLO MISSIONS</b> . . . . .	3-1
3.1 <u>INTRODUCTION</u> . . . . .	3-1
3.2 <u>NEAR-EARTH MISSIONS</u> . . . . .	3-1
3.2.1 LAUNCH VEHICLE AND CSM DEVELOPMENT MISSION - SHORT LOB . . . . .	3-2
3.2.2 LAUNCH VEHICLE AND CSM DEVELOPMENT MISSION - LONG LOB . . . . .	3-4
3.2.3 LIQUID HYDROGEN BEHAVIOR IN ORBIT AND S-IVB STAGE DEVELOPMENT MISSION . . . . .	3-6
3.2.4 LONG DURATION CSM OPERATIONS MISSION . . . . .	3-8
3.2.5 LM DEVELOPMENT MISSION . . . . .	3-10
3.2.6 CSM-LM OPERATIONS MISSION - DUAL LAUNCH . . . . .	3-12
3.2.7 FIRST SATURN V AND SPACECRAFT DEVELOPMENT MISSION . . . . .	3-14
3.2.8 SECOND SATURN V AND SPACECRAFT DEVELOPMENT MISSION . . . . .	3-16

Section	Page
3.2.9 LUNAR MISSION SIMULATION . . . . .	3-18
3.3 <u>LUNAR MISSION</u> . . . . .	3-20
3.3.1 TYPICAL LUNAR MISSION . . . . .	3-20
3.3.2 PHASES OF THE LUNAR MISSION . . . . .	3-20
3.3.2.1 Launch . . . . .	3-20
3.3.2.2 Earth Parking Orbit . . . . .	3-20
3.3.2.3 Translunar Injection Burn . . . . .	3-20
3.3.2.4 Translunar Trajectory . . . . .	3-22
3.3.2.5 Lunar Orbit Insertion . . . . .	3-22
3.3.2.6 Lunar Parking Orbit . . . . .	3-22
3.3.2.7 LM Descent . . . . .	3-22
3.3.2.8 LM Stay Time . . . . .	3-22
3.3.2.9 LM Ascent and Rendezvous . . . . .	3-23
3.3.2.10 Transearth Injection . . . . .	3-23
3.3.2.11 Transearth Trajectory . . . . .	3-23
3.3.2.12 Reentry and Recovery . . . . .	3-23
3.3.3 REFERENCE TRAJECTORIES . . . . .	3-24
3.4 <u>REFERENCES</u> . . . . .	3-30
<b>4.0 TRAJECTORY PREDICTION MODEL . . . . .</b>	<b>4-1</b>
4.1 <u>INTRODUCTION</u> . . . . .	4-1
4.2 <u>CONSTANTS FOR APOLLO</u> . . . . .	4-1
4.2.1 EARTH CONSTANTS . . . . .	4-1
4.2.2 LUNAR CONSTANTS . . . . .	4-5
4.2.3 GENERAL CONSTANTS . . . . .	4-8
4.3 <u>EPHEMERIS TAPE SYSTEM</u> . . . . .	4-8
4.4 <u>DRAG MODEL</u> . . . . .	4-9
4.4.1 ATMOSPHERIC MODEL FOR APOLLO . . . . .	4-9
4.4.2 DRAG EQUATIONS . . . . .	4-9
4.5 <u>FISCHER EARTH MODEL</u> . . . . .	4-11

Section	Page
4.6 <u>BASIC EQUIVALENTS AND CONVERSION FACTORS</u> . . . . .	4-12
4.7 <u>VENTING MODEL</u> . . . . .	4-13
4.7.1 S-V/S-IVB ULLAGE AND VENTING ACTION DURING EARTH ORBIT . . . . .	4-13
4.7.1.1 J2-Second Ignition . . . . .	4-14
4.7.2 VENTING EQUATIONS (CONTINUOUS VENTING) . . . . .	4-14
4.8 <u>REFERENCES</u> . . . . .	4-16

## 5.0 NAVIGATION AND COMMUNICATION SYSTEMS CHARACTERISTICS . . . . .

5.1 <u>INTRODUCTION</u> . . . . .	5-1
5.2 <u>ERROR MODEL AND ERROR SOURCES</u> . . . . .	5-1
5.2.1 STATISTICAL ERROR MODEL - NOISE AND BIAS . . . . .	5-1
5.2.2 GROUND-BASED SYSTEM ERROR SOURCES . . . . .	5-2
5.2.3 ONBOARD SYSTEM ERROR SOURCES . . . . .	5-2
5.3 <u>TIME AND TIME TAGGING</u> . . . . .	5-3
5.3.1 DEFINITIONS OF TIME . . . . .	5-3
5.3.1.1 Ephemeris Time . . . . .	5-3
5.3.1.2 Atomic Time . . . . .	5-3
5.3.1.3 Universal Time, or Greenwich Mean Time . . . . .	5-4
5.3.2 GROUND TIME TAGGING . . . . .	5-5
5.3.3 ONBOARD TIME TAGGING . . . . .	5-5
5.4 <u>THE MANNED SPACE FLIGHT NETWORK</u> . . . . .	5-6
5.4.1 STATION LOCATIONS . . . . .	5-6
5.4.2 C-BAND RADARS . . . . .	5-6

Section	Page
5.4.3 UNIFIED S-BAND SYSTEM . . . . .	5-7
5.4.3.1 Antenna Mounts . . . . .	5-7
5.4.3.2 Range Rate Measurements . . . . .	5-10
5.4.3.2.1 Destructive N count . . . . .	5-11
5.4.3.2.2 Nondestructive T count . . . . .	5-11
5.4.3.3 Two- and Three-Way Doppler . . . . .	5-11
5.4.3.4 Range Rate Uncertainties . . . . .	5-13
5.4.3.4.1 Noise . . . . .	5-13
5.4.3.4.1.1 Nondestructive T count . . . . .	5-13
5.4.3.4.1.2 Destructive N count . . . . .	5-15
5.4.3.4.2 Bias . . . . .	5-16
5.4.4 ONBOARD ANTENNA COVERAGE . . . . .	5-16
5.4.5 APOLLO SHIPS . . . . .	5-18
5.4.5.1 C-band Radar . . . . .	5-18
5.4.5.2 Unified S-band System . . . . .	5-18
5.4.5.3 Navigation Accuracy . . . . .	5-18
5.4.6 ATMOSPHERIC CORRECTION . . . . .	5-18
5.5 <u>ONBOARD NAVIGATION SYSTEM</u> . . . . .	5-19
5.5.1 GEOMETRICAL SENSORS . . . . .	5-19
5.5.1.1 Sextant . . . . .	5-19
5.5.1.2 Scanning Telescope . . . . .	5-19
5.5.1.3 LM Optical Rendezvous System . . . . .	5-20
5.5.1.4 Alignment Optical Telescope . . . . .	5-20
5.5.1.5 Rendezvous Radar . . . . .	5-20
5.5.2 INERTIAL SENSORS . . . . .	5-21
5.5.2.1 Inertial Measurement Unit . . . . .	5-21
5.5.2.2 Inertial Measurement Instruments Associated With The Abort Guid- ance System . . . . .	5-21

Section	Page
5.5.3 ENGINE CHARACTERISTICS . . . . .	5-22
5.6 <u>LUNAR LANDMARKS AND AGC STAR CATALOGUE</u> . . . . .	5-23
5.6.1 LUNAR LANDMARKS . . . . .	5-23
5.6.2 AGC STAR CATALOGUE . . . . .	5-23
5.7 <u>COMMUNICATION SYSTEMS</u> . . . . .	5-23
5.7.1 APOLLO SATURN NASCOM NETWORK . . . . .	5-23
5.7.2 DATA FRAME RATES . . . . .	5-26
5.7.3 SYSTEM RELIABILITY . . . . .	5-27
5.8 <u>REFERENCES</u> . . . . .	5-39
<b>6.0 NAVIGATION SOFTWARE CAPABILITIES</b> . . . . .	<b>6-1</b>
6.1 <u>INTRODUCTION</u> . . . . .	6-1
6.2 <u>RTCC, GROUND-BASED NAVIGATION PROGRAM</u> . . . . .	6-1
6.2.1 TWO-VEHICLE CAPABILITY . . . . .	6-1
6.2.2 COMPUTATIONAL METHOD . . . . .	6-2
6.2.3 OBSERVABLES PROCESSED . . . . .	6-3
6.2.4 DATA BATCH PROCESSING . . . . .	6-3
6.2.5 STATE ELEMENTS IN THE SOLUTION . . . . .	6-3
6.2.6 MODEL BIASES . . . . .	6-4
6.3 <u>CM AND LM ONBOARD PROGRAMS</u> . . . . .	6-4
6.3.1 ONBOARD TRAJECTORY PREDICTION MODEL . . . . .	6-5
6.3.1.1 Earth Orbit Phase . . . . .	6-5
6.3.1.2 Lunar Orbit Phase . . . . .	6-5
6.3.1.3 Translunar and Transearth Phases . . . . .	6-5



Section	Page
6.3.2 CM ONBOARD NAVIGATION PROGRAM . . . . .	6-5
6.3.2.1 CM Orbit in Translunar and Transearch Phases . . . . .	6-5
6.3.2.2 CM Orbit in Lunar Phase . . . . .	6-6
6.3.2.3 CM Landing Site Determination . . . . .	6-6
6.3.2.4 CM Rendezvous Navigation . . . . .	6-6
6.3.3 LM ONBOARD NAVIGATION PROGRAM . . . . .	6-6
6.4 <u>S-IVB ONBOARD PROGRAM</u> . . . . .	6-6
6.4.1 FREE-FLIGHT NAVIGATION . . . . .	6-6
6.4.2 POWERED-FLIGHT NAVIGATION . . . . .	6-7
6.5 <u>APOLLO SHIP TRACKING AND ACQUISITION PROGRAM</u> . . . . .	6-8
6.6 <u>REFERENCES</u> . . . . .	6-9

## TABLES

Table	Page
3-I	CORRELATION BETWEEN MISSION NUMBERS USED IN PREVIOUS ANWG DOCUMENTS AND TITLES USED IN THIS DOCUMENT . . . 3-25
3-II	INTEGRATED TRAJECTORY STATE VECTOR . . . . . 3-26
3-III	PATCHED CONIC, REFERENCE TRAJECTORY FOR A LUNAR LANDING MISSION
	(a) Rectangular coordinates . . . . . 3-27
	(b) Conic elements . . . . . 3-28
3-IV	SYMBOLS USED IN TABLES 3-II AND 3-III . . . . . 3-29
5-I	C-BAND RADAR TRACKING ACCURACIES AND LIMITATIONS . . . . 5-28
5-II	USBS TRACKING ERRORS AND LIMITATIONS
	(a) Acquisition time after spacecraft illumination (Elevation $\geq 5^\circ$ ) . . . . . 5-29
	(b) Maximum angular tracking rate . . . . . 5-29
	(c) Maximum tracking ranges using 20W transponder mode . . . . . 5-30
5-III	USBS TRACKING ERRORS AND LIMITATIONS - TRACKING ACCURACY
	(a) Angles . . . . . 5-31
	(b) Range . . . . . 5-31
	(c) Range rate . . . . . 5-31
5-IV	STATION LOCATIONS AND STATUS . . . . . 5-33
5-V	INERTIAL POSITION AND SPEED ERRORS FOR SHIPS . . . . . 5-34
5-VI	C-BAND BEACONS AND USB TRANSPONDERS . . . . . 5-34
5-VII	SUMMARY OF APOLLO SHIPS INSTRUMENTATION . . . . . 5-35

Table		Page
5-VIII	RESIDUAL ERRORS AFTER ATMOSPHERIC CORRECTION . . . . .	5-35
5-IX	LUNAR LANDMARKS AND THEIR UNCERTAINTIES . . . . .	5-36
5-X	APOLLO GUIDANCE COMPUTER STAR CATALOGUE REFERENCED TO 1967.0 . . . . .	5-37
5-XI	SUMMARY OF GEMINI GROUND SYSTEMS DOWN TIMES IN PER- CENT OF MISSION SUPPORT TIME FOR GTA-9, 10, 11, AND 12 . . . . .	5-38

## FIGURES

Figure		Page
3-1	Launch vehicle and CSM development mission - short lob . . . . .	3-3
3-2	Launch vehicle and CSM development mission - long lob . . . . .	3-5
3-3	Liquid hydrogen behavior in orbit and S-IVB stage development mission . . . . .	3-7
3-4	Long duration CSM operations mission. . . . .	3-9
3-5	LM development mission . . . . .	3-11
3-6	CSM-LM operations mission - dual launch . . . . .	3-13
3-7	First Saturn V and spacecraft development mission . . .	3-15
3-8	Second Saturn V and spacecraft development mission . . . . .	3-17
3-9	Lunar mission simulation . . . . .	3-19
3-10	Typical lunar landing mission . . . . .	3-21
3-11	Water recovery areas . . . . .	3-24
5-1	X-Y mount	
	(a) X-Y axes . . . . .	5-8
	(b) Angular coverage for X-Y mount . . . . .	5-8
5-2	Angle definitions for USBS X-Y antenna mounts	
	(a) 30-ft antenna . . . . .	5-9
	(b) 85-ft antenna . . . . .	5-9

Figure		Page
5-3	Two-way and three-way Doppler	
	(a) Two-way Doppler . . . . .	5-12
	(b) Three-way Doppler . . . . .	5-12
5-4	Autocorrelation function for range rate noise due to the random walk phase noise in the oscillator . . . .	5-14
5-5	High gain spacecraft (CSM S-band antenna coverage). . .	5-17
5-6	LM S-band steerable antenna coverage in LM body coordinates (separated from CSM). . . . .	5-17
5-7	Apollo/Saturn NASCOM communications network . . . . .	5-24

## ABBREVIATIONS

AGC	Apollo guidance computer
AGS	abort guidance system
ANWG	Apollo Navigation Working Group
AOT	alignment optical telescope
APS	ascent propulsion system
ARDC 1962	Air Research and Development Center model atmosphere
CM	command module
CSM	command and service modules
DPS	descent propulsion system
DSIF	Deep Space Instrumentation Facility
DSN	Deep Space Network
ETR	Eastern Test Range
FITH	fire in the hole. The ignition of an engine which is located between two space vehicles and which impinges on one of the vehicles.
G.m.t	Greenwich mean time
GSFC	Goddard Space Flight Center
IMU	inertial measurement unit
IRIG	Inter-Range Instrumentation Group
IU	instrument unit
JPL	Jet Propulsion Laboratory
LES	launch escape system
LGC	LM guidance computer

LH<sub>2</sub> liquid hydrogen  
LM lunar module  
loran long-range navigation  
LORS LM optical rendezvous system  
LOX liquid oxygen  
MPAD Mission Planning and Analysis Division  
MSFN Manned Space Flight Network  
NASA National Aeronautics and Space Administration  
NASCOM NASA World-Wide Communications Network  
OAMS orbit attitude maneuvering system  
PGNCS primary guidance and navigation control system  
PRA Patrick reference atmosphere  
RCS reaction control system  
RR rendezvous radar  
RTCC Real-Time Computer Complex  
S-IB Saturn IB (launch vehicle)  
S-IVB Saturn IVB (third stage)  
SLA spacecraft LM adapter  
SM service module  
SPS service propulsion system  
S-V Saturn V (launch vehicle)  
TEI transearth injection  
TLI translunar injection  
USBS unified S-band system  
UT universal time

## UNITS

AU	astronomical unit
cm	centimeter
cm/sec	centimeter per second
deg	degree
deg/sec	degrees per second
e.r.	earth radii
fps or ft/sec	feet per second
ft	feet
int. ft	international feet
int. stat. mi.	international statute mile
int. stat. mi./sec	international statute mile per second
hr	hour
Hz	Hertz (cycles per ephemeris second)
kbit	kilobit
kg	kilogram
kg m <sup>2</sup>	kilogram meters squared
km	kilometer
kW	kilowatt
lbf	pound force
lbm	pound mass



m	meter
min	minute
mrad	milliradian
msec	millisecond
m/sec or mps	meters per second
n. mi.	nautical mile
rad	radian
rad/sec	radians per second
sec	second

## 1.0 INTRODUCTION

The purpose of the Apollo Navigation Working Group (ANWG), as stated in the Apollo Program Directive No. 17, March 31, 1966, is to provide information and recommendations concerning the individual and combined use of Apollo tracking and navigation systems that will best support the Apollo missions. Emphasis is on the total system, rather than on the onboard and ground systems individually, so that the optimum combination can be achieved.

The information in this document, "Apollo Missions and Navigation Systems Characteristics," is to be used in all studies of Apollo navigation capability. It provides a standard for the studies by the various NASA centers and their contractors. The common standard facilitates comparisons of navigational accuracies by eliminating discrepancies due to model differences.

Recent advancements motivate the present revision. Chapter 2.0 list changes which make this revision substantially different from the January 17, 1967 revision (Technical Report AN-1.2). The organization in this revision is essentially the same as that of the last revision.

The information presented is divided into four areas, each influencing Apollo navigation analyses: brief updated descriptions of the Apollo missions, constants and equations affecting orbit prediction accuracy, descriptions of navigation and communication systems, and navigation software capabilities. The tracking and navigation system errors presented are conservative and are intended only for manned space flight navigational analyses; they are not specifications.

Because international English units are used in the Apollo program, they are also used in this document. However, certain constants in Chapter 4.0 are in units consistent with their definition or common usage.

## 2.0 CHANGES

### Chapter 3.0 - APOLLO MISSIONS

1. The descriptions of the Apollo missions have been updated.
2. Mission numbers have been deleted and replaced by a descriptive title for each mission.

### Chapter 4.0 - TRAJECTORY PREDICTION MODEL

1. The title of chapter was changed from TRAJECTORY PREDICTION CAPABILITY to TRAJECTORY PREDICTION MODEL.
2. The potential function description was changed from the back of the chapter to follow the corresponding constants description.
3. Section 4.3 - Conversion factor for the lunar ephemeris updated.
4. Section 4.3 - Ephemeris tape system updated.
5. Section 4.4.2 - Effective cross sectional area changed.
6. Section 4.7 - The venting model was updated, and the venting equations added.

### Chapter 5.0 - NAVIGATION AND COMMUNICATION SYSTEMS CHARACTERISTICS

The more pertinent changes were those made to the values in the tables. In addition, some headings were added for consistency and others were deleted for simplicity. Parts of the text were reworded.

### Chapter 6.0 - NAVIGATION SOFTWARE CAPABILITIES

The title of the chapter was changed from DATA PROCESSING PROCEDURES to NAVIGATION SOFTWARE CAPABILITIES; this chapter was expanded.

## 3.0 APOLLO MISSIONS

### 3.1 INTRODUCTION

The purpose of this chapter is to give a convenient summary of the Apollo missions. A reference trajectory of the lunar landing missions is also included.

The ANWG makes every effort to include in this document the concepts that are current when the document is published. The following brief descriptions of the objectives and flight plans for the early missions give an idea of recent thinking about the types of missions being considered.

### 3.2 NEAR-EARTH MISSIONS

Earth orbital and suborbital missions are the early Apollo missions whose objectives are the qualification of spacecraft systems and the practice of lunar orbital rendezvous techniques. The following sections give a brief description of each of the missions. The missions are not identified by number as in previous editions because mission numbers are constantly changing. Instead the missions have been given short descriptive titles; table 3-I gives the correlation between the mission numbers used in the previous edition of this document and the descriptive titles used in this edition.

### 3.2.1 LAUNCH VEHICLE AND CSM DEVELOPMENT MISSION - SHORT LOB

This mission, launched February 26, 1966, was a short lob of 37-minutes duration. The purpose of the mission was to test the launch vehicle and the CSM; major events of the mission were:

- Launch at  $105^{\circ}$  azimuth; suborbital S-IVB cutoff
- S-IVB/CSM separation
- Coast through apogee (6 min)
- First SM burn (184 sec)
- Second SM burn (10 sec); cutoff 3.5 min prior to entry
- CM/SM separation
- CM entry at 26 500 fps (8077.2 mps)
- Recovery near Ascension Island

NASA-S-67-6288

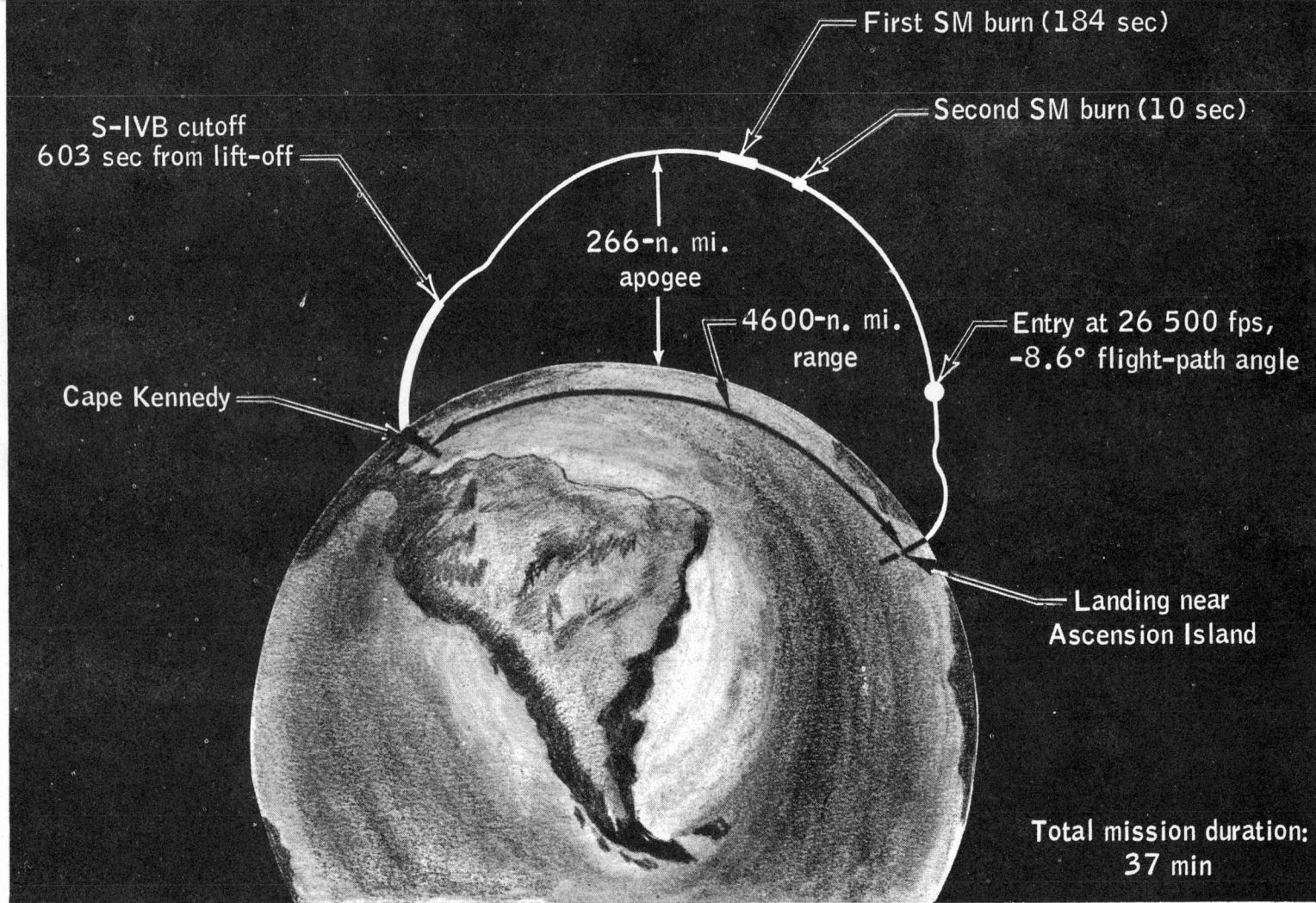


Figure 3-1.- Launch vehicle and CSM development mission - short lob.

### 3.2.2 LAUNCH VEHICLE AND CSM DEVELOPMENT MISSION - LONG LOB

This mission was a long lob of 93-minutes duration launched August 25, 1966. The purpose of the mission was to test the launch vehicle and the CSM; major mission events included:

- First stage flight at 105° azimuth
- Suborbital S-IVB cutoff and S-IVB/CSM separation
- S-IVB bulkhead test
- First SM burn (215 sec) after an 11-sec ullage, north of the Virgin Islands
- SM burns off northwest coast of Australia

Second SM burn (88 sec) after a 30-sec ullage

Third SM burn (3 sec) after a 10-sec ullage

Fourth SM burn (3 sec) after a 10-sec ullage

- CM/SM separation
- CM guided entry over New Guinea
- High heat load entry at 28 500 fps (8686.8 mps)
- Recovery near Wake Island

NASA-S-67-6287

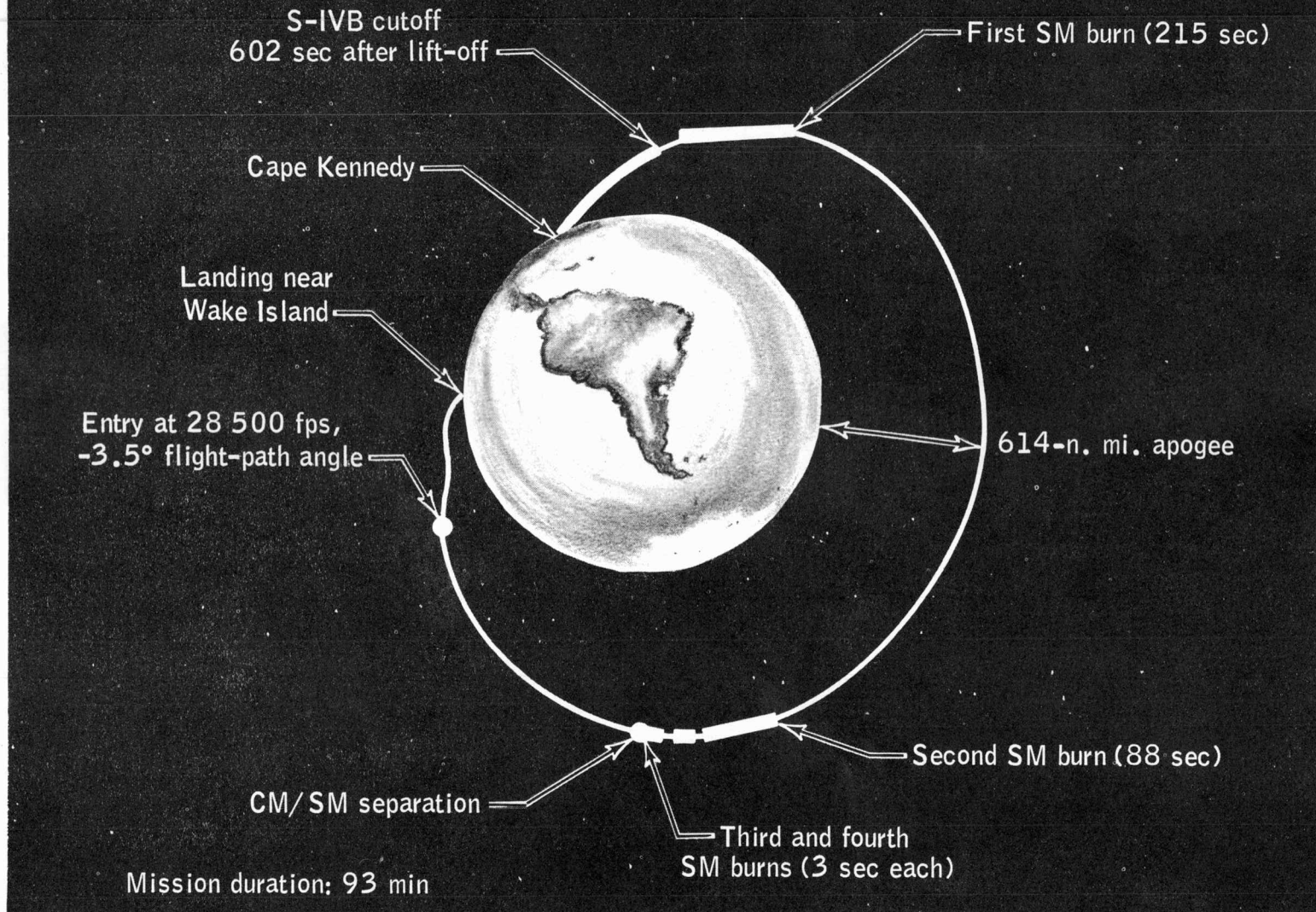


Figure 3-2.- Launch vehicle and CSM development mission - long lob.



### 3.2.3 LIQUID HYDROGEN BEHAVIOR IN ORBIT AND S-IVB STAGE DEVELOPMENT MISSION

This mission was launched July 5, 1966 and lasted approximately 6 hours; the purpose of the mission was to test the S-IVB stage and the behavior of liquid hydrogen in orbit. Major mission events were:

- Launch at  $72^{\circ}$  azimuth into a 100-n. mi. (185.2-km) circular orbit
- Coast and S-IVB stabilization
- $\text{LH}_2$  venting
- S-IVB start-cycle operation
- S-IVB bulkhead test
- No recovery

NASA-S-67-6290

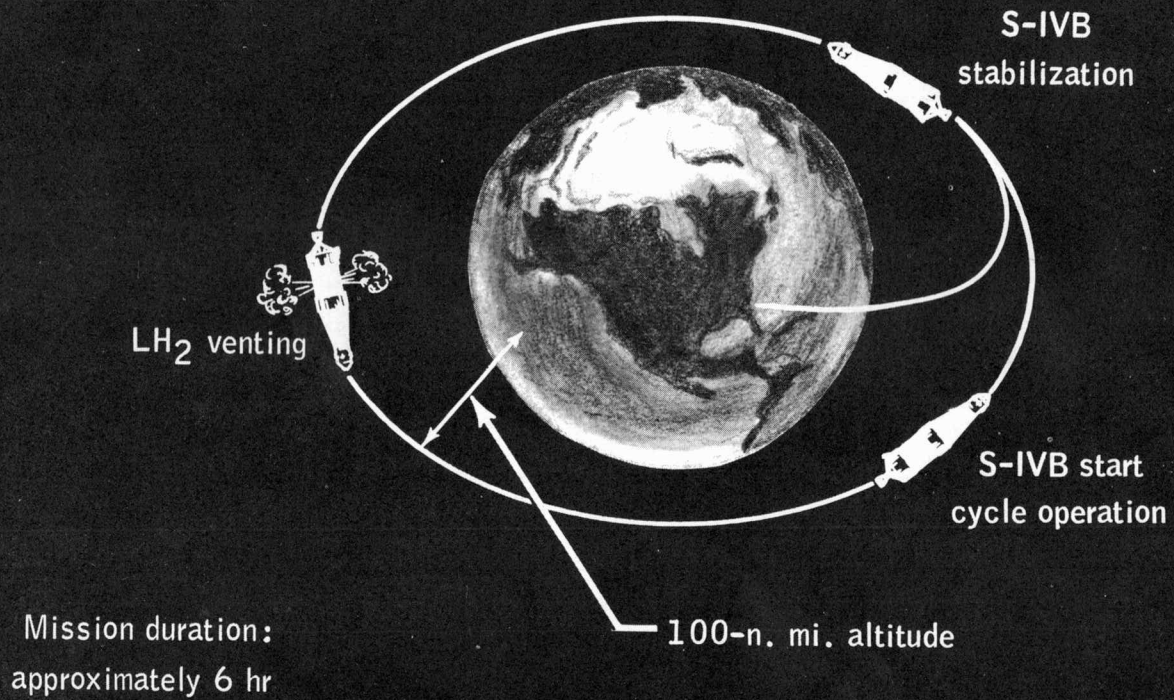


Figure 3-3.- Liquid hydrogen behavior in orbit and S-IVB stage development mission.

### 3.2.4 LONG DURATION CSM OPERATIONS MISSION

3-8

The objective of this mission is to test the CSM during a long-duration mission. Major mission events will include:

- Launch at 72° azimuth into a 120- by 150-n. mi. (222- by 278-km) orbit
- S-IVB/CSM separation
- CSM transposition maneuver
- SM burn to adjust phasing of S-IVB and CSM orbits
- CSM rendezvous with S-IVB on second day

Two SM burns

Coelliptic rendezvous simulation

- Minimum-impulse SM burn on third day
- SM burn on fifth day to raise apogee and lower perigee, changing the orbit to 95 by 220 n. mi. (176 by 407 km)
- Three out-of-plane SM burns of 0.5- to 57-sec duration during seventh to tenth days
- SM burn (11 sec) to deorbit on eleventh day
- Recovery in Atlantic

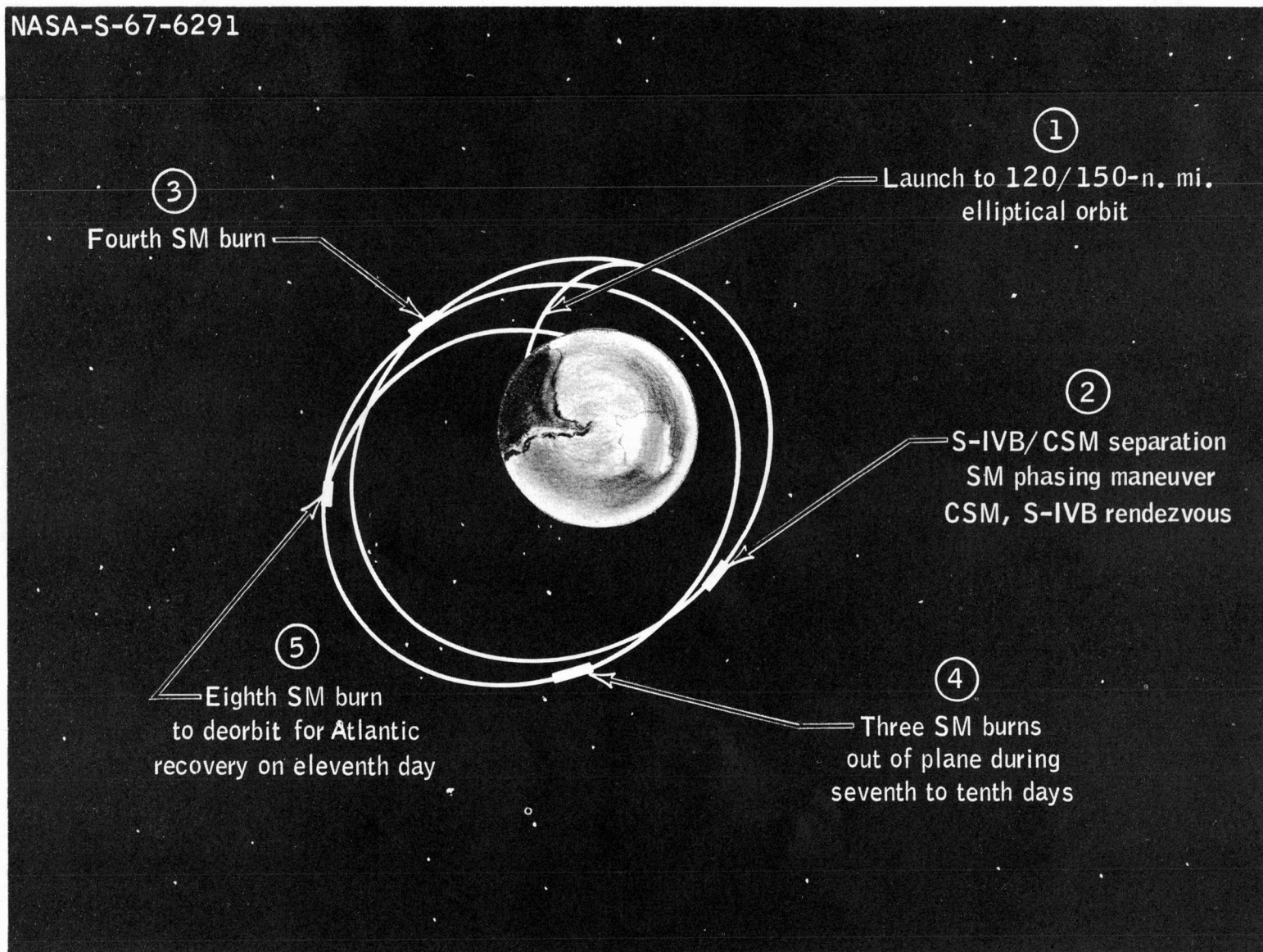


Figure 3-4.- Long duration CSM operations mission.

## 3.2.5 LM DEVELOPMENT MISSION

This mission will test the LM in earth orbit by simulating LM operations for the lunar landing mission. Major mission events will include:

- Launch at 72° azimuth into an 85- by 120-n. mi. (157- by 222-km) elliptical orbit; jettison CSM boilerplate with LES
- Deploy SLA, coast 30 minutes, separate LM
- Cold soak, LM attitude hold
- First DPS burn to change orbit to 120 by 180 n. mi. (222 by 333 km)
- Second DPS burn/FITH abort test consisting of DPS burn (5 sec), staging, and APS first burn (5 sec) with resulting orbit 168 by 187 n. mi. (311 by 346 km)
- Second APS burn with resulting orbit 128 by 172 n. mi. (237 by 318 km)
- Final coast; no recovery

NASA-S-67-6289

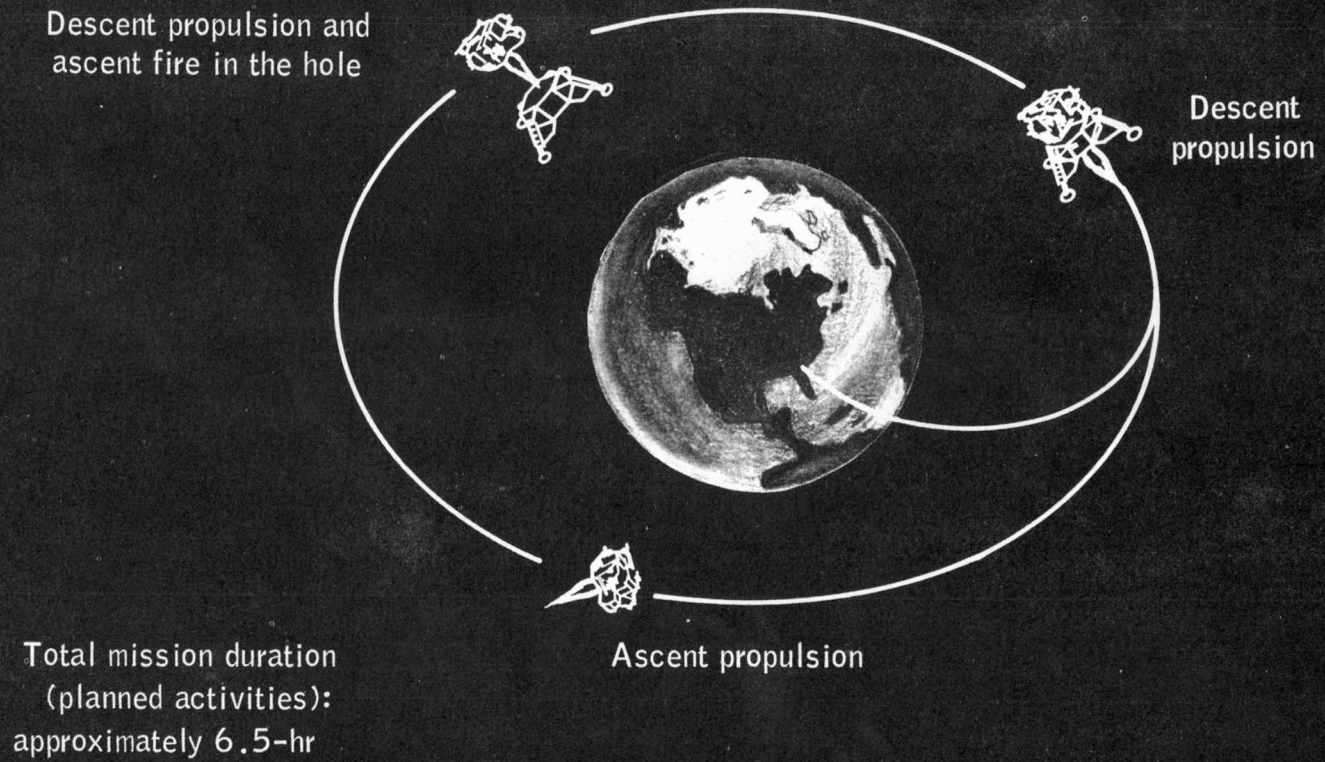


Figure 3-5.- LM development mission.

### 3.2.6 CSM-LM OPERATIONS MISSION - DUAL LAUNCH

3-12

This mission will provide a dual launch with the CSM being launched first. The objective of this mission is to test CSM-LM rendezvous operations. Major mission events will include:

- Launch CSM into a 100-n. mi. (185.2-km) circular orbit
- CSM separation from S-IVB
- SPS out-of-plane confidence burn
- Launch LM 1 day later into a 110-n. mi. (203.7-km) circular orbit
- CSM-active rendezvous and docking
- Use CSM RCS to separate LM from S-IVB
- Docked SPS burns, including "stroking test", resulting in a 125-n. mi. (231.5-km) circular orbit
- Extravehicular activities
- Docked out-of-plane DPS burn
- LM-active separation, equiperiod rendezvous, and docking
- Staging of LM descent stage
- CSM separation from unmanned LM
- APS burn to depletion
- CSM flyby rendezvous with LM descent stage in approximately 125-n. mi. (231.5-km) circular orbit
- SPS burn to 90- by 240-n. mi. (166- by 244-km) orbit
- SM burn to deorbit
- Recovery in Atlantic

NASA-S-67-6293

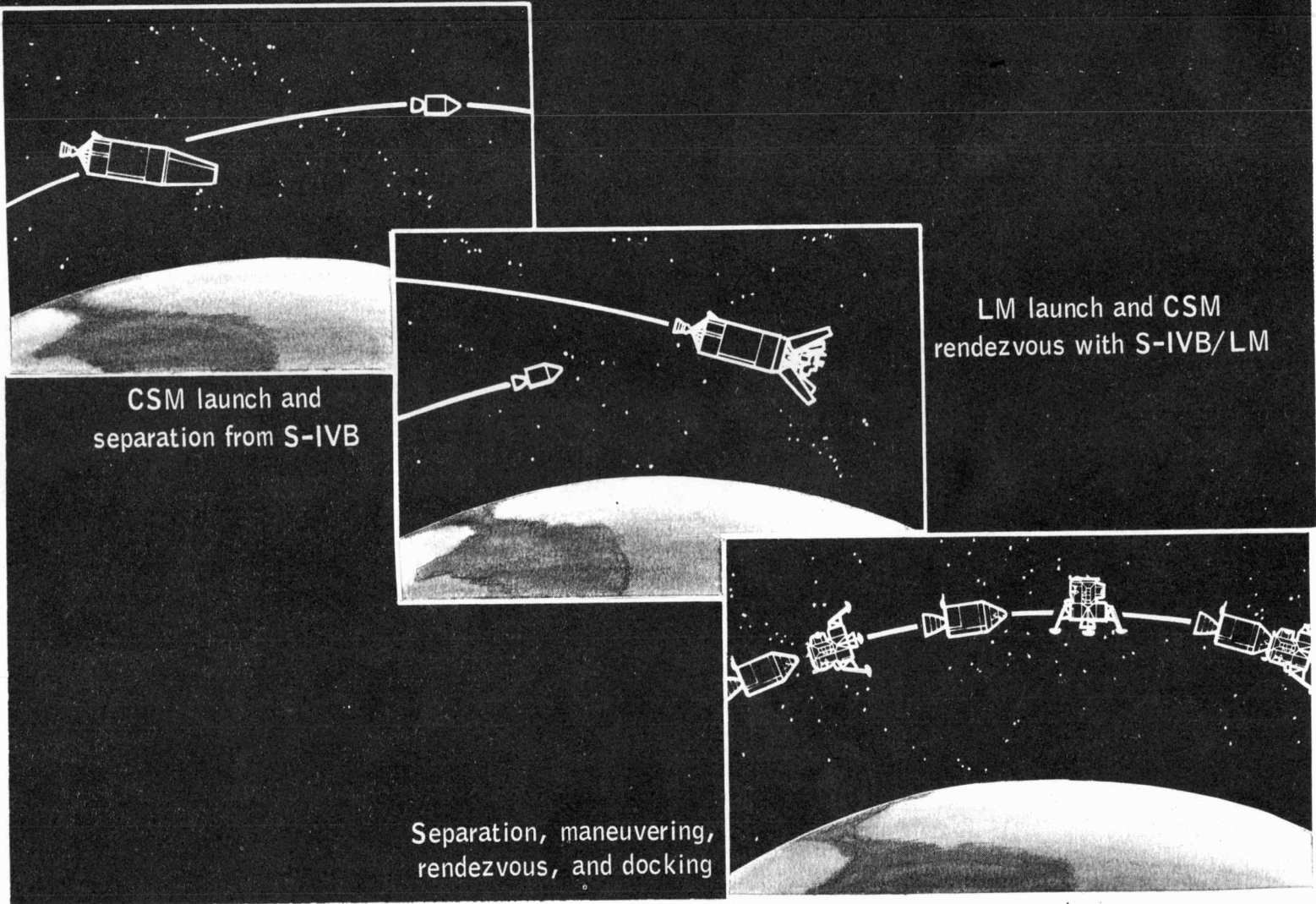


Figure 3-6.- CSM - LM operations mission - dual launch.



## 3.2.7 FIRST SATURN V AND SPACECRAFT DEVELOPMENT MISSION

This 9-hour mission will provide check out of the LM and CSM. Major mission events will include:

- Launch at  $72^\circ$  azimuth into a 100-n. mi. (185.2-km) circular parking orbit
- Two-orbit coast
- S-IVB nonoptimum burn to insert into earth-intersecting ellipse having a 9000-n. mi. (16 668-km) apogee altitude
- S-IVB/CSM separation
- SM burn (25 sec)
- SM burn 9265 sec prior to entry to simulate lunar return entry conditions; entry at 36 333 fps (11 074.3 mps)
- Recovery near Hawaii

NASA-S-67-6295

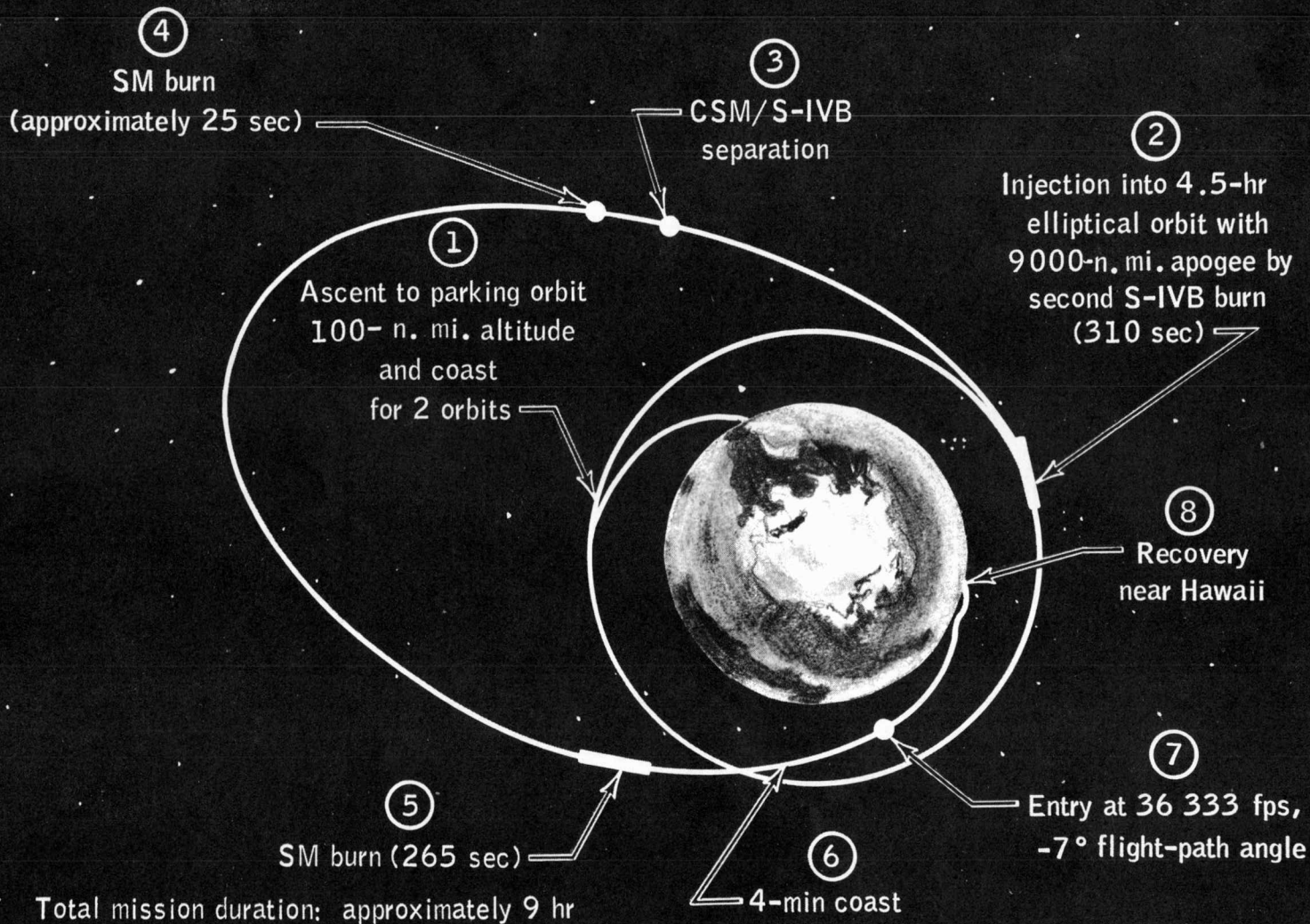
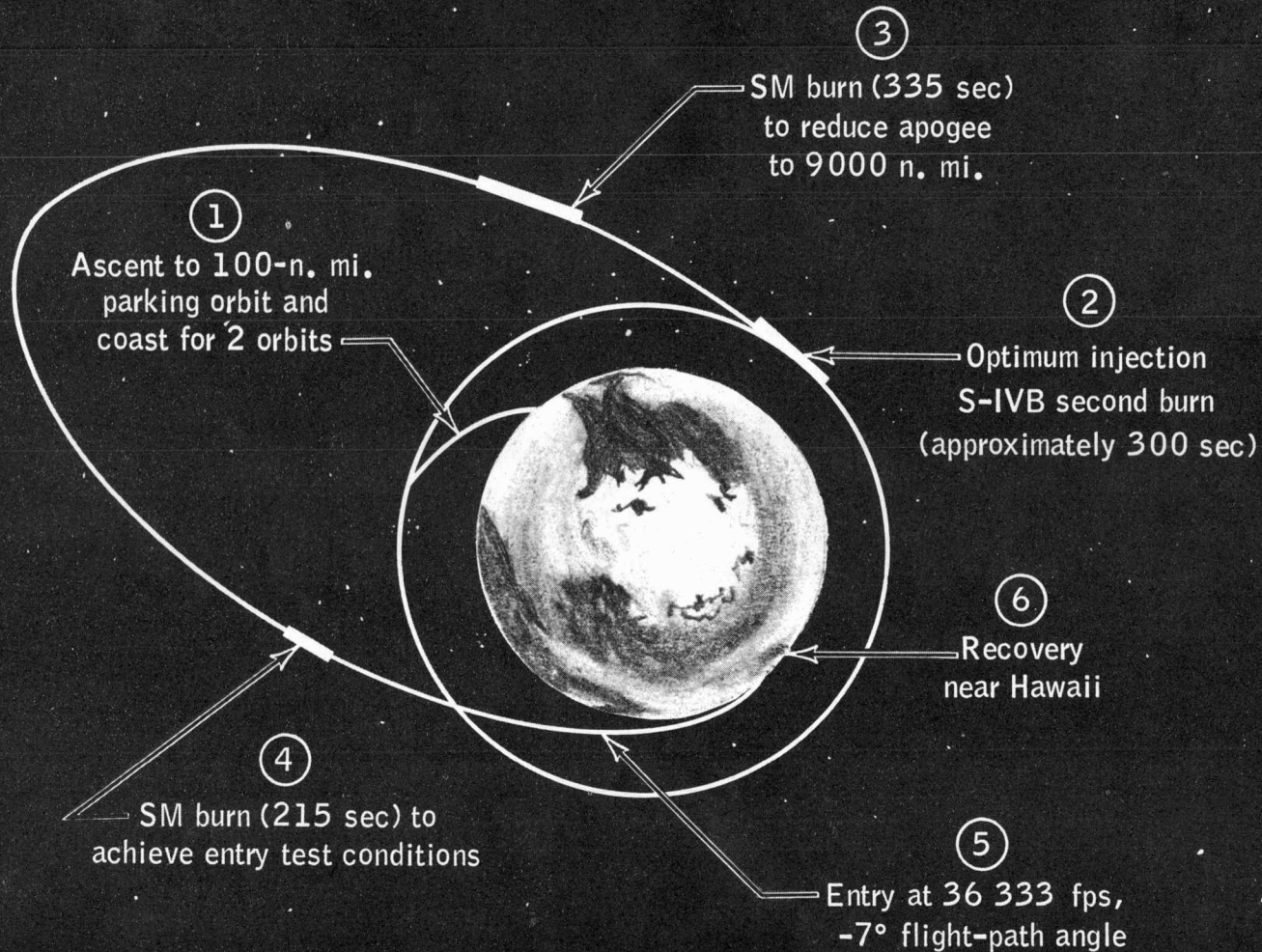


Figure 3-7.- First Saturn V and spacecraft development mission.

### 3.2.8 SECOND SATURN V AND SPACECRAFT DEVELOPMENT MISSION

The objective of this mission is to test the launch vehicle and CSM; major mission events will include:

- Launch at  $72^\circ$  azimuth into 100-n. mi. (185.2-km) parking orbit
- Two-orbit coast
- S-IVB optimum burn injecting S-IVB/CSM onto a 72-hr lunar transfer ellipse
- S-IVB/CSM separation
- SM burn to lower apogee to 9000 n. mi. (16 668 km)
- SM burn prior to entry to simulate lunar return entry conditions; entry at 36 333 fps (16 668 mps)
- Recovery near Hawaii



Total mission duration:  
approximately 9 hr

Figure 3-8.- Second Saturn V and spacecraft development mission.

### 3.2.9 LUNAR MISSION SIMULATION

The purpose of this mission is to simulate in earth orbit the operations of the lunar mission; the sequence of events will include:

- Launch into 100-n. mi. (185.2-km) parking orbit
- Spacecraft checkout and IMU alignment during two-orbit coast
- Second S-IVB burn to an elliptical orbit having a 4000-n. mi. (7408-km) apogee
- Perform transposition, docking, navigation, and midcourse corrections
- SM burn to circularize orbit at 130 n. mi. (234.8 km)
- LM DPS propulsion, LM and CSM rendezvous and docking exercises
- SM burn to simulate transearth injection
- SM burn to deorbit
- Recovery

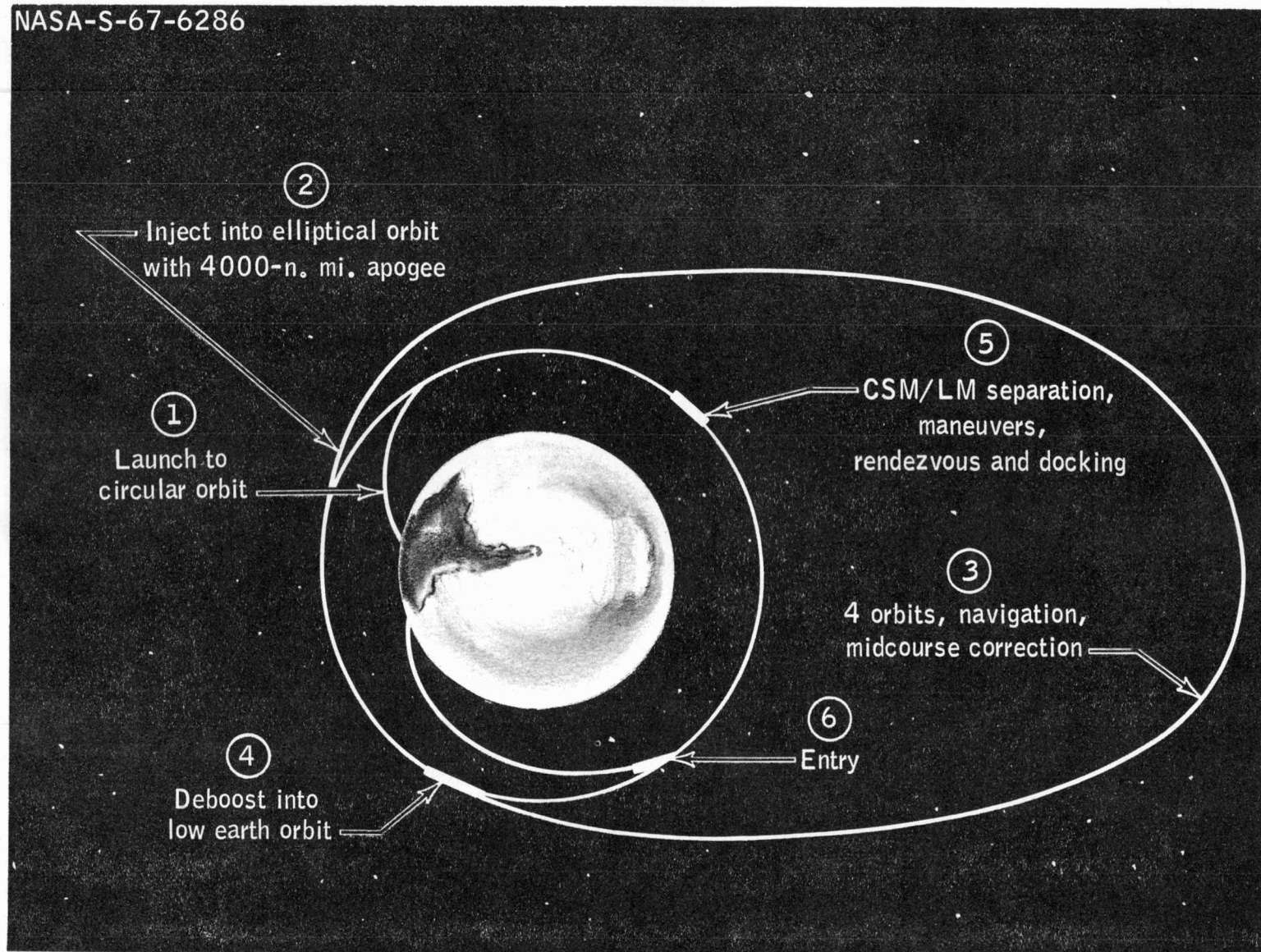


Figure 3-9.- Lunar mission simulation.

### 3.3 LUNAR MISSION

#### 3.3.1 TYPICAL LUNAR MISSION

The lunar mission may be called that mission during which the vehicle enters the lunar sphere of influence. It is commonly divided into 14 phases (see fig. 3-10). Within each phase the possible trajectories are limited by operational constraints. Operational constraints are governed by the day of launch of the mission, delay in the time of launch, contingencies that develop during a mission, and the performance of the ground and onboard systems.

The following sections contain guidelines to be used in constructing Apollo-type lunar missions for navigational study. These guidelines apply to conic type or patched-conic type construction. Listed by phase are the constraints on the geometry of the trajectory (ref. 1 and 2). It should be noted that the guidelines are consistent with a ground rule requiring the selection of a free-return translunar trajectory.

#### 3.3.2 PHASES OF THE LUNAR MISSION

##### 3.3.2.1 Launch

Launch is from Cape Kennedy. The launch azimuth varies between  $72^\circ$  and  $108^\circ$ . Insertion occurs approximately  $25^\circ$  downrange and at approximately 680 seconds after lift-off.

##### 3.3.2.2 Earth Parking Orbit

The plane of the trajectory and the location of the insertion vector are defined by the launch. The minimum operational daily launch window is approximately 2.5 hours. Operational launch azimuths are limited to a difference of  $26^\circ$  for each launch window.

The altitude of the nominal circular parking orbit is 100 n. mi. (185.2 km). The parking orbit lifetime based on the ARDC 1962 atmosphere shall be at least 10 orbits.

##### 3.3.2.3 Translunar Injection Burn

Two translunar injection opportunities are required after insertion into the earth parking orbit. The last one occurs no later than 4.5 hours after orbital insertion.

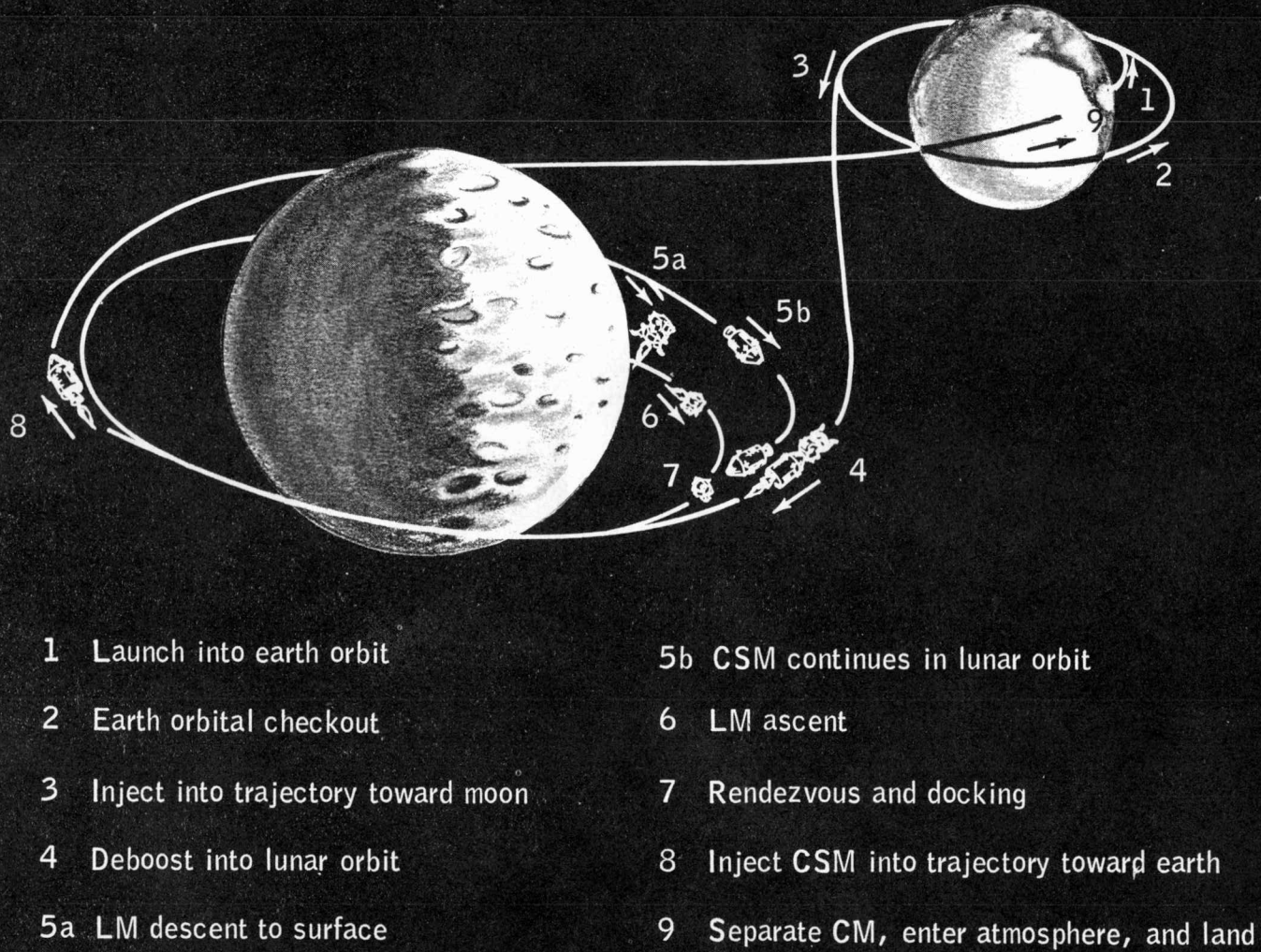


Figure 3-10.- Typical lunar landing mission.



#### 3.3.2.4 Translunar Trajectory

The translunar injection burn injects the spacecraft on a free-return trajectory with an inclination essentially the same as the earth parking orbit. The plane of the trajectory intersects the earth-moon plane and is coincident with the earth-moon line at the time of pericyynthion arrival. The travel time from perigee to pericyynthion varies between 60 and 75 hours, depending upon the earth-moon distance.

In the nominal mission, no midcourse corrections are required during translunar coast. However, two midcourse maneuvers are planned. The first maneuver is planned between 2 and 8 hours after translunar injection and the second maneuver near the lunar sphere of influence.

#### 3.3.2.5 Lunar Orbit Insertion

The lunar orbit insertion burn is targeted to put the landing site in the plane of the CSM orbit at the time of LM descent.

#### 3.3.2.6 Lunar Parking Orbit

Lunar orbit insertion is initiated to obtain the desired orbital plane. The insertion maneuver will not necessarily occur at pericynthion because of the allowance of pre- or post-pericynthion braking. The orbit is designed such that a transearth injection may be made from any known orbit.

The CSM is in a near-circular retrograde orbit of approximately 80-n. mi. (148-km) altitude. The nominal mission extends the lunar parking orbit phase after jettisoning the LM before transearth injection.

#### 3.3.2.7 LM Descent

The LM descent will be a Hohmann transfer from the lunar parking orbit to a pericynthion of 60 000 ft (18 288 m). The pericynthion of the Hohmann transfer orbit is targeted to be  $16^{\circ}$  from the landing site.

#### 3.3.2.8 LM Stay Time

Stay time on the lunar surface will be between 0 and 24 hours. The maximum total stay time on the lunar surface, including contingency, is 44 hours.

### 3.3.2.9 LM Ascent and Rendezvous

The pericyynthion of the LM ascent trajectory will be approximately 60 000 ft (18 288 m) above the lunar surface. The trajectory will be consistent with the concentric flight plan. Prior to LM ascent, the CSM will maneuver so that the LM will be in the CSM orbital plane.

### 3.3.2.10 Transearth Injection

The vehicle will not be visible to the earth for at least 20 minutes after termination of the transearth injection burn.

### 3.3.2.11 Transearth Trajectory

The inclination of the transearth trajectory plane to the equatorial plane will be between  $0^\circ$  and  $40^\circ$ . The vehicle must make a posigrade return with respect to the earth's rotation. The transearth injection from a lunar parking orbit allows for a plane change.

In the nominal mission no midcourse maneuvers are applied, but two are scheduled. The first is at the lunar sphere of influence, and the second is approximately 30 hours after the first maneuver.

The nominal vacuum perigee altitude is 25 n. mi. (46.3 km) with  $\pm 12$ -n. mi. (22.2-km) tolerance. The transearth transit time will not exceed 110 hours.

### 3.3.2.12 Reentry and Recovery

Reentry will begin at 400 000-ft (121 920-m) altitude. The down-range distance from reentry point to impact point is planned to lie between 1500 n. mi. (2778 km) and 2500 n. mi. (4630 km) in the primary mode. In the backup mode, dispersions of 1400 n. mi. (2592 km) to 3500 n. mi. (6482 km) could be encountered. Two landing areas are designated (see fig. 3-11). They take the shape of rectangles on the east side of the following two points.

Hawaii:

Latitude, deg N . . . . . 21.37

Longitude, deg W. . . . . 157.97

Pago Pago:

Latitude, deg S . . . . . 14.25

Longitude, deg W. . . . . 170.75

The rectangles have a longitudinal width of 400 n. mi. (740.8 km) and a latitudinal length of 2400 n. mi. (4445 km) which is 1200 n. mi. (2222.4 km) north and 1200 n. mi. (2222.4 km) south of the landing site.

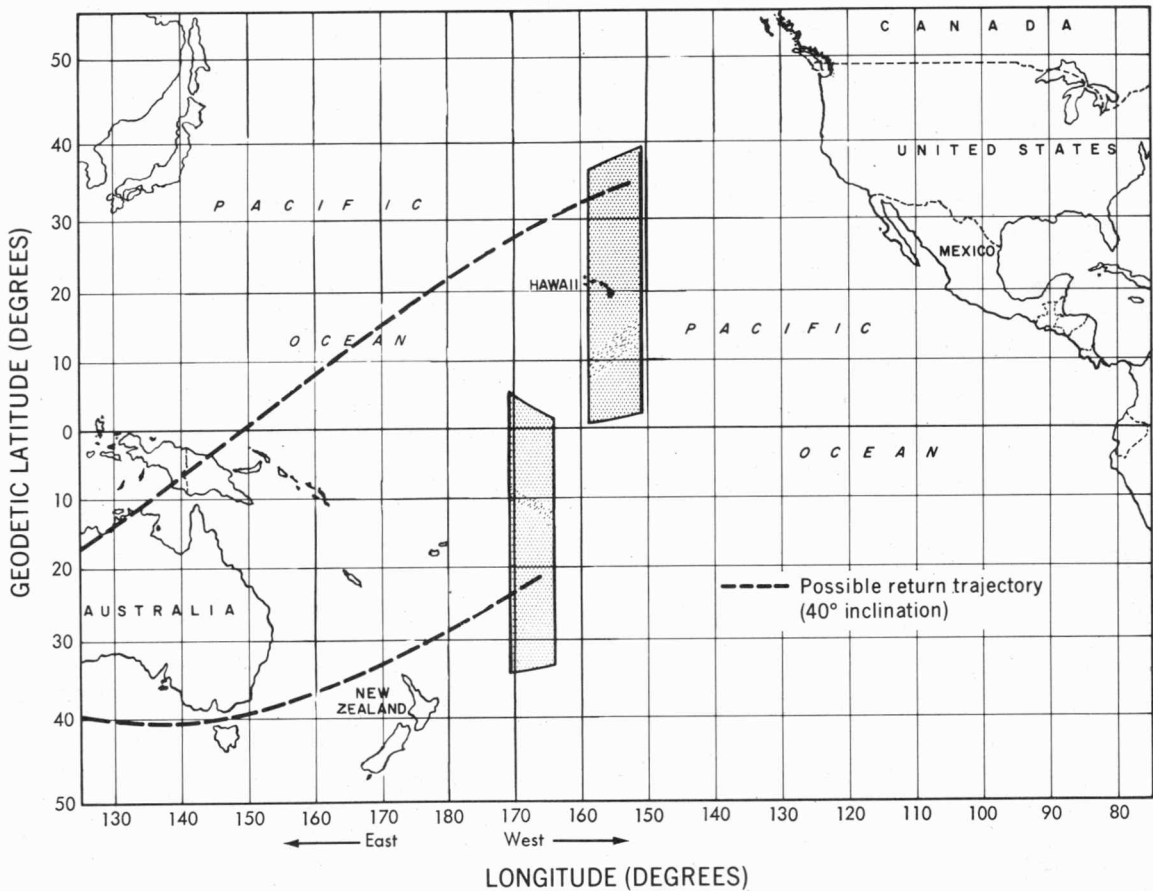


**Figure 3-11.- Water recovery areas.**

3.3.3 REFERENCE TRAJECTORIES

Specific examples of complete missions are often desired for error analysis studies. For a lunar landing mission, a reference trajectory (ref. 3) produced by MPAD is presented in both patched conic and integrated form in tables 3-I and 3-II, respectively.

TABLE 3-I.- CORRELATION BETWEEN MISSION NUMBERS USED IN PREVIOUS  
ANWG DOCUMENTS AND TITLES USED IN THIS DOCUMENT

Mission number	Descriptive title
AS-201	Launch vehicle and CSM development mission - short lob
AS-202	Launch vehicle and CSM development mission - long lob
AS-203	Liquid hydrogen behavior in orbit and S-IVB stage development mission
AS-204	Long duration CSM operations mission
AS-206	LM development mission
AS-207/208	CSM-LM operations mission - dual launch
AS-501	First Saturn V and spacecraft development mission
AS-502	Second Saturn V and spacecraft development mission
AS-503	Lunar mission simulation

TABLE 3-II.- INTEGRATED TRAJECTORY STATE VECTOR<sup>a</sup>

[September 17, 1969]

Event	Hours from midnight of day of launch	Reference system	x, n. mi. (km)	y, n. mi. (km)	z, n. mi. (km)	$\dot{x}$ , fps (mps)	$\dot{y}$ , fps (mps)	$\dot{z}$ , fps (mps)
Earth parking orbit insertion	13:01:08.5	Earth	-2234.9353 (-4139.1002)	+1982.0656 (3670.7855)	+1906.8056 (3531.4039)	-16705.129 (-5091.7233)	-19364.552 (-5902.3154)	+548.50787 (167.1851)
Translunar injection	15:55:14.5	Earth	-1979.0874 (-3665.2698)	+2328.1528 (4311.7389)	+1924.0770 (3563.3906)	-27937.154 (-8515.2445)	-21544.653 (-6566.8102)	+4916.3660 (1498.5083)
Lunar orbit insertion	77:10:12.2	Moon	165.63936 (306.7640)	-919.37695 (-1702.6861)	-415.86151 (-770.1755)	-5208.3665 (-1587.5101)	-817.04316 (-249.0347)	-268.21399 (-81.7516)
LM Hohmann descent	81:14:04.5	Moon	291.06763 (539.0572)	-892.26715 (-1652.4787)	-405.90489 (-751.7358)	-4963.9006 (-1512.9969)	-1378.4721 (-420.1580)	-526.42523 (-160.4544)
LM Hohmann ascent	117:13:25.0	Moon	-207.17281 (-383.6840)	+842.58758 (1560.4721)	+381.20313 (705.9881)	+5430.6187 (1655.2525)	+1213.0308 (369.7317)	+459.61653 (140.0911)
Transearth injection	121:59:12.3	Moon	+952.74342 (1764.4808)	-332.99696 (-616.7103)	-166.43166 (-308.2314)	-2725.8340 (-830.8342)	-6776.7037 (-2-65.5392)	-3294.6829 (-1004.2193)

<sup>a</sup>See table 3-IV for definition of symbols.

TABLE 3-III.- PATCHED CONIC, REFERENCE TRAJECTORY FOR A LUNAR LANDING MISSION<sup>a</sup>

[September 17, 1969]

(a) Rectangular coordinates

Event Time, hr:min:sec	x, e.r. x, e.r./hr	y, e.r. y, e.r./hr	z, e.r. z, e.r./hr	r, e.r. v, e.r./hr	r <sup>2</sup> , (e.r.) <sup>2</sup> v <sup>2</sup> , (e.r./hr) <sup>2</sup>	r <sup>3</sup> , (e.r.) <sup>3</sup> v <sup>3</sup> , (e.r./hr) <sup>3</sup>
Launch 00:00:45.773	-2.61907521E-01 -3.80045062E-00	8.38973331E-01 -1.86518437E-00	4.76986212E-01 1.19389898E-00	9.99993825E-01 4.39860576E-00	9.99987662E-01 1.93477324E+01	9.99981487E-01 8.51030469E+01
Start Earth Park Orbit 00:12:37.773	-6.06858200E-01 -3.00693446E-00	6.12262309E-01 -3.20127439E-00	5.61927658E-01 2.40666047E-01	1.02903098E-00 4.39860576E-00	1.05890475E-00 1.93477324E+01	1.08964579E-00 8.51030469E+01
End Earth Park Orbit 02:56:03.307	-1.99110475E-01 -3.87894809E-00	8.94833708E-01 -1.57067959E-00	4.67474461E-01 1.35442238E-00	1.02903098E-00 4.39860576E-00	1.05890475E-00 1.93477324E+01	1.08964579E-00 8.51080469E+01
End TL Injection 03:01:17.227	-5.73888361E-01 -4.81025964E-00	6.75075561E-01 -3.69884905E-00	5.61630416E-01 8.46055424E-01	1.04904890E-00 6.12665421E-00	1.10050359E-00 3.75358918E+01	1.15448208E-00 2.29969433E+02
Perigee TL Conic 02:58:55.225	-3.77181831E-01 -5.14285642E-00	8.11086261E-01 -3.17808247E-00	5.20740676E-01 1.22500001E-00	1.03503522E-00 6.16845244E-00	1.07129793E-00 3.80498055E+01	1.10883111E-00 2.34708416E+02
Start Lunar Brake 64:36:38.052	9.14372098E-02 -1.35900301E-00	-2.55935153E-01 -2.95845199E-01	-1.16563806E-01 -4.16477954E-01	2.95720625E-01 1.45184967E-00	8.74506867E-02 2.10786745E-00	2.58609718E-02 3.06030664E-00
Free Return Perigee 132:56:18.809	-1.87690558E-01 -3.51597363E-01	9.22975099E-01 -2.29643866E-00	3.53934580E-01 5.80210078E-00	1.00617120E-00 6.24992996E-00	1.01238048E-00 3.90616247E+01	1.01862808E-00 2.44132420E+02
Start Lunar Park Orbit 64:36:38.052	9.14372289E-02 -8.65258348E-01	-2.55935207E-01 -2.62905964E-01	-1.16563828E-01 -1.01488878E-01	2.95720625E-01 9.09995353E-01	8.74506867E-02 8.28091538E+01	2.58609718E-02 7.53559446E+01
End Lunar Park Orbit 111:15:40.684	2.82698664E-01 -2.66597763E-01	-7.70484251E-02 -7.95718211E-01	-3.99461126E-02 -3.51922849E-01	2.95720625E-01 9.09995353E-01	8.74506867E-02 8.28091538E-01	2.58609718E-02 7.53559446E-01
End T E Injection 111:15:40.684	2.82698664E-01 -4.00613683E-01	-7.70484251E-02 -1.18597727E-00	-3.99461126E-02 -5.47617799E-01	2.95720625E-01 1.36635232E-00	8.74506867E-02 1.86691865E-00	2.58609718E-02 2.55086863E-00
Return Perigee 199:21:34.200	-5.84317166E-01 -4.92805803E-00	7.16488701E-01 -2.34832311E-00	3.95784074E-01 -3.02438161E-00	1.00569759E-00 6.24077410E-00	1.01142766E-00 3.89472610E+01	1.01719037E-00 2.43061060E+02
Start Reentry 199:19:19.157	-3.92325053E-01 -5.28316671E-00	7.94397622E-01 -1.79985528E-00	5.03314632E-01 -2.69814485E-00	1.01897603E-00 6.19929957E-00	1.03831215E-00 3.84313151E+01	1.05801520E-00 2.38247237E+02

<sup>a</sup>See table 3-IV for definition of symbols.

TABLE 3-III.- PATCHED CONIC, REFERENCE TRAJECTORY FOR THE LUNAR LANDING MISSION<sup>a</sup>

[September 17, 1969]

(b) Conic elements

Phases; reference E, rad P <sub>x</sub> /p, e.r.	a, e.r. M, rad P <sub>y</sub> /p, e.r.	e, n.d. n, rad/hr P <sub>z</sub> /p, e.r.	i, rad T, hr r <sub>peri</sub> , e.r.	Ω, rad H <sub>x</sub> /h, (e.r.) <sup>2</sup> /hr r <sub>peri</sub> , e.r./hr	ω, rad H <sub>y</sub> /h, (e.r.) <sup>2</sup> /hr d <sub>o</sub> , (e.r.) <sup>2</sup> /hr	t <sub>p</sub> , hr H <sub>z</sub> /h, (e.r.) <sup>2</sup> /hr l/a, l/e.r.
Translunar; Earth 9.68387449E-09 -3.64414412E-01	4.72697008E 01 9.20423007E-08 7.83631605E-01	9.78103614E-01 1.37295079E-02 5.03113943E-01	5.71495003E-01 4.57640964E 02 1.03503557E 00	8.74071002E-01 4.14834416E-01 6.16845137E 00	2.76564268E 00 -3.47094378E-01 2.90572643E-07	2.98200703E 00 8.41093278E-01 2.11552000E-02
Translunar; Moon -1.72633491E-04 3.09201324E-01	-5.42156887E-01 -3.72931626E-04 -8.65462637E-01	1.54545210E-00 1.23963125E 00 -3.94168675E-01	2.63236672E 00 5.06859219E 00 2.95720613E-01	2.78988144E 00 1.67946595E-01 1.45184967E 00	-6.28742081E-01 4.57658923E-01 -4.65661287E-10	6.46106458E 01 -8.73122132E-01 -1.84448452E 00
Free return; Earth -2.20131457E-09 -1.86539386E-01	3.88108078E 01 -1.92089786E-08 9.17314172E-01	9.74074960E-01 1.84544128E-02 3.51763794E-01	1.45035979E 00 3.40470609E 02 1.00617146E 00	1.72592118E 00 9.80835509E-01 6.24992901E 00	1.93299429E 00 1.53384295E-01 -5.96046448E-08	1.32938558E 02 1.20145589E-01 2.57660180E-02
Transearth; Moon -1.72633491E-04 9.55965233E-01	-1.16204329E-00 -5.13829362E-04 -2.60544917E-01	1.25448330E 00 3.95044962E-01 -1.35080704E-01	2.70490575E 00 1.59049876E 01 2.95720607E-01	-3.11126426E 00 -1.28251018E-02 -1.36635233E-00	-1.24520184E 00 4.22745109E-01 -7.12461770E-08	1.11261413E 02 -9.06157863E-01 -8.60553133E-01
Transearth; Earth -5.59658986E-09 -5.81006861E-01	3.08202034E 01 -4.34560633E-08 7.12429553E-01	9.67368877E-01 2.60781038E-02 3.93541813E-01	6.74212325E-01 2.40937197E 02 1.00569780E 00	-3.21336824E-01 -1.97170329E-01 6.24077338E 00	-2.25285298E 00 -5.92327696E-01 -1.34110451E-07	1.99359500E 02 7.81198919E-01 3.24462482E-02

<sup>a</sup>See table 3-IV for definition of symbols.

TABLE 3-IV.- SYMBOLS USED IN TABLES 3-II and 3-III

a	orbital semimajor axis
$d_o$	the dot product of the initial position and velocity vectors, $\bar{R}_o \cdot \dot{\bar{R}}_o$
e	orbital eccentricity
E	eccentric anomaly
$H_x/h, H_y/h, H_z/h$	unit angular momentum vector
i	orbital inclination
M	mean anomaly
n	mean motion
$P_x/p, P_y/p, P_z/p$	unit vector in direction of periapsis
r	scalar position of a vehicle
$r_{peri}$	radius of periapsis
t	elapsed time from the base time, hr:min:sec. The base time (G.m.t.) is 12 hr 49 min and 08.4 sec from midnight of the day of launch.
$t_p$	time of perigee passage
T	orbital period
v	scalar velocity of a vehicle
$v_{peri}$	velocity magnitude at periapsis
x, y, z	inertial, right-handed, rectangular coordinates, either geocentric or selenocentric corresponding to the use of either the earth or the moon as the primary reference body. x points toward the mean equinox of the date of launch, z points north.
$\omega$	argument of perigee
$\Omega$	right ascension of ascending node



3.4 REFERENCES

1. Mayer, John P.: Apollo Operational Nominal Trajectory Ground Rules, Memorandum, July 2, 1965.
2. Jenkins, Morris V.: Apollo Operational Nominal Ground Rules, NASA 64-OM-4, 1964.
3. Apollo Mission Planning Task Force: Design Reference Mission, Vol. I Mission Description, published by Grumman Aircraft Engineering Corporation, Bethpage, N. Y. Contract No. NAS 9-1100, Report No. LED-540-12, October 30, 1964.

## 4.0 TRAJECTORY PREDICTION MODEL

### 4.1 INTRODUCTION

The trajectory prediction model is of interest since it influences the accuracy with which the orbit may be computed at some initial time and future times. The error in the computed orbit due to the predictor may be determined by investigating the influence of the error in gravitational constants, atmospheric drag, S-IVB venting, etc.

This chapter presents the values and associated uncertainties of the constants to be used in the trajectory prediction model. Also presented are a drag model, a venting model, the earth and moon potential models, and a designation of the celestial body ephemeris system to be used. A list of conversion factors and a description of potential equations are also included.

Uncertainties (one sigma) are presented, if available. For some quantities, more decimal digits are given than are justified by the uncertainties, for purposes of consistent conversion between units. The values presented are in agreement with those adopted by NASA Headquarters. (See ref. 1.)

### 4.2 CONSTANTS FOR APOLLO

#### 4.2.1 EARTH CONSTANTS

##### Equatorial Earth Radius (gravitational)

$$1 \text{ e.r.} = 6.378\,165 \text{ } (+0.000\,025) \times 10^6 \text{ m (ref.2)}$$

$$1 \text{ e.r.} = 2.092\,573\,819 \text{ } (+0.000\,008\,2) \times 10^7 \text{ int. ft.}$$

$$1 \text{ e.r.} = 3.443\,933\,585 \text{ } (+0.000\,013\,5) \times 10^3 \text{ n. mi.}$$

##### Flattening (accepted number based on 1960 Fischer ellipsoid)

$$1/f = 298.30 \pm 0.05 \text{ (ref. 3)}$$

$$f = 3.352\,329\,869\,259\,14 \times 10^{-3}$$

6,378,135.5<sup>m</sup> WGS7

6378140 ± 3<sup>m</sup> (188)

298.26 (WGS72)  
298.257 (1981)

3.35281 × 10<sup>-3</sup>  
81

Gravitational Parameter ( $GM_e = \mu_e = \mu$  earth)

$\mu$  earth = 3.986 032 (+0.000 030)  $\times 10^{14}$  m<sup>3</sup>/sec<sup>2</sup> (ref. 4)

$\mu$  earth = 1.407 653 92 (+0.000 010 6)  $\times 10^{16}$  (int. ft)<sup>3</sup>/sec<sup>2</sup>

$\mu$  earth = 1.990 941 65 (+0.000 015)  $\times 10$  (e.r.)<sup>3</sup>/hr<sup>2</sup>

Mass of the earth

$M_e = 5.975 \times 10^{24}$  kg

Angular velocity of the earth rotation

The following equation is taken from reference 1.

$$\omega = \frac{2\pi}{86\,164.098\,92 + 0.001\,64T} \text{ rad/sec.}$$

Where  $T$  is the number of Julian centuries of 36 525 days from 1900 January 0.5 UT (Julian date = 241 502 0.0).

$\omega = 7.292\,115\,06 \times 10^{-5}$  rad/sec (1966-1972)

$\omega = 2.625\,161\,42 \times 10^{-1}$  rad/hr

$\omega = 4.178\,074\,16 \times 10^{-3}$  deg/sec

Gravitational potential function The four forms in use follow with the associated constants.

$$U = \frac{\mu_e}{r} \left[ 1 - \frac{J_2}{2} \left(\frac{R_e}{r}\right)^2 (3 \sin^2\phi - 1) - \frac{J_3}{2} \left(\frac{R_e}{r}\right)^3 (5 \sin^3\phi - 3 \sin\phi) - \frac{J_4}{8} \left(\frac{R_e}{r}\right)^4 (35 \sin^4\phi - 30 \sin^2\phi + 3) + 3J_{22} \left(\frac{R_e}{r}\right)^2 \cos^2\phi \cos 2(\lambda - \lambda_{22}) \right]$$

*75/100*  
*Relative to Precessing System (Sideris)*

*Non Precessing System*

*1975 86164.14505*  
*1980 86164.10925*  
*1985 86164.00731*  
*(1975) 7.292115072x10<sup>-5</sup>*  
*(1980) 7.292114807x10<sup>-5</sup> rad/sec*  
*(1985) 7.292113029x10<sup>-5</sup> rad/sec*

*Baseline year - Fixed by length of Tropical year*  
*365.242198781 days of 86400 sec = (ea)*

$$\begin{aligned}
 U = \frac{\mu_e}{r} & \left[ 1 + \frac{C_{2,0}}{2} \left( \frac{R_e}{r} \right)^2 (3 \sin^2 \phi - 1) \right. \\
 & + \frac{C_{3,0}}{2} \left( \frac{R_e}{r} \right)^3 (5 \sin^3 \phi - 3 \sin \phi) \\
 & + \frac{C_{4,0}}{8} \left( \frac{R_e}{r} \right)^4 (35 \sin^4 \phi - 30 \sin^2 \phi + 3) \\
 & \left. + 3J_{22} \left( \frac{R_e}{r} \right)^2 \cos^2 \phi \cos 2(\lambda - \lambda_{22}) \right] \\
 U = \frac{\mu_e}{r} & \left[ 1 + \frac{J}{3} \left( \frac{R_e}{r} \right)^2 (1 - 3 \sin^2 \phi) \right. \\
 & + \frac{H}{5} \left( \frac{R_e}{r} \right)^3 (3 \sin \phi - 5 \sin^3 \phi) \\
 & + \frac{D}{35} \left( \frac{R_e}{r} \right)^4 (3 - 30 \sin^2 \phi + 35 \sin^4 \phi) \\
 & \left. + 3J_{22} \left( \frac{R_e}{r} \right)^2 \cos^2 \phi \cos 2(\lambda - \lambda_{22}) \right]
 \end{aligned}$$

The fourth order term of the previous equation is sometimes written as follows:

$$+ \frac{K}{30} \left( \frac{R_e}{r} \right)^4 (3 - 30 \sin^2 \phi + 35 \sin^4 \phi)$$

(277x36525 - 27)

T 86164.10015<sub>d</sub>

$W_e(1975) = 7.292115042 \times 10^{-5}$

$W_e(1980) = 86164.10023$   
 $7.292115035 \times 10^{-5}$

$W_e(1985) = 86164.10031$

$7.292115029 \times 10^{-5}$

The associated definitions and constants are:

$\mu_e$  = gravitational parameter for the earth

$R_e$  = equatorial earth radius (gravitational)

$$J_2 = 1082.3 (\pm 0.2) \times 10^{-6} \text{ (ref. 2)}$$

$$J_3 = -2.3 (\pm 0.1) \times 10^{-6} \text{ (ref. 2)}$$

$$J_4 = -1.8 (\pm 0.2) \times 10^{-6} \text{ (ref. 2)}$$

$$\lambda_{22} = -21^\circ 0 (\pm 3^\circ 0)$$

$$J_{22} = 1.9 (\pm 0.2) \times 10^{-6}$$

$r$  = distance from the center of the earth to the vehicle

$\phi$  = declination of the vehicle

$\lambda$  = longitude of vehicle

$$J = 1.62345 (\pm 0.00030) \times 10^{-3}$$

$$H = -0.575 (\pm 0.025) \times 10^{-5}$$

$$D = 0.7875 (\pm 0.0876) \times 10^{-5}$$

$$K = 6.750 (\pm 0.075) \times 10^{-6}$$

$$C_{2,0} = -1.08230 (\pm 0.0002) \times 10^{-3}$$

$$C_{3,0} = 2.3 (\pm 0.1) \times 10^{-6}$$

$$C_{4,0} = 1.8 (\pm 0.2) \times 10^{-6}$$

Relations between the above are as follows:

$$J_2 = \frac{2}{3} J, J_3 = \frac{2}{5} H, J_4 = \frac{-4}{15}, K = -\frac{8}{35} D$$

$$J_2 = -C_{2,0}, J_3 = -C_{3,0}, J_4 = -C_{4,0}$$

## 4.2.2 LUNAR CONSTANTS

Earth-moon mass ratio (ref. 2)

$$M_e/M_m = 81.3015 (\underline{+0.0033})$$

Mean lunar radius (ref. 3)

$$R_m = 1.738\ 09 (\underline{+0.000\ 07}) \times 10^6 \text{ m}$$

$$R_m = 5.702\ 395 (\underline{+0.000\ 23}) \times 10^6 \text{ int. ft}$$

$$R_m = 2.725\ 06 (\underline{+0.000\ 011}) \times 10^{-1} \text{ e.r.}$$

Principal axes

$$a = 1.738\ 57 (\underline{+0.000\ 07}) \times 10^6 \text{ m}$$

$$b = 1.738\ 21 (\underline{+0.000\ 07}) \times 10^6 \text{ m}$$

$$c = 1.737\ 49 (\underline{+0.000\ 07}) \times 10^6 \text{ m}$$

where a is directed toward the center of the earth, c is coincident with the moon's rotational axis, and b is perpendicular to a and c.

Moments of inertia about principal rotational axes

$$A = 0.887\ 817\ 983\ 4 (\underline{+0.000\ 24}) \times 10^{35} \text{ kg-m}^2$$

$$B = 0.888\ 001\ 954\ 2 (\underline{+0.000\ 24}) \times 10^{35} \text{ kg-m}^2$$

$$C = 0.888\ 369\ 781\ 7 (\underline{+0.000\ 24}) \times 10^{35} \text{ kg-m}^2$$

Gravitational potential function The three forms in use follow with the associated constants. This model will be expanded when final Langley Lunar Orbiter data are available.

$$U = \frac{\mu_m}{r} \left[ 1 - \frac{J_2 R_m^2}{2r^2} (3 \sin^2 \phi - 1) + \frac{3 J_{22} R_m^2}{r^2} \cos^2 \phi \cos 2\theta \right]$$

$$U = \frac{\mu_m}{r} \left[ 1 + \frac{J}{3} \left( \frac{R_m}{r} \right)^2 (1 - 3 \sin^2 \phi) + L \left( \frac{R_m}{r} \right)^2 \cos^2 \phi \cos 2\theta \right]$$

$$U = \frac{\mu_m}{r} \left[ 1 + \frac{C_{2,0}}{2} \left( \frac{R_m}{r} \right)^2 (3 \sin^2 \phi - 1) \right]$$

$$+ 3 C_{2,2} \left( \frac{R_m}{r} \right)^2 \cos^2 \phi \cos 2\theta \left. \right]$$

$$J_2 = 2.071 \ 08 \ (\underline{+0.2}) \times 10^{-4}$$

$$J_{22} = 2.071 \ 60 \ (\underline{+0.6}) \times 10^{-5}$$

$$J = 3.106 \ 6 \ (\underline{+0.3}) \times 10^{-4}$$

$$L = 6.214 \ 8 \ (\underline{+1.8}) \times 10^{-5}$$

$$L = 3 J_{22} \text{ and } J = \frac{3}{2} J_2$$

$$C_{2,0} = -J_2 \text{ and } C_{2,2} = J_{22}$$

$(x, y, z)$  = selenographic position vector of the vehicle

$$\sin \phi = z/r, \quad \cos \phi = \sqrt{\frac{x^2 + y^2}{r^2}}$$

$$\cos \theta = x/\sqrt{x^2 + y^2}, \quad \sin \theta = \frac{y}{\sqrt{x^2 + y^2}}$$

$r$  = distance from the center of the moon to the vehicle

$$R_m = 1.738\ 09 \times 10^6 \text{ m}$$

Reference 5 contains preliminary values from the Lunar Orbiter. These preliminary results indicate that the potential functions must be expanded through fifth order and degree for study, and programs should be modified accordingly. A procedure and computer program is described in reference 6.

Rotational rate of the moon (ref. 1)

$$\omega_m = \frac{2\pi}{2360\ 591.545 + 0.014\ T} \text{ rad/sec}$$

where  $T$  is the number of Julian centuries of 36 525 days from 1900 January 0.5 UT.

$$\omega_m = 2.661\ 699\ 477 \times 10^{-6} \text{ rad/sec (1968-1970)}$$

$$\omega_m = 9.582\ 118\ 118 \times 10^{-3} \text{ rad/hr}$$

$$\omega_m = 1.525\ 041\ 464 \times 10^{-4} \text{ deg/sec}$$



Gravitational parameters for the moon  $(GM_m = \mu_m = \mu_{\text{moon}})$

$$\mu_{\text{moon}} = 4.902\ 778\ (+0.000\ 2) \times 10^{12}\ \text{m}^3/\text{sec}^2\ (\text{ref. 2})$$

$$\mu_{\text{moon}} = 1.731\ 399\ 71\ (+0.000\ 071) \times 10^{14}\ (\text{int. ft})^3/\text{sec}^2$$

$$\mu_{\text{moon}} = 2.448\ 837\ 57\ (+0.000\ 10) \times 10^{-1}\ (\text{e.r.})^3/\text{hr}^2$$

Mean distance of moon with respect to earth

$$3.844\ 020 \times 10^8\ \text{m}$$

$$6.026\ 84 \times 10^1\ \text{e.r.}$$

$$2.075\ 60 \times 10^5\ \text{n. mi.}$$

#### 4.2.3 GENERAL CONSTANTS

Astronomical unit (ref. 2)

$$\text{AU} = 1.495\ 990\ 00 \times 10^{11}\ \text{m}$$

Velocity of light in a vacuum

$$c = 2.997\ 925\ (+0.000\ 001) \times 10^8\ \text{m/sec}\ (\text{ref. 2})$$

$$c = 9.835\ 712\ (+0.000\ 0033) \times 10^8\ \text{int. ft/sec}$$

$$c = 4.700\ 294\ (+0.000\ 0016) \times 10\ \text{e.r./sec}$$

Gravitational parameters for the sun

$$\mu_{\text{sun}} = 1.327\ 154\ 45 \times 10^{20}\ \text{m}^3/\text{sec}^2\ (\text{ref. 2})$$

$$\mu_{\text{sun}} = 4.686\ 801\ 71 \times 10^{21}\ (\text{int. ft})^3/\text{sec}^2$$

$$\mu_{\text{sun}} = 6.628\ 865\ 68 \times 10^6\ (\text{e.r.})^3/\text{hr}^2$$

#### 4.3 EPHEMERIS TAPE SYSTEM

The ephemeris tape system to be used for Apollo missions is provided by JPL and is called the JPL Ephemeris Tapes Development Ephemeris 19 (DE 19). For additional information see reference 7.

The one sigma uncertainty for the radius vector of the moon with respect to the earth is one hundred meters.

The following values are used to convert the ephemeris tape units to km. (ref. 7)

$$AU = 149\,597\,900. \pm 200. \text{ km (Scale factor for planetary ephemerides.)}$$

$$b = 6378.1495 \pm 0.0020 \text{ km (Scale factor for lunar ephemeris.)}$$

$$M_e/M_m = 81.302 \pm 0.001 \text{ (Ratio of earth mass to moon mass.)}$$

#### 4.4 DRAG MODEL

##### 4.4.1 ATMOSPHERIC MODEL FOR APOLLO

The following atmospheric model for Apollo has been approved by the Apollo Program Director (ref. 1).

a. Launch atmosphere model for Cape Kennedy and Merritt Island, Florida:

1. The 1963 Patrick Atmosphere, which is described in reference 8, is to be used for the launch phase.

2. Expected deviations from this model for use in error analysis studies are given in reference 9.

b. The 1962 "U. S. Standard Atmosphere" (ref. 10) is to be used for the earth orbit and translunar phase.

c. Entry atmosphere model:

1. Above 90 km - 1962 U. S. Standard Atmosphere (ref. 10).

2. Below 90 km - Interim Supplemental Atmospheres (ref. 11).

##### 4.4.2 DRAG EQUATIONS

$$\ddot{\mathbf{R}}_D = -\frac{1}{2} C_D \rho (A/M) (\dot{\mathbf{R}} - \boldsymbol{\Omega} \times \mathbf{R}) \left| \dot{\mathbf{R}} - \boldsymbol{\Omega} \times \mathbf{R} \right|$$

or in component form:

$$\ddot{x}_D = -\frac{1}{2} C_D \rho (A/M) (\dot{x} + \omega y) v$$

$$\ddot{y}_D = -\frac{1}{2} C_D \rho (A/M) (\dot{y} - \omega x) v$$

$$\ddot{z}_D = -\frac{1}{2} C_D \rho (A/M) (\dot{z}) v$$

$$v = [(\dot{x} + \omega y)^2 + (\dot{y} - \omega x)^2 + \dot{z}^2]^{1/2}$$

where

$\ddot{x}_D, \ddot{y}_D, \ddot{z}_D$  = components of acceleration due to drag

$x, y, z$  = inertial position components of vehicle

$C_D$  = drag coefficient

$A$  = effective cross sectional area of vehicle

$M$  = mass of vehicle

$\rho$  = density of atmosphere at given altitude ( $z_1$ )

$\dot{R}$  = inertial velocity vector of vehicle

$R$  = position vector to vehicle from the center of earth

$\ddot{R}_D$  = acceleration vector due to drag

$\Omega$  = earth's rotational vector =  $(0, 0, \omega)$

$v$  = speed of vehicle with respect to rotating earth

$$z_1 = r - \frac{r}{d}$$

$$d = \left( \frac{x^2 + y^2}{a^2} + \frac{z^2}{b^2} \right)^{1/2}$$

$$r = (x^2 + y^2 + z^2)^{1/2}$$

$$a = 6.378\,178 \times 10^6 \text{ m}$$

$$b = 6.356\,797 \times 10^6 \text{ m}$$

for the ellipsoid used in the 1962 U. S. Standard Atmosphere.

The following values have been adopted for the drag model.

Drag coefficient

$$C_D = 2.0 \pm 0.2 \text{ (above 400 000 ft)}$$

Area

$$A = 129.4 \text{ ft}^2 \text{ (12.02 m}^2\text{)}$$

Mass

$$M = 280\ 000 \text{ lb (127\ 000 kg) (parking orbit) (for the lunar landing mission)}$$

$$M = 130\ 000 \text{ lb (59\ 000 kg) (after translunar thrust)}$$

$$M = 11\ 000 \text{ lb (5\ 000 kg) (reentry)}$$

Uncertainties in mass, area and density are included in the  $C_D$  uncertainty.

#### 4.5 FISCHER EARTH MODEL

The following constants describe the Fischer earth model (1960) which is used for the location of radar stations for Apollo (ref. 1).

Equatorial earth radius

$$a = 6.378\ 166\ 000 \times 10^6 \text{ m (exact)}$$

$$a = 2.092\ 574\ 147 \times 10^7 \text{ int. ft}$$

Flattening

$$f = \text{flattening} = 1 - b/a$$

$$f = 1/298.30$$

Polar earth radius

$$b = 6.356\ 784\ 284 \times 10^6 \text{ m}$$

$$b = 2.085\ 559\ 148 \times 10^7 \text{ int. ft}$$

Eccentricity of ellipsoid

$$e = \sqrt{\frac{a^2 - b^2}{a^2}}$$

$$e = 8.181\ 333\ 402 \times 10^{-2}$$

$$e^2 = 2f - f^2$$

$$e^2 = 6.693\ 421\ 623 \times 10^{-3}$$

4.6 BASIC EQUIVALENTS AND CONVERSION FACTORS

$$1 \text{ int. ft} = 3.048 \times 10^{-1} \text{ (exact) m (ref. 2)}$$

$$1 \text{ n. mi.} = 1.852 \text{ (exact) km (ref. 2)}$$

$$1 \text{ m} = 3.280\ 839\ 895\ 013\ 12 \text{ int. ft}$$

$$1 \text{ m}^2 = 1.076\ 391\ 041\ 670\ 97 \times 10 \text{ (int. ft)}^2$$

$$1 \text{ n. mi.} = 6.076\ 115\ 485\ 564\ 30 \times 10^3 \text{ int. ft}$$

$$1 \text{ U. S. Survey foot} = 3.048\ 006\ 096\ 012\ 192 \times 10^{-1} \text{ m}$$

$$1 \text{ int. stat. mi.} = 5.28 \times 10^3 \text{ (exact) int. ft}$$

$$\pi = 3.141\ 592\ 653\ 589\ 793\ 238\ 47 \text{ (ref. 1)}$$

$$1 \text{ deg} = 1.745\ 329\ 251\ 994\ 329\ 577 \times 10^{-2} \text{ rad}$$

$$1 \text{ rad} = 5.729\ 577\ 951\ 308\ 232\ 1 \times 10 \text{ deg}$$

$$1 \text{ lbm} = 4.535\ 923\ 7 \times 10^{-1} \text{ kg (exact)}$$

$$1 \text{ kg} = 2.204\ 622\ 621\ 848\ 78 \text{ lbm}$$

$$1 \text{ lbf} = 1 \text{ lbm} \times 3.2\ 174\ 048\ 556 \times 10 \text{ int. ft/sec}^2$$

$$1 \text{ km} = 1.567\ 849\ 060\ 035\ 292 \times 10^{-4} \text{ e.r.}$$

$$1 \text{ e.r.} = 6.378\ 165 \times 10^3 \text{ km (exact for scaling)}$$

$$1 \text{ km/sec} = 5.644 \ 256 \ 616 \ 127 \ 052 \times 10^{-1} \text{ e.r./hr}$$

$$1 \text{ e.r./hr} = 1.771 \ 712 \ 5 \text{ (exact) km/sec}$$

$$1 \text{ e.r./hr} = 5.812 \ 705 \ 052 \ 493 \ 438 \times 10^3 \text{ int. ft/sec}$$

$$1 \text{ int. ft/sec} = 1.720 \ 369 \ 416 \ 595 \ 526 \times 10^{-4} \text{ e.r./hr}$$

$$1 \text{ km} = 5.399 \ 568 \ 034 \ 557 \ 235 \ 42 \times 10^{-1} \text{ n. mi.}$$

#### 4.7 VENTING MODEL

There are three primary vent sources. They are the non-propulsive liquid hydrogen (LH) tank blowdown, the liquid oxygen (LOX) tank blowdown, and the LH low level continuous vent. The LOX blowdown is included in a maneuver table and the LH blowdown may be neglected.

The low level continuous vent occurs from insertion into earth parking orbit to CSM/S-IVB separation or injection. (ref. 12)

##### 4.7.1 S-V/S-IVB ULLAGE AND VENTING ACTION DURING EARTH ORBIT

<u>Seconds from Insertion</u>	<u>Disturbance Description</u>
0 - 360	Continuous LH <sub>2</sub> vent force along the roll axis with a constant thrust of 55-lb force with 1-σ uncertainty of 2-lb force.
360 - 2520	Continuous LH <sub>2</sub> vent force along the roll axis drops from 55-lb force to 22-lb force with a constant slope and a 2-lb force 1-σ uncertainty.
2520 - 16200	Continuous LH <sub>2</sub> vent force along the roll axis drops from 22-lb force to 15-lb force with a constant slope and a 2-lb force 1-σ uncertainty.

2088 - 2091  
 4320 - 4323  
 8280 - 8283

There will be three oxygen pressure relief ventings. Each will last about 3 seconds and will be of 150-lb thrust. These ventings will work off a pressure relief valve canted at  $22.7^\circ$  with respect to the vehicle roll axis. The resulting torque will be canceled by the attitude maneuvering system. A deflector may be added which may cause the cant angle to change from its current value.

#### 4.7.1.1 J2 - Second Ignition

Prior to J2 second ignition (translunar injection) there will be a 322-second ullage via the two 72-lb OAMS engines canted at  $10^\circ$  from the roll axis. This is followed by a J2 fuel lead (chill down) at 900-lb thrust for 5 seconds.

#### 4.7.2 VENTING EQUATIONS ( CONTINUOUS VENTING )

$$\ddot{R}_v = \frac{cgK}{w} \frac{(H \times R)}{hr}$$

where

$\ddot{R}_v$  is the venting acceleration in  $\text{ft}/\text{sec}^2$

$R, \dot{R}$  are position and velocity vectors of the vehicle

$$r = |R|$$

$$H = R \times \dot{R}$$

$$h = |H|$$

$w$  is the mass of the vehicle in pounds mass. This constant is also used in the drag equations.

$K$  is the vent thrust magnitude in pounds force.

$g = 32.174048$  and converts pounds mass to slugs

$c$  is the constant to convert  $\text{ft}/\text{sec}^2$  to units used for acceleration in the prediction program.

The magnitude of the vent is found from a linear interpolation of a small table of vent force magnitude versus time from insertion.

Current values for the vent table are given below.

t, hours from insertion	K, lbf
$t_1 = 0.0$	0.0
$t_2 = 0.0$	55.0
$t_3 = 0.7$	22.0
$t_4 = 4.5$	15.0
$t_5 = 4.51$	0.0
$t_6 = 4.52$	0.0
$t_7 = 4.53$	0.0
$t_8 = 4.54$	0.0
$t_9 = 4.55$	0.0
$t_{10} = 4.56$	0.0



4.8 REFERENCES

1. NASA M-DE-8020-008B, " Natural Environment and Physical Standards for the Apollo Program," April 1965.
2. Clarke, Victor C. Jr.,: Constants and Related Data for Use in Trajectory Calculations. Technical Report No. 32-604, California Institution of Technology, Pasadena, California, March 6, 1964.
3. Makemson, M. W.; Baker, R.M.L., Jr.; and Westrom, G. B.: Analysis and Standardization of Astrodynamic Constants. Journal of Astronautical Sciences, Vol. 8, No. 1, Spring 1961.
4. Kaula, William M.: A Review of Geodetic Parameters. Goddard Space Flight Center, Greenbelt, Maryland. Technical Note D-1847, May 1963.
5. Michael, William H., Jr.: Tolson, Robert H.; and Gapcynski, John P.: "Preliminary Results on the Gravitational Field of the Moon From Analysis of Lunar Orbiter Tracking Data', American Geophysical Union Annual Meeting, Langley Research Center. April 17-20, 1967.
6. Flanagan, Paul; and Austin, George: Perturbation Forces in the Lunar Gravitational Potential. MSC Internal Note No. 67-FM-76, June 7, 1967.
7. Lawson, C. L.: Announcement of JPL Development Ephemeris No. 19. Technical Memorandum No. 162, JPL, Section 314, April 13, 1967.
8. NASA TMX-53139, "A Reference Atmosphere for Patrick Air Force Base Florida, Annual (1963 Revision). (A Reference Atmosphere for Cape Kennedy Defined to 90 km - Extended to 700 km.)"
9. NASA TMX-53328, "Terrestrial Environment (Climatic) Criteria Guidelines for Use in Space Vehicle Development," May 1, 1966.
10. U. S. Government Printing Office: U. S. Standard Atmosphere, 1962.
11. Air Force Interim Supplemental Atmospheres to 90 Kilometers; Air Force Surveys in Geophysics No. 153.
12. Wood, C. C.: Variations in S-IVB/V Continuous Vent Thrust. MSFC Memorandum, December 15, 1966.

## 5.0 NAVIGATION AND COMMUNICATION SYSTEMS CHARACTERISTICS

### 5.1 INTRODUCTION

Several measuring systems exist for the determination of vehicle position and velocity. For the purpose of this document they are classified as being either onboard or ground based. This chapter is concerned with the measurement accuracy of these systems, the location accuracy of the ground-based systems, limitations in system coverage, system reliability, and the data transmission capability of the ground communication network. The ground-based systems discussed in this document consist of the MSFN and the three USBS DSN stations.

The conservative tracking and navigation system error estimates presented in this document are intended only for manned space flight analyses and are not to be construed as specifications.

### 5.2 ERROR MODEL AND ERROR SOURCES

#### 5.2.1 STATISTICAL ERROR MODEL - NOISE AND BIAS

In the ANWG statistical error model, errors are classified as either bias or noise. Bias errors are defined as those which are essentially time invariant during the time of observation. Typical biases are station location and time tagging errors. Noise errors are defined as those which vary appreciably during the time of observation and have an average value of zero. A typical source of Gaussian distributed noise is the thermal noise in electronic systems. The quantization error, which results from counting only an integral number of Doppler cycles, is an example of non-Gaussian distributed noise. In some cases the correlation between measurements is not negligible. (See, for example, section 5.4.3.2.)

### 5.2.2 GROUND-BASED SYSTEM ERROR SOURCES

The C-band radar and USBS errors presented in tables 5-I, 5-II, and 5-III include all tracking uncertainties with the exception of those associated with the following:

1. Station location, which is given in table 5-IV.
2. Velocity of light (section 4.2.3). The effects of the velocity of light uncertainty on orbit determination and error analysis are under study and are not included in the range and range-rate uncertainties given in this document.
3. Time tagging (section 5.3).
4. Atmospheric correction residuals (section 5.4.6).

### 5.2.3 ONBOARD SYSTEM ERROR SOURCES

Only estimates of errors due to equipment limitations are presented. Errors such as those associated with data processing and time tagging, which must also be considered for a proper error analysis, are not included. It is suggested that the bias on the observable be increased by 50 percent to account for these effects, and that the uncertainty in prediction be accounted for by increasing the uncertainty in the gravitational parameter,  $\mu$ , by 50 percent. There are several error sources which degrade the ground's knowledge of position and velocity through a burn. These include uncertainties associated with the vehicle platform, accelerometer, navigation system, and engine. The current error model assumes that the primary error sources can be attributed to platform misalignment and drift, accelerometer scale factor error, accelerometer bias, and uncertainties associated with specific engine impulse, mass, and mass flow. The platform and accelerometer errors are listed in section 5.5.2. The specific impulse and mass flow errors in the engines are listed in section 5.5.3.

The following is a list of navigation and propulsion system equipment which must be considered in any error analysis of onboard navigation system performance (ref. 1). The mass of the spacecraft must also be considered.

Following is the equipment for the CSM:

1. Sextant.
2. Scanning telescope (SCT).
3. Inertial measurement unit (IMU) accelerometers and gyros.
4. Service propulsion system (SPS).
5. Reaction control system (RCS).

The equipment for the LM consists of the following:

1. LM optical rendezvous system (LORS).
2. Rendezvous radar (RR).
3. Landing radar.
4. Alignment optical telescope (AOT).
5. Ascent engine.
6. Descent engine.
7. Backup inertial system.

The S-IVB engine has the IMU accelerometers and gyros.

### 5.3 TIME AND TIME TAGGING

#### 5.3.1 DEFINITIONS OF TIME<sup>a</sup>

##### 5.3.1.1 Ephemeris Time

Ephemeris time is the fundamental unit of time and is based on the period of orbital motion of the earth about the sun. Thus the time unit is in years. An ephemeris second is a subdivision of a period, or, in exact terms, it is  $31\,556\,925.9747^{-1}$  of the tropical year for 1900. A tropical year is the time required for the earth to rotate one revolution about the sun passing through the point of vernal equinox.

##### 5.3.1.2 Atomic Time

Atomic time is based on the time required to accumulate a fixed number of vibrational periods of transition frequency of atoms under a

---

<sup>a</sup>References 2 and 3.

prescribed condition. The frequency of the atomic transition and thus the period of the frequency or any multiple thereof is so constant that by comparison with the ephemeris time it takes at least a century to be certain of any atomic time variation.

The Twelfth General Conference of Weights and Measures, which met in October 1964, designated "an atomic or molecular frequency standard to be employed temporarily for the physical measurement of time" and further declared "that the standard to be employed is the transition between the hyperfine levels  $F = 4, m_f = 0$  and  $F = 3, m_f = 0$  of the fundamental state  $2S_{1/2}$  of the atom of cesium 133, not perturbed by external fields and that the value 9 192 631 770 Hertz is assigned to the frequency of this transition."  $F, m_f,$  and  $2S_{1/2}$  represent numbers which identify the quantum states and energy levels associated with a particular atomic transition, and hence with a particular spectral line (or frequency) of emission.

#### 5.3.1.3 Universal Time, or Greenwich Mean Time

Universal time (UT) is based on the earth's period of rotation about its axis. The fundamental time unit is thus in solar days. Since apparent solar days vary in length with the season, mean solar time was devised, and the tabulation of the difference between the apparent value and the mean value is called the equation of time. Because of its definition, universal time is dependent upon the observer's position, and thus a reference based on the prime meridian at Greenwich, England, was established. Universal time is therefore synonymous with Greenwich mean time (G.m.t.).

There are four kinds of universal time, namely:

- a. Universal time 0 (UT 0) is the uncorrected universal time or mean solar time.
- b. Universal time 1 (UT 1) is universal time corrected for polar variations and has a period of approximately 14 months. The correction is dependent on latitude.
- c. Universal time 2 (UT 2) is universal time corrected for seasonal as well as polar variations. The seasonal variations, which can vary from year to year, account for an excursion of approximately +30 msec.
- d. Universal time coordinated (UTC) is a time scale coordinated with atomic time to provide an approximation within +100 msec of UT 2. This time scale is an attempt to provide uniform universal time on a

yearly basis, since all other universal time scales are non-uniform. The Bureau International de L'Heure announces yearly the rate of change of UTC with respect to atomic time.

### 5.3.2 GROUND TIME TAGGING

The clocks associated with the tracking equipment of the MSFN, DSN, and tracking ships are synchronized by timing signals received from the National Bureau of Standards radio station WWV. WWV-transmitted time signals are derived from the United States Frequency Standard. This time is also referred to as UTC. In order to obtain UT 2, corrections have to be applied to UTC. The corrections are broadcast each hour, and the  $\sigma$  uncertainty of the corrections is 4.4 msec corresponding to a probable error of 3 msec (ref. 2). The  $\sigma$  synchronization uncertainty to WWV at the station is 3 msec, which includes radio wave propagation delay uncertainties. Thus, the uncertainty of synchronization at a station to UTC is 3 msec and to UT 2 is  $\sqrt{4.4^2 + 3^2} = 5.4$  msec. The uncertainty of synchronization between stations is  $3\sqrt{2} = 4.2$  msec.

At the ETR C-band radar sites, where the principal time synchronization source is loran C, the timing generators are synchronized to UT 2 within the following  $\sigma$  values: MLA, CNV, PAFB, GBI, and ANT, 10  $\mu$  sec; ASC and PRE, 5 msec (ref. 4). At present, timing accuracy data for SSI is not available. The corresponding  $\sigma$  uncertainties of synchronization to UTC are MLA, CNV, PAFB, GBI, GTI, and ANT, 4.4 msec; ASC and PRE, 6.6 msec. (Table IV identifies the call letters.)

### 5.3.3 ONBOARD TIME TAGGING

The navigation or tracking data transmitted to the ground are time tagged by the onboard guidance computer clock. The CM clock is synchronized to UTC prior to launch. The LM clock is synchronized to UTC by the MSFN prior to CM/LM separation. Each clock is resynchronized whenever it has drifted a prescribed amount,  $\Delta t$ , (currently 30 msec) from UTC. The onboard clocks are synchronized to the particular MSFN station in contact with the spacecraft. The ground has knowledge of onboard clock drift and can compensate for it, whereas the onboard computer cannot. It is expected that the allowable drift will be reduced below the present value of 30 msec.

In time tagging, the bias and noise errors due to truncation can be as large as 5 and 2.9 msec, respectively. An additional  $\sigma$  noise

error of 2.9 msec due to roundoff is introduced by the ground station (ref. 5). As indicated in section 5.3.2, the station time can have a bias up to 3 msec relative to UTC.

The onboard time tagging errors introduced by these error sources are thus:

	Bias, msec	Noise, msec
CM or LM relative to UTC	$\sqrt{3^2 + 5^2 + \Delta t^2}$	$2.9\sqrt{2} = 4.1$
CM relative to LM	$\sqrt{5^2 + \Delta t^2}$	$2.9\sqrt{2} = 5.8$

#### 5.4 THE MANNED SPACE FLIGHT NETWORK

##### 5.4.1 STATION LOCATIONS

The land-based station locations, site status and associated location uncertainties are presented in table 5-IV. The position and speed uncertainties associated with the tracking ships are given in table 5-V (ref. 6, 7, and 8).

##### 5.4.2 C-BAND RADARS

The C-band radars measure range, azimuth, and elevation. All radars use azimuth-elevation antenna mounts. Table 5-VI indicates which Apollo spacecraft either have carried or are scheduled to carry C-band transponders (ref. 9 and 10).

Table 5-I presents the range performance of the C-band radars operating against the particular spacecraft transponder and antenna systems associated with either the CM, LM, or IU (ref. 9 through 12). Skin tracking of the CM during reentry is also included. The following range limits are presented:

1. Maximum range for the listed tracking accuracy.
2. Maximum range for acquisition and tracking with degraded accuracy.
3. Maximum unambiguous range.

### 5.4.3 UNIFIED S-BAND SYSTEM

The USBS measures range, range rate, and two angles. The stations are equipped with either 85-ft or 30-ft diameter antennas. There are always two 85-ft stations located close together; one being a MSFN, the other, a DSIF station. The 85-ft antennas associated with either station can be utilized to simultaneously track two spacecraft. That is, each such 85-ft "dual site" employs two frequency-separated, receive-transmit links to permit simultaneous tracking and communication with two spacecraft provided both craft are within the antenna beam. Accurate angle data are obtained only for the spacecraft onto which the antenna is locked. As indicated in table 5-IV, some of the 30-ft antennas also have dual capability (ref. 13). The beacons and transponders carried on the spacecraft during the different missions are listed in table 5-VI (ref. 9, 10, and 13).

#### 5.4.3.1 Antenna Mounts

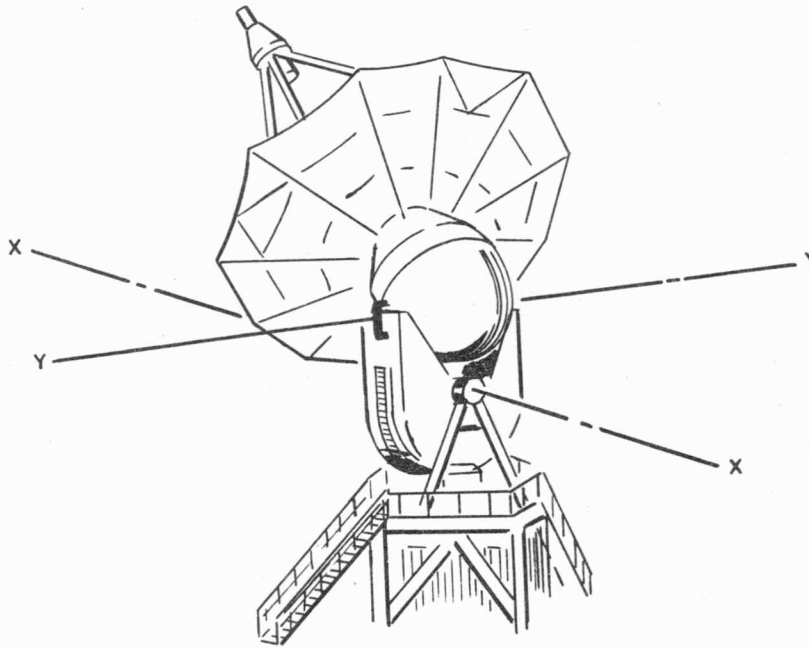
The land-based USBS antennas of the MSFN have X-Y mounts. The X and Y axes are perpendicular as shown in figure 5-1(a). These antennas cover a hemisphere with the exception of  $0^\circ$  to  $2^\circ$  elevation and a blind spot (keyhole) around the X axis, as shown in figure 5-1(b). Individual USBS site masking data (ref. 14) are now being collected by the Manned Space Engineering Section of GSFC. The results, which are to be published as a GSFC technical report, will be summarized in a future revision of this ANWG document. The 30-ft antennas [fig. 5-2(a)] have the X axis oriented north-south, the 85-ft antennas [fig. 5-2(b)] have the X axis oriented east-west. The X axis is always tangent to the earth's surface. The conversions from x and y angles to azimuth (Az) and elevation (El) angles are given by

$$\begin{array}{l} \text{30-ft antenna} \\ \text{85-ft antenna} \end{array} \left\{ \begin{array}{l} \sin \text{El} = \cos x \cos y \\ \tan \text{Az} = \sin x \cot y \\ \sin \text{El} = \cos x \cos y \\ \tan \text{Az} = - \frac{\tan y}{\sin x} \end{array} \right.$$

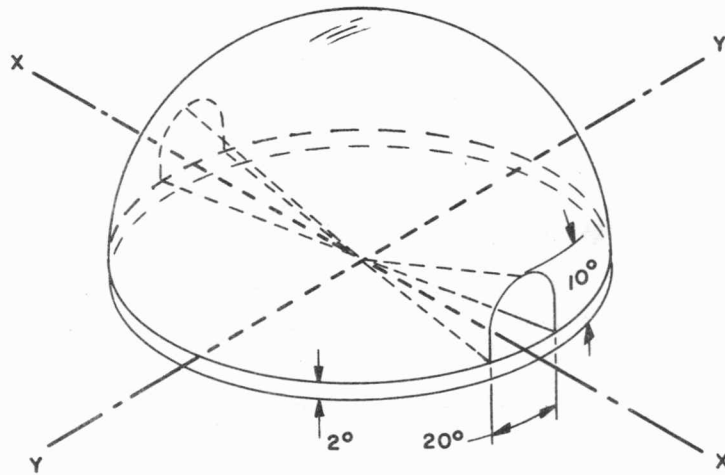
Positive x and y angles are as defined in figure 5-2 (ref. 15).

The DSIF 85-ft antennas employ polar (also referred to as hour-angle - declination) mounts where one of the two axes is always aligned parallel to the earth's rotational axis.



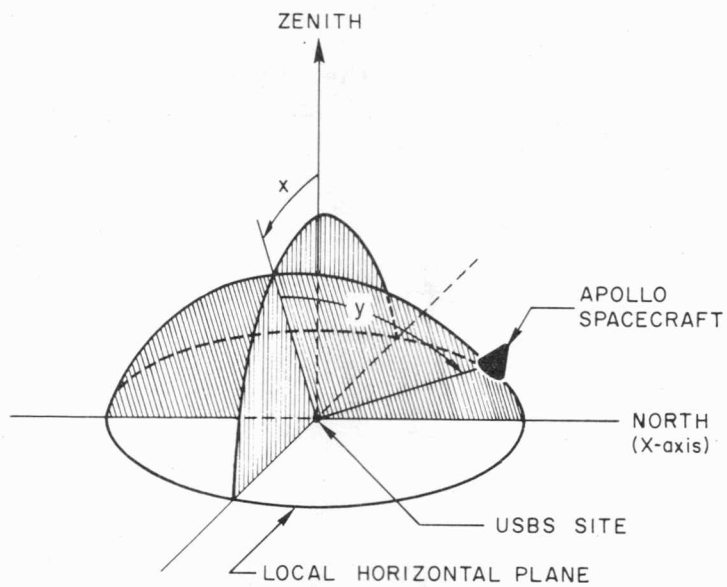


(a) X-Y axes

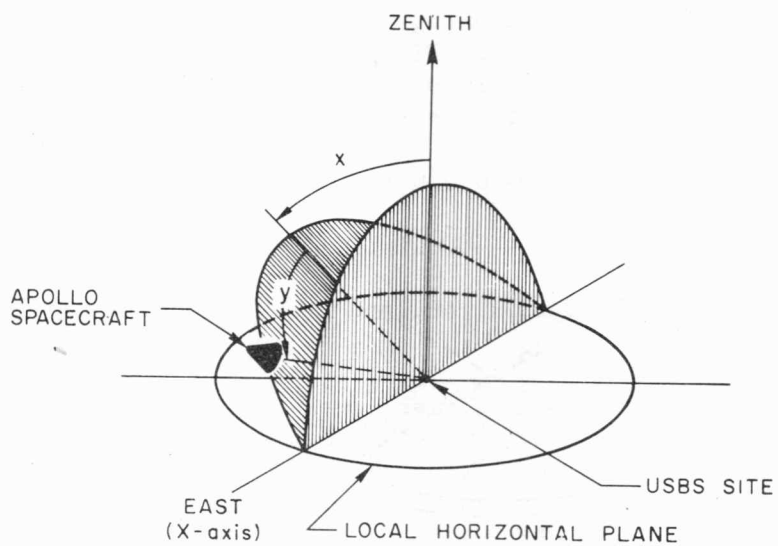


(b) Angular coverage for X-Y mount

Figure 5-1.- X-Y mount.



(a) 30-ft antenna



(b) 85-ft antenna

Figure 5-2.- Angle definitions for USBS X-Y antenna mounts.  
(Positive angles shown.)

The shipborne USBS antennas have azimuth-elevation (Az-El) mounts.

For the X-Y tracking antenna, the reference point for range measurements is the intersection of the Y axis with the radio frequency axis of the antenna (ref. 16). The X and Y axes cannot be made coincident, and an error in the measurement of range ( $r$ ) and range rate ( $\dot{r}$ ) will result due to the axis separation ( $b$ ).

This error, which cannot be calibrated out at the site, is given for the X-Y mount (MSFN) by:

$$\delta r = b \cos y$$

$$\delta \dot{r} = -b \dot{y} \sin y$$

where

$y$  = angle about the Y axis

$\delta r$  = range bias error due to axis separation

$\delta \dot{r}$  = range rate bias error due to axis separation

$b$  = axis separation

For polar as well as Az-El mounts, the antenna reference point is the intersection of the axis that is fixed with respect to the antenna surface and the radio frequency axis of the antenna (ref. 16). The error due to separation of axes with a polar mount (DSN) is given by

$$\delta r = b \cos D$$

$$\delta \dot{r} = -b \dot{D} \sin D$$

where  $D$  = declination angle and  $\delta R$ ,  $\delta \dot{R}$ , and  $b$  are as defined for the X-Y mount.

The separation between antenna axes (ref. 17, 18, and 19) is 8 ft for the MSFN 30-ft mount and 22 ft for the MSFN and DSN 85-ft mounts.

#### 5.4.3.2 Range Rate Measurements

The system is capable of measuring a change in range,  $\Delta r$ , during a finite time interval  $T$ . That is, the system measures an average range rate,  $\dot{r}$ , during the time interval,  $T$  (ref. 20).

$$\text{range rate} = \dot{r} = \frac{\Delta r}{T}$$

For brevity, the term "range rate," as used in this document will be taken to mean an average range rate.

The change in range,  $\Delta r$ , is measured by counting Doppler cycles plus the cycles of a superimposed bias frequency. Two counting methods are available.

5.4.3.2.1 Destructive N count.- The time,  $T$ , is measured for a predetermined constant number of Doppler-plus-bias cycles. Due to the superimposed bias frequency the measured time (integration time) is approximately 0.8 seconds and varies only slightly with changes in Doppler frequency. For this method no continuous Doppler count is obtained over a longer time period than 0.8 seconds and the quantization errors are negligible. The highest sampling rate with a 0.8-second integration time is 1 measurement per second. The destructive N-count can also be used with 0.08-second integration time, yielding a maximum sampling rate of 10 measurements per second.

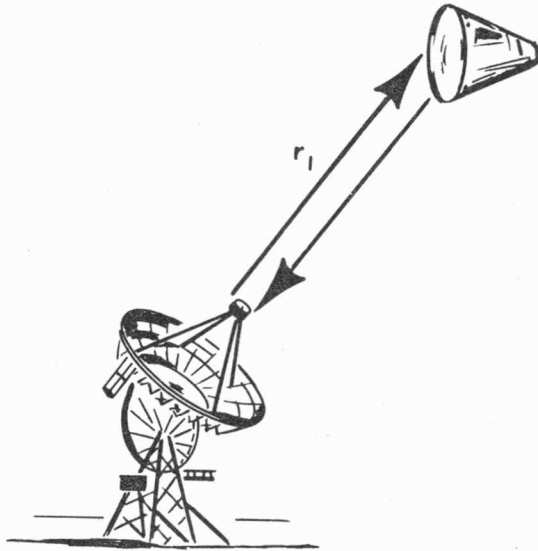
5.4.3.2.2 Nondestructive T count.- Doppler-plus-bias cycles are counted continuously and the counter is read out at constant time intervals  $T$  without destroying the information in the counter. The Doppler counter may be read out either one or ten times per second. Since the readout is nondestructive, lower sampling rates are obtained by discarding intermediate readouts.

Prior to overflow, the counter can accumulate 35 binary digits, corresponding to a total count time of 9 to 10 hours. The exact time to overflow depends on slant range. Since the 35 binary digits remain correct during overflow, the only effect is a measurement ambiguity. Both the low and the high speed data formats are capable of transmitting the 35 binary range rate digits (ref. 21). For this method a continuous Doppler count over longer time periods is obtained and the negatively correlated quantization errors are not negligible.

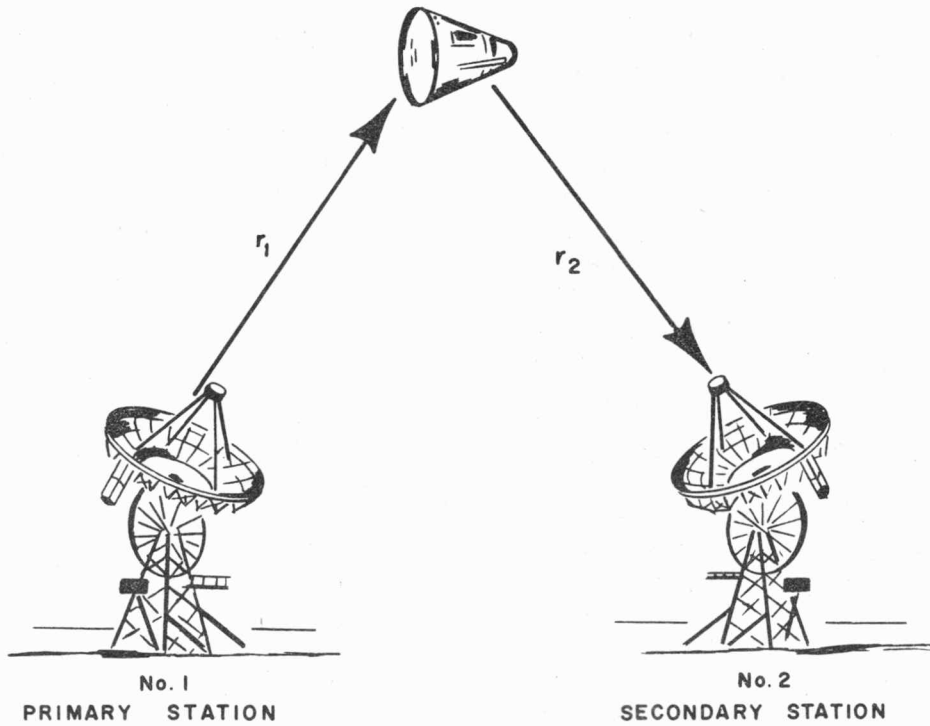
#### 5.4.3.3 Two- and Three-Way Doppler

The two basic modes of operation available are the two-way and the three-way modes indicated in figure 5-3. In the two-way mode a single station both transmits and receives the signal. The received signal is compared with the same oscillator that generated the transmitted signal.

In the three-way mode the primary station transmits the signal while the secondary station receives the signal. The received signal is compared with an oscillator at the secondary station. The signal is thus compared to an oscillator other than the one used for signal generation. Any frequency difference between the two oscillators shows up as a bias in the three-way Doppler.



(a) Two-way Doppler



(b) Three-way Doppler

Figure 5-3.- Two-way and three-way Doppler.

The two-way Doppler count is proportional to  $2\dot{r}_1$ , and the three-way Doppler is proportional (ref. 20) to  $(\dot{r}_1 + \dot{r}_2)$ . (Figure 5-3 defines  $\dot{r}_1$  and  $\dot{r}_2$ .) Three-way Doppler may be simultaneously obtained from more than one secondary station. A primary station can simultaneously obtain two-way Doppler.

#### 5.4.3.4 Range-Rate Uncertainties

5.4.3.4.1 Noise.— Three classes of noise are recognized: quantization noise, white phase noise, and random walk phase noise (ref. 22 and 23). The following discussions relate the classes of noise to the two Apollo USBS Doppler counting schemes.

5.4.3.4.1.1 Nondestructive T count: For the two-way Doppler mode with nondestructive T count the total  $1\sigma$  noise,  $\sigma(\dot{r}_1)$ , for  $\dot{r}_1$  is given for the land-based USBS by

$$\left[\sigma(\dot{r}_1)\right]^2 = \left[\left(\frac{0.09}{T}\right)^2 + \left(\frac{0.08}{T}\right)^2\right] (\text{ft/sec})^2 \quad (5-1a)$$

where

$\left(\frac{0.09}{T}\right)^2$  = the term due to the quantization error. The correlation coefficient  $\rho = -0.5$  for adjacent measurements and  $\rho = 0$  for nonadjacent measurements.

$\left(\frac{0.08}{T}\right)^2$  = the term due to random walk and white phase noise. The correlation coefficient  $\rho = -0.5$  for adjacent measurements and  $\rho = 0$  for nonadjacent measurements.

T = the count or integration time in seconds.

Equation (5-1a) assumes that the wave propagation time  $\tau_d < T$ .

For the case that  $\tau_D > T$  the total  $1\sigma$  noise is given by

$$\left[\sigma(\dot{r}_1)\right]^2 = \left(\frac{0.09}{T}\right)^2 + \left(\frac{0.08}{T}\right)^2 + \frac{(0.013)^2}{T} \quad (5-1b)$$

where the correlation properties for the first two terms are the same as above. The normalized autocorrelation function for the third term is shown in figure 5-4 (ref. 24).

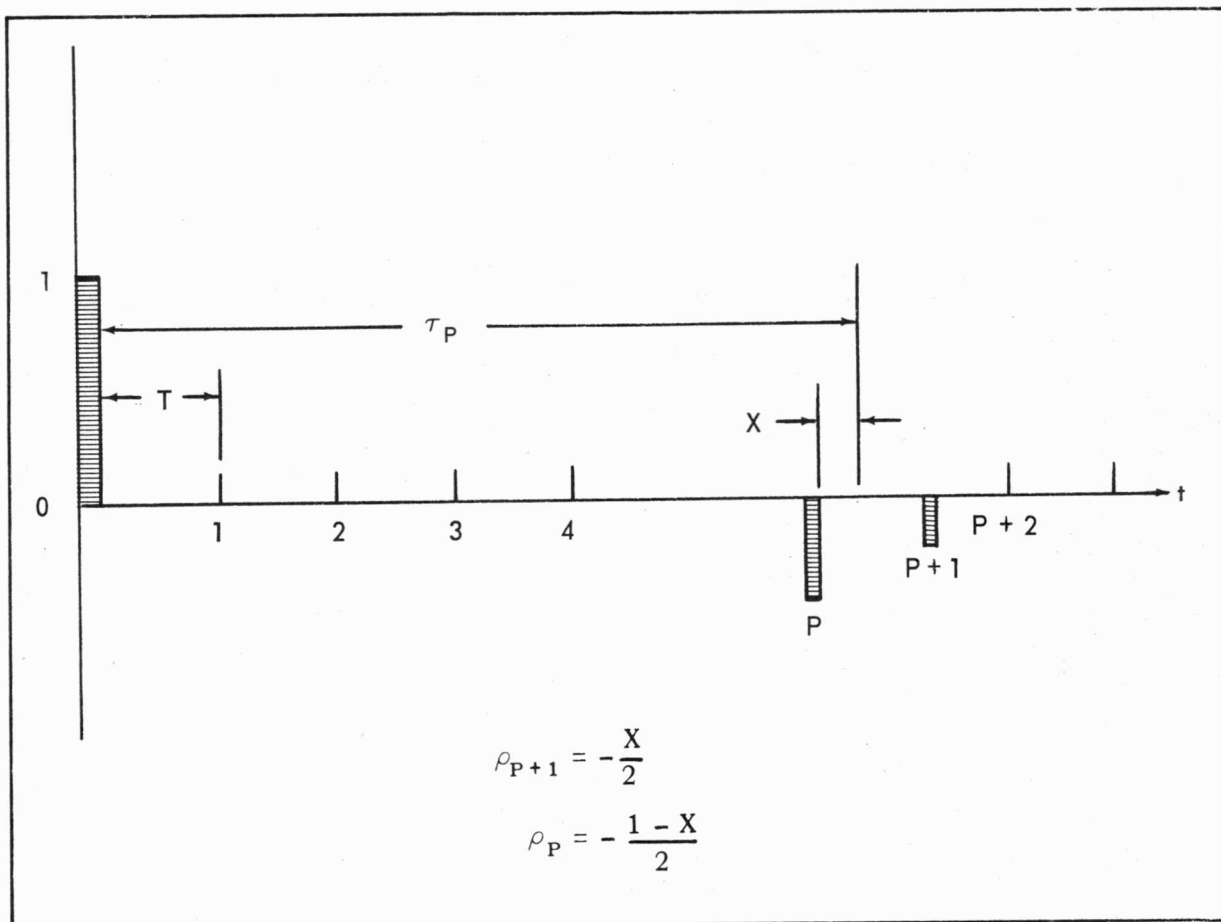


Figure 5-4.- Autocorrelation function for range rate noise due to the random walk phase noise in the oscillator.

For the shipborne USBS, a term is added to account for the noise resulting from antenna motion caused by the roll and pitch of the ship. Thus

$$\left[ \sigma(\dot{r}_1) \right]^2 = \left[ \left( \frac{0.09}{T} \right)^2 + \left( \frac{0.08}{T} \right)^2 + \left( \frac{0.5}{T} \right)^2 \right] (\text{ft/sec})^2 \quad (5-2a)$$

where the first two terms are identical to equation (5-1a) and where

$\left( \frac{0.5}{T} \right)^2$  = the term due to antenna motion of the ship. The correlation coefficient is  $\rho = -0.5$  for adjacent measurements and  $\rho = 0$  for nonadjacent measurements.

For the three-way Doppler mode (land-based USBS only) with non-destructive T count, the  $1\sigma$  noise,  $\sigma(\dot{r}_1 + \dot{r}_2)$ , for  $(\dot{r}_1 + \dot{r}_2)$  is given by

$$\left[\sigma(\dot{r}_1 + \dot{r}_2)\right]^2 = \left[\left(\frac{0.18}{T}\right)^2 + \left(\frac{0.13}{T}\right)^2 + \frac{(0.017)^2}{T}\right] (\text{ft/sec})^2 \quad (5-2b)$$

where

$\left(\frac{0.18}{T}\right)^2$  = the term due to quantization. The correlation coefficient is  $\rho = -0.5$  for adjacent measurements and  $\rho = 0$  for non-adjacent measurements.

$\left(\frac{0.13}{T}\right)^2$  = the term due to white noise. The correlation coefficient is  $\rho = -0.5$  for adjacent measurements and  $\rho = 0$  for non-adjacent measurements.

$\frac{(0.017)^2}{T}$  = the term due to random walk phase noise. The correlation coefficient for all measurements is  $\rho = 0$ .

T = the count or integration time.

5.4.3.4.1.2 Destructive N count: Quantization errors for destructive N count are negligible. "White" noise and random walk errors are the same as for nondestructive readout. The count time is approximately 0.08 or 0.8 seconds independent of sampling rate.

By equation (5-1) the two-way Doppler noise error is

$$\sigma(\dot{r}_1) = 0.10 \text{ ft/sec for } T = 0.8 \text{ sec}$$

or

$$\sigma(\dot{r}_1) = 1.0 \text{ ft/sec for } T = 0.08 \text{ sec}$$

and for the three-way mode

$$\sigma(\dot{r}_1 + \dot{r}_2) = 0.16 \text{ ft/sec for } T = 0.8 \text{ sec}$$

or

$$\sigma(\dot{r}_1 + \dot{r}_2) = 1.6 \text{ ft/sec for } T = 0.08 \text{ sec.}$$



Because of the time gap between measurements (approximately 0.2 seconds for a one-per-second sampling rate) the correlation coefficient for adjacent measurements is for all practical purposes zero.

5.4.3.4.2 Bias.- A conservative value for two-way Doppler bias is 0.03 ft/sec (1 cm/sec).

In the three-way Doppler mode the dominating bias source is the frequency difference between oscillators at the primary and secondary stations. A conservative estimate of the relative difference in oscillator frequency is  $2 \times 10^{-10}$ , which corresponds to a three-way Doppler bias of 0.2 ft/sec (6 cm/sec). The tracking errors and limitations for the USBS are compiled in table 5-III.

Except for extremely short observation times, the bias is the principal error source in orbit determination.

#### 5.4.4 ONBOARD ANTENNA COVERAGE

A priori acquisition information at the C-band sites normally permits spacecraft acquisition prior to an elevation pointing of  $5^\circ$ . Since the spacecraft has omnidirectional C-band antennas, no significant tracking interruptions are anticipated for all vehicles above the radio horizon.

USBS acquisition times are indicated in table 5-II. The spacecraft S-band omnidirectional antenna system is used prior to and during transposition and docking. In order to approximate spherical coverage both the CM and LM employ two "omnidirectional antenna" switch positions (ref. 10). Occasional loss of lock, necessitating reacquisition, can be anticipated as a result of antenna switching as well as antenna pattern nulls.

After transposition and docking the CSM high gain antenna is deployed. The coverage of the CSM and LM high gain antennas is indicated in figures 5-5 and 5-6, respectively (ref. 25). During this mission phase, frequent tracking and communication interruptions can be anticipated as a result of spacecraft rotation. One rotation each 24 minutes is expected (ref. 26). Since pointing procedures for the high gain antennas are not yet established, estimates of acquisition time are not included in this revision. Assuming spacecraft rotation and use of the high gain antenna, a conservative estimate for the periodic loss of tracking data is 9 minutes of interruption following each 15 minutes of satisfactory tracking.

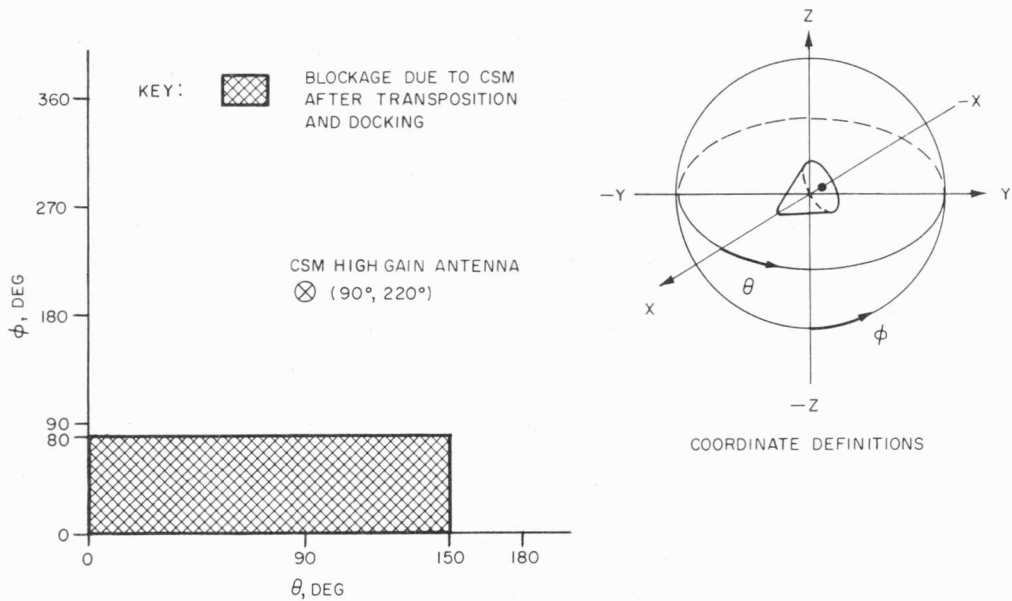


Figure 5-5.- High gain spacecraft (CSM) S-band antenna coverage.

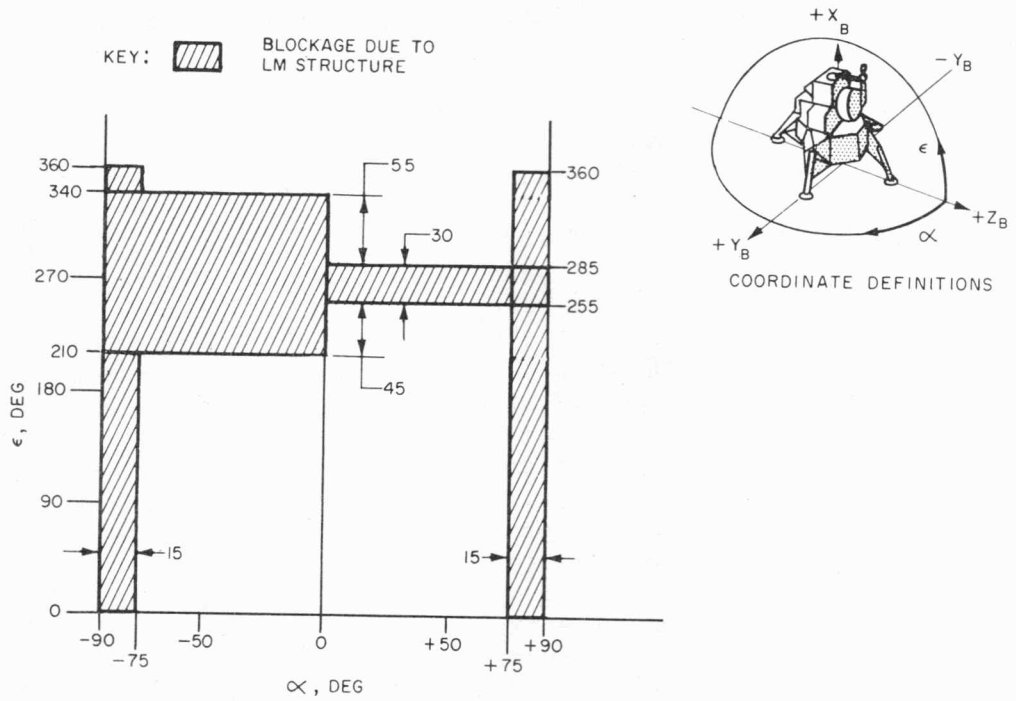


Figure 5-6.- LM S-band steerable antenna coverage in LM body coordinates (separated from CSM).

#### 5.4.5 APOLLO SHIPS

Table 5-VII indicates the class, designation, name, primary function, and tracking equipment associated with the Apollo instrumentation ships.

##### 5.4.5.1 C-band Radars

Range and angular accuracies for the shipborne C-band radars are listed in table 5-I.

##### 5.4.5.2 Unified S-band System

Range, range rate, and angular accuracies for the shipborne USBS are listed in table 5-III. Note that the errors listed include the ship's attitude errors.

##### 5.4.5.3 Navigation Accuracy

Position and speed errors for the ships are listed in table 5-V. The insertion ship in the Atlantic Ocean will be covered by the loran-C radio navigation system. Ships in other locations must rely on inertial or bathymetric navigation (ref. 27).

#### 5.4.6 ATMOSPHERIC CORRECTION

Tracking data will be corrected for the effects of the troposphere. Corrections for the effects of the ionosphere are not considered at this time. The atmospheric residual errors in range, range rate, and angles remaining after correcting for the effect of the troposphere are listed in table 5-VIII (ref. 28). These errors, which include the effects of the daytime ionosphere (i.e., a worst case), are for the following conditions:

1. Elevation angle  $\geq 5^\circ$ .
2. Height  $\geq 430$  n. mi. (800 km).
3. Average cloud cover.
4. Daily estimates of surface refractivity are assumed available for the tropospheric correction.

RECEIVED

JAN 14 1970

GEORGE SILVER 5-19

5.5 ONBOARD NAVIGATION SYSTEMS

5.5.1 COMMAND MODULE

5.5.1.1 Sextant

The sextant is a high magnification (28X), narrow field of view ( $1.8^\circ$ ) dual line of sight optical device on the Apollo CM. It is designed to determine the line of sight to a star, to an earth or lunar landmark, or to the LM. The sextant is also used to determine the angle between a star and an earth or lunar landmark, or between a star and the earth or lunar horizon. The estimated sextant angular errors for cislunar navigation (star-landmark, star-horizon) are the following.

1 $\sigma$  instrument noise = 0.05 mrad per axis

Instrument bias = 0.025 mrad per axis

The estimated sextant angular errors for unit vector determination with respect to the IMU (LM or landmark tracking and IMU alignment) are the following.

1 $\sigma$  instrument noise = 0.2 mrad per axis

Instrument bias = 0.2 mrad per axis

5.5.1.2 Scanning Telescope

The scanning telescope is a unity power, wide field of view ( $60^\circ$ ), single line of sight optical device. It is used for coarse acquisition prior to sighting with the sextant or for measurement of the line of sight with respect to the IMU. The estimated scanning telescope errors for unit vector determination with respect to the IMU are the following.

1 $\sigma$  instrument noise = 1.0 mrad per axis

Instrument bias = 1.0 mrad per axis

## 5.5.1.3 Command Module Stable Member (IMU)

1 $\sigma$  misalignment, per axis

Free fall = 0.2 mrad

Prelaunch, azimuth = 2.4 mrad

Vertical = 0.24 mrad

1 $\sigma$  gyro drift bias, per axis

Free fall = 0.52 mrad/hr

Powered flight<sup>a</sup> = 1.34 mrad/hr

1 $\sigma$  accelerometer bias, per axis

Bias = 0.067 cm/sec<sup>2</sup>

Scale factor = 116 ppm

## 5.5.1.4 Earth and Lunar Horizons

Earth horizon error<sup>b</sup>

1 $\sigma$  noise = 2.2 km

Bias = 3.0 km

Lunar horizon error<sup>b</sup>

1 $\sigma$  noise = 1.5 km

Bias = 0.7 km

---

<sup>a</sup>To simplify the calculation of drift rates and accelerometer errors at various attitudes, an average of 0.5g acceleration in each axis has been assumed. This assumption results in a simple, convenient model which is slightly more pessimistic than the exact mathematical models. However, a nominal SPS maneuver is made along one gyro/accelerometer axis within the alignment accuracy.

<sup>b</sup>These errors are functions of range. To determine total angular error, divide the kilometer error by the range to the horizon from the spacecraft.

## 5.5.1.5 VHF Ranging System

The VHF ranging system is a part of the CM navigation system and is used to determine the range to the LM during rendezvous navigation.

Slant range, n. mi.	Ranging only, ft	Ranging/voice, ft	Ranging only, ft	Ranging/voice, ft
	$1\sigma$ noise		Bias	
200	11	25	132	140
10	10	34	118	119

## 5.5.1.6 Command Module Reaction Control System (RCS)

Engine characteristics	Nominal value	$1\sigma$ error
Thrust, lb . . . . .	96	+1.20 -1.23
Specific impulse, sec . . . . .	272	$\pm 2.3$
Oxidizer to fuel mixture ratio . . . . .	2.09/1	+0.047 -0.040
Total propellant flow rate, lb/sec . . . . .	.353	$\pm 0.005$

These parameters are represented by a nominal value with a maximum and a minimum tolerance. The tolerances include engine-to-engine variation, instrumentation error, propellant inlet condition variations, and a propellant temperature range of 40° to 105° F.

## 5.5.1.7 Service Module Reaction Control System (RCS)

Engine characteristics	Nominal value	1 $\sigma$ error
Thrust, lb . . . . .	102.8	+1.13 -1.27
Specific impulse, sec . . . . .	277.3	+2.93 -4.53
Oxidizer to fuel mixture ratio . . . .	2.05/1	$\pm$ .043
Total propellant flow rate, lb/sec . . . . .	.371	+0.0047 -0.0040

These parameters are representative of nominal conditions. The tolerances include engine-to-engine variation, instrumentation, propellant inlet conditions variations, and a propellant inlet temperature range of 40° to 85° F.

## 5.5.1.8 Service Propulsion System (SPS)

The following data are the performance predictions and associated dispersions for the SPS engines.

Engine characteristics	Nominal value	1 $\sigma$ error
Thrust, lb . . . . .	20 880	$\pm 147.2$
Specific impulse, sec . . . . .	313.8	$\pm 1.193$
Oxidizer to fuel mixture ratio . . .	1.6/1	$\pm .008$
Oxidizer flow rate, lb/sec . . . . .	40.90	$\pm .238$
Fuel flow rate, lb/sec . . . . .	25.64	$\pm .184$
Tail-off impulse (dual bore engine), lb-sec . . . . .	13 500	$\pm 833.33$
Tail-off impulse, (single bore engine), lb-sec . . .	12 500	$\pm 833.33$



## 5.5.2 LUNAR MODULE

## 5.5.2.1 Lunar Module Stable Member (IMU)

1 $\sigma$  misalignment, per axis

Free fall = 0.33 mrad

Lunar surface = 0.46 mrad

1 $\sigma$  gyro drift bias, per axis

Free fall = 0.52 mrad/hr

Powered flight<sup>a</sup> = 1.34 mrad/hr

Lunar surface = 0.66 mrad/hr

1 $\sigma$  accelerometer, per axis

Bias = 0.067 cm/sec<sup>2</sup>

Scale factor = 100 ppm

## 5.5.2.2 Lunar Module Abort Guidance System (AGS)

The abort guidance system (AGS) is a backup guidance and navigation system to be used in the event of a primary guidance and navigation system failure. The system includes a computer along with gyros and accelerometers which are rigidly fastened to the vehicle body axes. The independent inertial system is aligned to the primary system prior to lunar ascent and descent and operates independent of the primary system during the entire lunar ascent and descent stages.

---

<sup>a</sup>To simplify the calculation of drift rates and accelerometer errors at various attitudes, an average of 0.5g acceleration in each axis has been assumed. This assumption results in a simple, convenient model which is slightly more pessimistic than the exact mathematical models. However, a nominal SPS maneuver is made along one gyro/accelerometer axis within the alignment accuracy.

5-21(a)

1σ misalignment

Overall PGNC errors per axis for coasting flight transmitted to AGS; includes the error between the ASA and IMU; does not include PGNC drift since last PGNC alignment

0.37 mrad

Overall PGNC errors per axis for the lunar surface transmitted to AGS; includes the error between the ASA and IMU; does not include PGNC drift since last PGNC alignment

0.51 mrad

1σ gyro drift bias, per axis

Free fall, X = 5.76 mrad/hr  
Y = 4.36 mrad/hr  
Z = 4.36 mrad/hr

Powered descent<sup>a</sup>, X = 5.06 mrad/hr  
Y = 5.76 mrad/hr  
Z = 5.41 mrad/hr

Powered ascent<sup>a</sup>, X = 5.93 mrad/hr  
Y = 6.63 mrad/hr  
Z = 6.46 mrad/hr

1σ accelerometer bias, per axis

Powered flight, 80 μg

Scale factor, 46 ppm

---

<sup>a</sup>To simplify the calculation of drift rates and accelerometer errors at various attitudes, an average of 0.5g acceleration in each axis has been assumed. This assumption results in a simple, convenient model which is slightly more pessimistic than the exact mathematical models. However, a nominal SPS maneuver is made along one gyro/accelerometer axis within the alignment accuracy.

## 5.5.2.3 Rendezvous Radar (With IMU)

Shaft and trunnion angles<sup>a</sup> (used to determine the line of sight direction)

Line of sight bias = 5 mrad

1 $\sigma$  line of sight noise as a function of range:

Range	1 $\sigma$ noise
400 n. mi. to 200 n. mi. . . . .	Varies linearly with range <sup>b</sup> from 1.7 mrad to 1 mrad
200 n. mi. to 5 n. mi. . . . .	Constant at 1 mrad
5 n. mi. to 1 n. mi. . . . .	Increases linearly from 1 mrad to 3.7 mrad with increasing range
1 n. mi. to 80 ft . . . . .	Constant at 3.7 mrad

## Range

1 $\sigma$  noise = greater of 0.33 percent of range and 27 feet

Bias = 170 feet for range greater than 50.8 n. mi.  
27 feet for range less than 50.8 n. mi.

## Range rate

1 $\sigma$  noise = greater of 0.43 percent of range rate and  
0.43 fps

Bias = 0.33 fps

<sup>a</sup>The angle bias errors specified in the PGNCs and AGS P&I specification include the error between the PGNCs navigation base and the RR and are the total vector sum of the errors per axis.

<sup>b</sup>The RR and PGNCs P&I specification random angle errors are different because of errors which result from vibrations between the RR base and the PGNCs navigation base. The random angle errors in the AGS P&I specification include the effects of RR display resolver errors, of tape display errors, and of astronaut readout errors. These errors are not present in RR data used by the PGNCs. The AGS random angle errors are not included for ranges less than 5 n. mi. because the AGS does not require RR data in this region.

## 5.5.2.4 Rendezvous Radar (With AGS)

The use of the RR in the AGS is similar to its use in the IMU (i.e., to track the CM during rendezvous navigation). The range and range rate are not read by the AGS automatically but rather are displayed on a tape meter on the LM displays. The crewman must read these data from the tape meters and insert them into the AGS.

Shaft and trunnion angles<sup>a</sup>

Line of sight bias = 5 mrad

1 $\sigma$  line of sight noise as a function of range as follows

Range	1 $\sigma$ noise
400 n. mi. to 200 n. mi. . . . .	2.7 mrad to 2.3 mrad <sup>b</sup>
200 n. mi. to 5 n. mi. . . . .	Constant at 2.3 mrad

Range rate

1 $\sigma$  noise = greater of 0.43 percent of range rate and 0.43 fps

1 $\sigma$  display error = 0.17 fps

Bias = 0.33 fps

Range

1 $\sigma$  random error as a function of range:

Range	Range random error	Display error
400 n. mi. to 10 n. mi.	Greater of 0.083% of range and 300 ft	0.33 n. mi.
10 n. mi. to 5 n. mi.	300 ft	17 ft
5 n. mi. to 1000 ft	Greater of 0.33% of range and 80 ft	17 ft
1000 ft to 80 ft	80 ft	1 ft

Bias = 27 feet for range less than 50.8 n. mi.

Bias = 170 feet for range greater than 50.8 n. mi.

<sup>a</sup>See footnote a for section 5.5.2.3.

<sup>b</sup>See footnote b for section 5.5.2.3.

## 5.5.2.5 Lunar Module Reaction Control System (RCS)

Preliminary studies by Power and Propulsion Division at MSC indicate that the LM RCS engine performance is the same as the SM RCS engine performance.

Engine characteristics	Nominal value	1 $\sigma$ error
Thrust, lb . . . . .	102.8	+1.13 -1.27
Specific impulse, sec . . . . .	277.3	+2.93 -4.53
Oxidizer to fuel mixture ratio . . . . .	2.05/1	$\pm$ 0.043
Total propellant flow rate, lb/sec . . . . .	0.371	+0.0047 -0.0040

## 5.5.2.6 Lunar Module Ascent Propulsion System (APS)

The following data are for the performance predictions and associated dispersions for the class of APS engines.

Engine characteristics	Nominal value	1 $\sigma$ error
Thrust, lb . . . . .	3463	$\pm$ 40.4
Specific impulse, sec . . . . .	309.3	$\pm$ 1.51
Oxidizer to fuel ratio . . . . .	1.601/1	$\pm$ 0.0054
Oxidizer flow rate, lb/sec . . . . .	6.89	$\pm$ 0.074
Fuel flow rate, lb/sec . . . . .	4.303	$\pm$ 0.045
Tail-off impulse, lb-sec . . . . .	299.0	$\pm$ 68.0

## 5.5.2.7 Lunar Module Descent Propulsion System (DPS)

The following table presents the best data available at this time; these data are to be used for all dispersions analyses until better data are available. Preliminary LM-3 DPS performance summary data are presented. Data applicable to all DPS engines is expected soon; however, because this is the only data available at present, it will have to suffice until that time. Tail-off uncertainty will be determined when the DPS data become available.

Engine characteristics	Nominal	1 $\sigma$ error
Engine at fixed throttle point (FTP)		
Thrust, lb . . . . .	9903	$\pm 44.8$
I <sub>sp</sub> , sec . . . . .	301.8	$\pm 1.36$
Mixture ratio . . . . .	1.581/1	$\pm .009$
Total propellant flow rate, lb/sec . . . . .	32.82	$\pm .132$
Engine at 40% FTP		
Thrust, lb . . . . .	4214	--
I <sub>sp</sub> , sec . . . . .	295.0	--
Fuel oxidizer ratio . . . . .	1.602/1	--
Total propellant flow rate, lb/sec . . . . .	14.29	--
Engine at 25% FTP		
Thrust, lb . . . . .	2645	$\pm 25.4$
I <sub>sp</sub> , sec . . . . .	293.5	$\pm 2.57$
Fuel-to-oxidizer ratio . . . . .	1.617/1	$\pm .008$
Total propellant flow rate, lb/sec . . . . .	9.01	$\pm .03$
Engine at 11.5% FTP		
Thrust, lb . . . . .	1197	$\pm 11.0$
I <sub>sp</sub> , sec . . . . .	289.7	$\pm 2.41$
Fuel-to-oxidizer mixture ratio . . . . .	1.619/1	$\pm .008$
Total propellant flow rate, lb/sec . . . . .	4.14	$\pm .014$

The estimated range rate ( $1\sigma$ ) errors are

- a. Noise = 0.4 percent of range rate or 0.4 ft/sec, whichever is greater
- b. Bias = 0.3 ft/sec

The angle errors are

- a. Noise due to shaft = 0.33 mrad
  - b. Noise due to trunnion = 0.28 mrad
  - c. Bias due to shaft =  $-1.33 + 0.00428\beta + 0.03 \sin \omega t$  (mrad)
  - d. Bias due to trunnion =  $2.42 - 0.018\beta - 0.1 \sin \omega t$  (mrad)
- where  $\beta$  is the shaft angle (deg) and  $\omega$  is the angle rate, i.e.,

$$\omega = \frac{9 \pi}{60 - \beta} \text{ (rad/min).}$$

The angular bias is solved for by the LM onboard filter program.

## 5.5.2 INERTIAL SENSORS

### 5.5.2.1 Inertial Measurement Unit

The  $1\sigma$  errors for the accelerometers and gyros are classified, but they can be obtained from the following references:

CSM IMU . . . . .	references 32 and 33
LM IMU . . . . .	reference 30 or 32
S-IVB IMU . . . . .	reference 32 or 34

### 5.5.2.2 Inertial Measurement Instruments Associated

with the Abort Guidance System

The abort guidance system (AGS) is a backup inertial measurement system to be used by the LM guidance computer in the event of a LM IMU failure. The system includes gyros and accelerometers which are rigidly aligned to the vehicle body axes rather than mounted on a stabilized platform. This system is aligned with the primary guidance and navigation

system before descent to the lunar surface and again prior to ascent. It will navigate throughout the LM's descent and ascent independent of the primary system.

The estimated backup LM IMU <sup>(AGS)</sup> Gaussian errors about each axis are given below.

- a. Accelerometer bias =  $90 \times 10^{-4}$  percent of measured acceleration
- b. Accelerometer scale factor error =  $410 \times 10^{-4}$  percent of measured acceleration
- c. AGS timing error =  $\left[67 + (10.3t)^2\right]^{1/2}$  (min) where t = time in hours to previous PGNCs IMU alignment
- d. Gyro drift (coast phase) = 0.52 deg/hr (inflight calibration)  
= 0.81 deg/hr (prelaunch calibration)
- e. Gyro drift (boost phase) = 1.02 deg/hr (inflight calibration)  
= 1.20 deg/hr (prelaunch calibration)  
See ref. 35.

### 5.5.3 ENGINE CHARACTERISTICS

The engine characteristics, specific impulse and mass flow, may be found in the following references:

RCS of the CM, SM, and LM . . . . .	reference 32 or 36
SMRCS . . . . .	reference 33
LM ascent engine . . . . .	reference 32 or 36
LM descent engine . . . . .	reference 32
S-IVB engine . . . . .	reference 32 or 34

In all cases total vehicle mass can be determined to within 0.25 percent prior to launch and 0.5 percent thereafter.



## 5.6 LUNAR LANDMARKS AND AGC STAR CATALOGUE

### 5.6.1 LUNAR LANDMARKS

Table 5-IX presents ten lunar landmarks and the corresponding lo uncertainties in both the horizontal and vertical components of the associated position vector references to the center of a spheroidal moon with mean radius of 938.5 n. mi. (1738 km). (See ref. 37.) The ten lunar landmarks, which have been recommended for optical sightings by the Lunar Surface Technology Branch of the MSC, lie within approximately  $\pm 5^\circ$  of the lunar equator. The number of lunar landmark uncertainties indicated in table 5-IX are expected to be reduced as knowledge of the lunar surface is improved by means of the current Langley Lunar Orbiter mapping missions.

### 5.6.2 AGC STAR CATALOGUE

Table 5-X is the AGC star catalogue referenced to 1967.0.

## 5.7 COMMUNICATION SYSTEMS

### 5.7.1 APOLLO SATURN NASCOM NETWORK

Figure 5-7 indicates that portion of the NASCOM network which will handle the relay of tracking and communication data during the forthcoming Apollo missions. The first letter of the four letter station designations in figure 5-7 is a prefix indicating the general location of the nearest switching center. The next three letters are the usual station call letters such as those of the tracking sites indicated in table 5-IV (ref. 38). Those stations which currently possess no tracking capability but are capable of voice communication and/or VHF telemetry reception and recording as required include Tananarive, Nigeria, and Canton Island. Details of the NASCOM network implementation, operation, and scheduling can be obtained in reference 39, which is updated on a regular basis.

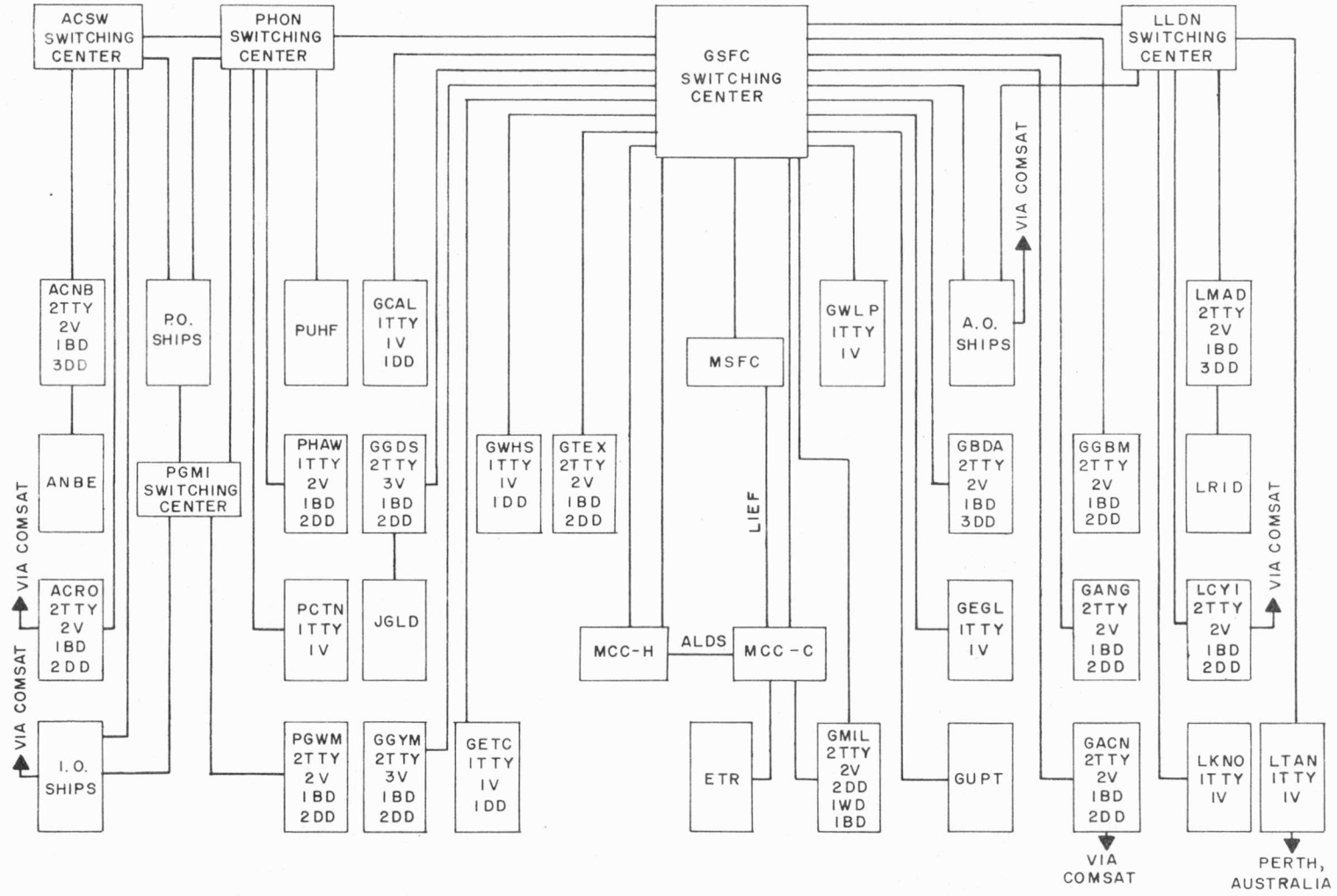


Figure 5-7.- Apollo/Saturn NASCOM communications network.

The communication capacity referred to in figure 5-7 is described below:

- a. Teletype (TTY) - 60 words/min and 100 words/min
- b. Voice (V) - 0.3 to 3.0 kHz bandwidth
- c. Biomedical data (BD) - 0.3 to 3.0 kHz
- d. High speed digital data (DD) - 2400 bit/sec except 600 to 1200 bit/sec via HF links for ASC and Apollo ships
- e. Wideband (WD) - 40.8 kbit/sec

For tracking data rates refer to section 5.7.2. For tracking station call letters refer to table 5-IV. The NASCOM prefixes are A, Australia; P, Pacific; L, London; and G, Goddard.

The following list defines the abbreviations used in figure 5-7.

- a. ACSW - NASCOM switching center at Canberra
- b. ALDS - Spollo Launch Data System
- c. A.O. Ships - Atlantic Ocean Ships. One insertion ship (3TTY, 3BD) is tentatively located in the Atlantic Ocean. Communication satellite instrumentation will provide an alternate communications path (2TTY, 2V, BD, 3DD) between the ship and the MCC-H.
- d. ETR - Eastern test range. Includes C-band radars in CNV, MLA, PAT, GBI, SSI, GTK, ANT, ASC, and PRE.
- e. GSFC - Goddard Space Flight Center
- f. GUPT - Patrick Air Force Base, DOD/NASCOM tentative interface point for Apollo aircraft communications.
- g. I.O. Ships - Indian Ocean Ships. One injection ship (2TTY, 3BD) and one CSQ-type ship (2TTY, 1BD) are tentatively located in the Indian Ocean. Communication Satellite instrumentation will provide an alternate communication path (2TTY, 2V, 1BD, 3DD) between the ship and MCC-H.
- h. LIEF - Launch Information Exchange Facility

- i. LLDN - NASCOM switching center in London, England
- j. MCC-C - Mission Control Center-Cape Kennedy
- k. MCC-H - Mission Control Center-Houston
- l. MSFC - Marshall Space Flight Center
- m. PGMI - NASCOM switching center at Guam
- n. PHON - NASCOM switching center at Honolulu
- o. P.O. Ships - Pacific Ocean Ships. One injection ship (2TTY, 3BD), two reentry ships (2TTY, 1BD) and one RKV-type ship are tentatively located in the Pacific Ocean. Communication satellite instrumentation on the injection ship will provide an alternate communication path (2TTY, 2V, 1BD, 3DD) between the ship and MCC-H.
- p. PUHF - Hickam Air Force Base DOD/NASCOM interface tentative interface point for Apollo aircraft communications.

#### 5.7.2 DATA FRAME RATES

The data frame rates for USBS are

- a. High speed format - 240 bits/frame which, except for ASC and ships, can be transmitted at 10, 5, 2.5, and 1 frame/sec. From ASC: 5, 2.5, or 1 frame/sec.
- b. Low speed format data word rates are selectable at 1 per 6 sec, 1 per 10 sec, 1 per 30 sec, 1 per min, and 1 per 10 min.

The rates for C-band are

- a. High speed format - 240 bits/frame only available from BDA and CRO. Frame rates are 10 per sec and 5 per sec.
- b. Low speed - 100 words/min from ETR  
- 60 words/min MSFN

Ships USBS and C-band (ref. 39) have the following rates:

- a. High speed data - two state vectors per second during powered flight. One state vector per 2 seconds during free flight. No high speed data during reentry.
- b. Low speed data - one state vector per 6 seconds.

### 5.7.3 SYSTEM RELIABILITY

An estimate of future MSFN performance may be inferred from the network's performance during the Gemini missions. Table 5-XI presents a summary of the average downtime of the Gemini ground system during Gemini flights 9 through 12 (ref. 40).

TABLE 5-1.- C-BAND RADAR TRACKING ACCURACIES AND LIMITATIONS

Station	Type of C-band radar	Angular tracking limits				Tracking accuracies						Maximum range						Unambiguous range, n. mi.
		Azimuth		Elevation		Azimuth		Elevation		Range		High accuracy <sup>a</sup>			Degraded accuracy			
		Angle limit, deg	Maximum angular rate deg/sec	Angle limit, deg	Maximum angular rate deg/sec	Noise, mrad	Bias, mrad	Noise, mrad	Bias, mrad	Noise, ft	Bias, ft	IU, n. mi.	CM, n. mi.	LM, n. mi.	IU, n. mi.	CM, n. mi.	LM, n. mi.	
CNV	FPS-16	360	42	-10 to 190	22	0.2	0.4	0.2	0.4	30	60	4 800	3 000	700	15 000	9 500	2 300	1 000
MLA	TPQ-18	360	28	-2 to 85	28	0.15	0.3	0.15	0.3	20	40	16 500	10 300	2 500	52 100	32 500	7 800	32 000
PAFB	FPQ-6	360	28	-2 to 85	28	0.15	0.3	0.15	0.3	20	40	16 500	10 300	2 500	52 100	32 500	7 800	32 000
GBI	FPS-16	360	42	-10 to 190	22	0.2	0.4	0.2	0.4	30	60	1 900	1 200	300	6 000	3 700	900	1 000
	TPQ-18	360	28	-2 to 85	28	0.15	0.3	0.15	0.3	20	40	16 500	10 300	2 500	52 100	32 500	7 800	32 000
SSI	FPS-16	360	42	-10 to 190	22	0.2	0.4	0.2	0.4	30	60	1 900	1 200	300	6 000	3 700	900	1 000
GTI	TPQ-18	360	28	-2 to 85	28	0.15	0.3	0.15	0.3	20	40	16 500	10 300	2 500	52 100	32 500	7 800	32 000
ANT	FPS-6	360	28	-2 to 85	28	0.15	0.3	0.15	0.3	20	40	16 500	10 300	2 500	52 100	32 500	7 800	32 000
BDA	FPS-16	360	42	-10 to 190	22	0.2	0.4	0.2	0.4	30	60	2 800	1 800	400	8 800	5 500	1 300	32 000
	FPQ-6	360	28	-2 to 85	28	0.15	0.3	0.15	0.3	20	40	9 500	6 000	1 400	30 000	19 000	4 500	32 000
CYI	MPS-26	360	56	0 to 89.5	28	1.0	2.0	1.0	2.0	60	120	2 150	1 350	340	6 600	4 100	1 000	2 500
ASC	TPQ-18	360	28	-2 to 85	28	0.15	0.3	0.15	0.3	20	40	16 500	10 300	2 500	52 100	32 500	7 800	32 000
	FPS-16	360	42	-10 to 190	22	0.2	0.4	0.2	0.4	30	60	1 900	1 200	300	6 000	3 700	900	1 000
PRE	MPS-25	360	42	-10 to 190	22	0.2	0.4	0.2	0.4	30	60	3 500	2 200	520	11 500	7 200	1 700	1 000
CRO	FPQ-6	360	28	-2 to 85	28	0.15	0.3	0.15	0.3	20	40	16 500	10 300	2 500	52 100	32 500	7 800	32 000
WOM	FPS-16	360	42	-10 to 90	22	0.2	0.4	0.2	0.4	30	60	1 900	1 200	300	6 000	3 700	900	500
HAW	FPS-16	360	42	-10 to 190	22	0.2	0.4	0.2	0.4	30	60	6 800	4 250	1 000	21 500	13 500	3 200	32 000
CAL	FPS-16	360	42	-10 to 190	22	0.2	0.4	0.2	0.4	30	60	6 800	4 250	1 000	21 500	13 500	3 200	32 000
WHS	FPS-16	360	42	-10 to 190	22	0.2	0.4	0.2	0.4	30	60	4 800	3 000	700	15 000	9 500	2 300	32 000
EGL	FPS-16	360	42	-10 to 190	22	0.2	0.4	0.2	0.4	30	60	1 900	1 200	300	6 000	3 700	900	200
Insertion and injection ships <sup>b</sup>	FPS-16 (V)	360	45	-10 to 70	25	0.4	0.8	0.4	0.8	30	60	3 500	2 200	520	11 500	7 200	1 700	32 000
Reentry ship T-AGM-6 <sup>b,c</sup> Watertown	CAPRI	360	48	-10 to 85	28	0.4	0.8	0.4	0.8	30	60	--	80	--	--	140	--	4 000
Reentry ship <sup>b,c</sup> T-AGM-7 Huntsville	Modified CAPRI	360	48	-10 to 85	28	0.4	0.8	0.4	0.8	30	60	--	200	--	--	350	--	4 000

<sup>a</sup>No C-band beacon aboard CM or LM beyond Mission 503, IU jettisoned at 6200 n. mi. altitude. High accuracy S/N = 20 db. Degraded accuracy S/N = 10 db.

<sup>b</sup>Includes ship attitude errors.

<sup>c</sup>Skin track of CM during reentry; target cross-section = 1 m<sup>2</sup>

TABLE 5-II.- USBS TRACKING ERRORS AND LIMITATIONS

(a) Acquisition time after spacecraft illumination. (Elevation  $\geq 5^\circ$ .)

Spacecraft antenna (a)	Angles, sec	Range rate, sec	Range, sec	Telemetry, sec
Omnidirectional	30	25	30	15

(b) Maximum angular tracking rate

Rate, deg/sec			30 ft Ship insertion and injection, deg/sec (b)		12 ft Ship reentry, deg/sec (b)	
30 ft MSFN	85 ft MSFN	85 ft DSIF	Azimuth	Elevation	Azimuth	Elevation
4	3	0.8	50	30	50	30

<sup>a</sup>No information currently available for LM or CSM high gain antenna.

<sup>b</sup>See reference 41.

TABLE 5-II.- USBS TRACKING ERRORS AND LIMITATIONS - Concluded

(c) Maximum tracking ranges using 20W transponder mode

Ground antenna	Measurements taken	CSM or LM omnidirectional antenna, n. mi.	CSM high gain antenna, n. mi.		LM high gain antenna, n. mi.
			Beamwidth = 4.6°	Beamwidth = 68°	Beamwidth = 13°
30 ft 85 ft	Range <sup>a</sup>	4.3 × 10 <sup>4</sup> 9.1 × 10 <sup>4</sup>	1.4 × 10 <sup>6</sup> 3.0 × 10 <sup>6</sup>	1.3 × 10 <sup>5</sup> 2.7 × 10 <sup>5</sup>	4.6 × 10 <sup>5</sup> 9.8 × 10 <sup>5</sup>
30 ft 85 ft	Range rate and angles <sup>b</sup>	1.9 × 10 <sup>5</sup> 4.0 × 10 <sup>5</sup>	6.3 × 10 <sup>6</sup> 1.3 × 10 <sup>7</sup>	5.6 × 10 <sup>5</sup> 1.2 × 10 <sup>6</sup>	2.1 × 10 <sup>6</sup> 4.3 × 10 <sup>6</sup>
30 ft 85 ft	Range rate and angles <sup>c</sup>	4.3 × 10 <sup>5</sup> 9.1 × 10 <sup>5</sup>	1.6 × 10 <sup>7</sup> 3.0 × 10 <sup>7</sup>	1.3 × 10 <sup>6</sup> 2.7 × 10 <sup>6</sup>	4.6 × 10 <sup>6</sup> 9.8 × 10 <sup>6</sup>

<sup>a</sup>Using range code modulation only. The range will be less if other modulation is added. The ranges given are based upon minimum required signal at MSFN for 99.6 percent probability of acquisition in 9 seconds.

<sup>b</sup>Using maximum modulation (range code, voice, telemetry, etc.), receiver bandwidth setting at MSFN = 50 Hz, and carrier-to-noise ratio = 12 db.

<sup>c</sup>Using no modulation, receiver bandwidth setting at MSFN = 50 Hz, and carrier-to-noise ratio = 12 db.



TABLE 5-III.- USBS TRACKING ACCURACY

(a) Angles

Station	1σ noise, mrad	1σ bias, mrad
Land based (X-Y mount)	0.8	1.6
Ship based (Az-El mount)	1.0	2.0

(b) Range

Station	1σ noise, ft	1σ bias, ft
Land based	30	60
Ship based	30	60

(c) Range rate

Land based two-way Doppler - nondestructive T count

Sampling rate	1σ noise				Total noise $\sigma(\dot{r}_1)$ , $\sigma^2 = \sigma_q^2 + \sigma_w^2$ , fps	1σ bias $\sigma(\dot{r}_1)$ , fps
	Quantization		White noise and random phase walk			
	$\sigma_q(\dot{r}_1)$ , fps	Correlation coefficient	$\sigma_w(\dot{r}_1)$ , fps	Correlation coefficient		
1 per sec	0.09	-0.5	0.08	-0.5	0.12	0.03
1 per 6 sec	0.015	-0.5	0.013	-0.5	0.02	This bias accounts for various model errors and must not be solved for.
1 per 60 sec	0.0015	-0.5	0.0013	-0.5	0.002	

Land based two-way Doppler - destructive N count

Sampling rate	Count time, sec	1σ noise		1σ bias $\sigma(\dot{r}_1)$ , fps
		$\sigma(\dot{r}_1)$ , fps	Correlation coefficient	
10 per sec and lower	0.08	1.0	0	0.03
1 per sec and lower	0.8	0.1	0	This bias accounts for various model errors and must not be solved for

TABLE 5-III.- USBS TRACKING ACCURACY - Concluded

## Land based three-way Doppler - nondestructive T count

Sampling rate	1 $\sigma$ noise						Total noise $\sigma(\dot{r}_1 + \dot{r}_2)$ , $\sigma^2 = \sigma_q^2 + \sigma_w^2 + \sigma_r^2$ , fps	1 $\sigma$ bias $\sigma(\dot{r}_1 + \dot{r}_2)$ , fps
	Quantization		White noise		Random phase walk			
	$\sigma_q(\dot{r}_1 + \dot{r}_2)$ , fps	Correlation coefficient	$\sigma_w(\dot{r}_1 + \dot{r}_2)$ , fps	Correlation coefficient	$\sigma_r(\dot{r}_1 + \dot{r}_2)$ , fps	Correlation coefficient		
1 per sec	0.18	-0.5	0.13	-0.5	0.017	0	0.22	0.2
1 per 6 sec	0.030	-0.5	0.022	-0.5	0.0069	0	0.038	If the three-way bias is solved for, the bias must not be reduced below 0.06 fps
1 per 60 sec	0.0030	-0.5	0.0022	-0.5	0.0022	0	0.0042	

## Land based two-way Doppler - nondestructive T count

Sampling rate	1 $\sigma$ noise						Total noise $\sigma(\dot{r}_1)$ , $\sigma^2 = \sigma_q^2 + \sigma_w^2 + \sigma_a^2$ , fps	1 $\sigma$ bias $\sigma(\dot{r}_1)$ , fps
	Quantization		White noise and random phase walk		Antenna motion			
	$\sigma_q(\dot{r}_1)$ , fps	Correlation coefficient	$\sigma_w(\dot{r}_1)$ , fps	Correlation coefficient	$\sigma_a(\dot{r}_1)$ , fps	Correlation coefficient		
1 per sec	0.09	-0.5	0.08	-0.5	0.5	-0.5	0.5	0.03
1 per 6 sec	0.015	-0.5	0.013	-0.5	0.008	-0.5	0.09	This bias accounts for various model errors and must not be solved for
1 per 60 sec	0.0015	-0.5	0.0013	-0.5	0.008	-0.5	0.009	

TABLE 5-IV.- STATION LOCATIONS AND STATUS

Call letters	Station	Site	Site status <sup>a</sup>	Operational date <sup>a</sup>	Geodetic coordinates			Geocentric rectangular coordinates <sup>b</sup>		
					Latitude	Longitude	Height above ellipsoid, m	U, m	V, m	W, m
CNV	Cape Kennedy	FPS-16	Operational	Now	28°28'54.36"±1.0"	- 80°34'35.45"±1.2"	14±40	918 608±32	-5 534 781±38	3 023 564±34
MLA	Merritt Island	TPQ-18	Operational	Now	28°25'29.5 ±1.0"	- 80°39'51.9 "±1.2"	12±40	910 604±32	-5 539 146±38	3 018 018±34
MIL		USBS 30' MSFN (Dual <sup>c</sup> )	Operational	Now	28°30'29.78"±1.0"	- 80°41'36.3 "±1.2"	10±40	907 086±32	-5 535 257±38	3 026 143±34
PAFB	Patrick Air Force Base	FPQ-6	Operational	Now	28°13'35.59"±1.0"	- 80°35'57.45"±1.2"	15±40	918 602±32	-5 548 399±38	2 998 673±34
GBI	Grand Bahama Island	TPQ-18	Operational	Now	26°38'10.86"±1.0"	- 78°16'03.8 "±1.2"	12±41	1 160 070±32	-5 585 912±39	2 842 277±34
		FPS-16	Operational	Now	<sup>d</sup> 26°36'56.80"	<sup>d</sup> - 78°20'52.20"	14	1 152 464	-5 588 531	2 840 241
GBM		USBS 30' MSFN	Test Phase	Now	26°37'58.29"±1.0"	- 78°14'15.59"±1.2"	5±41	1 163 032.7±32	-5 585 466.3±39	2 841 928.2±34
SSI	San Salvador Island	FPS-16	Operational	Now	24°07'07.77"±1.0"	- 74°30'14.89"±1.2"	5±42	1 556 154±33	-5 612 886±40	2 590 317±34
GTI	Grand Turk Island	TPQ-18	Operational	Now	21°27'46.40"±1.0"	- 71°07'55.61"±1.2"	28±42	1 920 453±33	-5 619 460±40	2 319 190±34
ANT	Antigua Island	FPQ-6	Operational	Now	17°08'38.51"±1.1"	- 61°47'34.29"±1.2"	58±42	2 881 618±35	-5 372 588±40	1 868 098±34
ANG		USBS 30' MSFN	Test Phase	May 1968	17°01' 0.09"±1.1"	- 61°45'09.68"±1.2"	50±42	2 887 336±35	-5 374 200±40	1 854 648±34
BDA	Bermuda	FPS-16	Operational	Now	32°20'53.17"±1.2"	- 64°39'13.68"±1.4"	18±43	2 308 904±39	-4 874 347±41	3 393 132±39
		FPQ-6	Operational	Now	32°20'52.67"±1.2"	- 64°39'13.47"±1.4"	19±43	2 308 912±39	-4 874 354±41	3 393 120±39
		USBS 30' MSFN	Operational	Now	32°21'04.63"±1.2"	- 64°39'29.45"±1.4"	21±43	2 308 451±34	-4 874 356±41	3 393 432±39
CYI	Grand Canary Island	MPS-26	Operational	Now	27°45'47.54"±4.6"	- 15°38'05.33"±5.1"	168±32	5 439 177±77	-1 532 209±138	2 953 405±127
		USBS 30' MSFN	Test Phase	Feb 1968	27°45'52.33"±4.6"	- 15°38'05.33"±5.1"	173±32	5 439 115±77	-1 522 192±138	2 953 537±127
ASC	Ascension Island	TPQ-18	Operational	Now	-07°58'21.94"±3.4"	- 14°24'06.10"±3.5"	143±32	6 118 555±43	-1 571 172±103	- 878 821±105
		FPS-16	Operational	Now	<sup>d</sup> -07°56'05.45"	<sup>d</sup> - 14°24'45.38"	110	6 118 540	-1 572 409	- 876 490
ACN		USBS 30' MSFN (Dual <sup>d</sup> )	Operational	Now	-07°57'18.20"±3.4"	- 14°19'39.28"±3.5"	562±32	6 121 247±43	-1 563 425±103	- 876 940±105
PRE	Pretoria, South Africa	MPS-25	Operational	Now	-25°56'37.44"±1.4"	28°21'30.56"±1.5"	1626±43	5 051 635±43	-2 726 681±43	-2 774 184±43
CRO	Carnarvon, Australia	FPQ-6	Operational	Now	-24°53'50.65"±1.9"	113°42'57.88"±2.2"	62±66	-2 328 319±60	5 300 017±64	-2 668 811±60
		USBS 30' MSFN (Dual <sup>c</sup> )	Operational	Now	-24°54'27.33"±1.9"	113°43'27.29"±2.2"	58±66	-2 328 882±60	5 299 247±64	-2 669 833±60
WOM	Woomera, Australia	FPS-16	Operational	Now	<sup>d</sup> -30°49'11.02"	<sup>d</sup> 136°50'13.16"	151	-3 998 928	3 750 388	-3 248 840
GWM	Guam	USBS 30' MSFN (Dual <sup>c</sup> )	Operational	Now	13°18'33.28"±6.4"	144°44'03.89"±6.6"	127±32	-5 068 804±125	3 584 345±163	1 458 757±193
HAW	Hawaii	FPS-16	Operational	Now	22°07'19.53"±1.4"	-159°39'55.38"±1.6"	1140±43	-5 544 019±53	-2 054 603±74	2 387 385±73
		USBS 30' MSFN (Dual <sup>c</sup> )	Operational	Now	22°07'29.63"±1.4"	-159°39'53.96"±1.6"	1150±43	-5 543 904±53	-2 054 604±74	2 387 676±73
CAL	Pt. Arguello, California	FPS-16	Operational	Now	34°34'58.45"±1.0"	-120°33'40.14"±1.2"	646±40	-2 673 158±33	-4 527 065±36	3 600 253±34
GYM	Guaymas, Mexico	USBS 30'	Operational	Now	27°57'47.54"±1.0"	-110°43'15.06"±1.2"	19±41	-1 994 696±32	-5 273 004±38	2 972 930±33
WHS	White Sands, New Mexico	FPS-16	Operational	Now	32°21'29.60"±1.0"	-106°22'10.43"±1.2"	1232±40	-1 520 192±31	-5 175 317±37	3 394 730±33
TEX	Corpus Christi, Texas	USBS 30' MSFN (Dual <sup>c</sup> )	Operational	Now	27°39'13.50"±1.0"	- 97°22'42.49"±1.1"	10±40	- 726 061±30	-5 606 849±38	2 942 592±32
EGL	Eglin Air Force Base	FPS-16	Operational	Now	30°25'18.36"±1.0"	- 86°47'53.21"±1.2"	28±40	307 465±31	-5 496 185±38	3 210 810±33
MAD	Madrid, Spain	USBS 85' MSFN (Dual <sup>c</sup> )	Test Phase	Now	<sup>d</sup> 40°27'19.29"	<sup>d</sup> 4°10'02.62"	825	4 847 850	- 353 231	4 117 146
RID	(Cerebros)	USBS 85' DSN (Dual <sup>c</sup> )	Test Phase	Now	<sup>d</sup> 40°27'10.74"	<sup>d</sup> 4°22'00.36"	778	4 846 727	- 370 108	4 116 915
CNB	Canberra, Australia	USBS 85' MSFN (Dual <sup>c</sup> )	Operational	Now	-35°35'50.0 "±1.9"	148°58'45.0 "±2.2"	1097±66	-4 450 343±63	2 676 239±60	-3 692 602±61
NBE	Tidbinbilla, Australia	USBS 85' DSN (Dual <sup>c</sup> )	Operational	Now	<sup>d</sup> -35°24'08.04"	<sup>d</sup> 148°58'48.21"	673±66	-4 460 857	2 682 467	-3 674 741
GDS	Goldstone, California	USBS 85' MSFN (Dual <sup>c</sup> )	Operational	Now	35°20'30.10"±1.1"	-116°52'23.84"±1.2"	965±40	-2 354 748±34	-4 646 829±37	3 669 433±35
GLD	(Pioneer)	USBS 85' DSN (Dual <sup>c</sup> )	Operational	Now	35°23'22.81"±1.1"	-116°50'56.62"±1.2"	1029±40	-2 351 415±34	-4 645 122±37	3 673 811±35

<sup>a</sup>Operational implies the capability to support manned missions.<sup>b</sup>The geocentric rectangular coordinate system consists of a U-axis at the intersection of the earth's equatorial plane with the Greenwich meridian, a W-axis along the earth's rotational axis, and a V-axis such to complete a right-handed coordinate system.<sup>c</sup>Dual indicates a common antenna and two receivers and transmitters. Geodetic coordinates referenced to the Fischer Ellipsoid of 1960.<sup>d</sup>Uncertainties not available.

HONEY SUCKLE HSK

TABLE 5-V.- INERTIAL POSITION AND SPEED ERRORS FOR SHIPS

Ship	1 $\sigma$ position, n. mi.	1 $\sigma$ speed, fps
Insertion <sup>a</sup>	0.5	0.5
Injection and reentry <sup>b</sup>	1.0 or 3.0	0.5

<sup>a</sup> Assumes star fix or bench mark available.

<sup>b</sup> 1 n. mi. assumes loran C coverage; 3.0 n. mi. assumes star fix 30 hours prior to tracking.

TABLE 5-VI.- C-BAND BEACONS AND USB TRANSPONDERS

Mission	IU		CSM		IM	
	C-band beacon	USB transponder	C-band beacon	USB transponder	C-band beacon	USB transponder
201	X		X			
202	X		X	X		
203	X					
204	X				X	X
205	X		X	X		
206	X				X	X
207	X		X	X	X	X
501	X	X	X	X		
502	X	X	X	X		
503	X	X	X	X	X	X
504	X	X		X		X
505	X	X		X		X
506	X	X		X		X

TABLE 5-VII.- SUMMARY OF APOLLO SHIPS INSTRUMENTATION<sup>a</sup>

Class	T-AGM-19	T-AGM-20	T-AGM-21	T-AGM-6	T-AGM-7
Name	Vanguard	Redstone	Mercury	Watertown	Huntsville
Primary function	Insertion	Injection	Injection	Reentry	Reentry
Unified S-band					
Capability	Single	Dual	Dual	Single	Single
Antenna	30 ft	30 ft	30 ft	12 ft	12 ft
Mount	Az-El	Az-El	Az-El	Az-El	Az-El
Acquisition aids	Mounted on antenna	Mounted on antenna	Mounted on antenna	None	None
C-Band Radar					
Type	FPS-16(V)	FPS-16(V)	FPS-16(V)	Capri	Modified Capri
Antenna	16 ft	16 ft	16 ft	16 ft	16 ft
Mount	Az-El	Az-El	Az-El	Az-El	Az-El
Acquisition aids	Mechanical scan	Mechanical scan	Mechanical scan	Mechanical scan	Mechanical scan Az. Electronic scan El. 23° Az × 6° El in 5 sec

TABLE 5-VIII.- RESIDUAL ERRORS AFTER ATMOSPHERIC CORRECTION<sup>b</sup>

Frequency, GHz	Range		Range rate		Azimuth and elevation	
	1 $\sigma$ noise, ft	1 $\sigma$ bias, ft	1 $\sigma$ noise, fps	1 $\sigma$ bias, fps	1 $\sigma$ noise, mrad	1 $\sigma$ bias, mrad
2 (S-band)	0.1	30	0	0.007	0.1	0.1
5 (C-band)	0.1	7	0	0.007	0.1	0.1

<sup>a</sup>For tracking accuracies see table 5-I for C-band systems and 5-III for USBS.

<sup>b</sup>See section 5.4.6 for conditions.

TABLE 5-IX.- LUNAR LANDMARKS AND THEIR UNCERTAINTIES

Landmark name	Selenocentric coordinates			Uncertainties, $1\sigma$ (a)	
	Latitude, deg	Longitude, deg	Altitude, ft	Horizontal component, ft	Vertical component, ft
Taruntius-G	1.904	49.483	- 4140.0	2540.0	2180.0
Messier-B	-0.856	48.135	-13461.0	2460.0	2219.0
Toricelli-C	-2.664	25.978	39.0	1321.0	2690.0
E. Pickering	-2.831	6.994	9170.0	739.0	2860.0
Rhaeticus-A	1.754	5.186	8924.0	690.0	2861.0
Gambert-C	3.350	-11.785	4268.0	854.0	2840.0
Turner	-1.358	-13.180	7146.0	885.0	2830.0
Lansberg-D	-2.975	-30.574	1516.0	1518.0	2620.0
Hortensius-A	4.388	-30.678	1572.0	1522.0	2610.0
Damoiseau-E	-5.195	-58.325	- 4508.0	2810.0	1910.0

<sup>a</sup>The lunar-centered coordinate system is one whose axes are oriented to the moon's polar axis, equator, and mean libration point. Altitude is measured from a mean sphere of 938.5-n. mi. (1738.00 km) radius.

TABLE 5-X.- APOLLO GUIDANCE COMPUTER STAR CATALOGUE REFERENCED TO 1967.0

No.	Star name	Spectral magnitude	Spectral class	Right ascension, hr:min:sec	Declination, deg:min:sec
1	$\alpha$ Andromedae	2.1	A0	0:06:40.6	+28:54:30
2	$\beta$ Ceti	2.2	K0	0:41:56.0	-18:10:30
3	$\gamma$ Cassiopeiae	2.2	B0	0:54:42.1	+60:32:19
4	$\alpha$ Eridani (Achernar)	0.6	B5	1:36:29.2	-57:24:15
5	$\alpha$ Ursae Minoris (Polaris)	2.1	F8	2:00:56.6	+89:06:43
6	$\theta$ Eridani	3.4	A2	2:57:00.5	-40:26:10
7	$\alpha$ Ceti	2.8	M2	3:00:33.1	+ 3:57:41
8	$\alpha$ Persei	1.9	F5	3:21:57.4	+49:44:43
9	$\alpha$ Tauri (Aldebaran)	1.1	gK5	4:34:01.5	+16:26:40
10	$\beta$ Orionis (Rigel)	0.3	cB8	5:12:57.1	- 8:14:19
11	$\alpha$ Aurigae (Capella)	0.2	gG0	5:14:14.9	+45:57:59
12	$\alpha$ Carinae (Canopus)	-0.9	F0	6:23:13.1	-52:40:38
13	$\alpha$ Canis Majoris (Sirius)	-1.6	A0	6:43:41.7	-16:40:10
14	$\alpha$ Canis Minoris (Procyon)	0.5	F5	7:37:34.5	+ 5:18:39
15	$\gamma$ Velorum	1.9	O0	8:08:30.9	-47:14:19
16	$\iota$ Ursae Majoris	3.1	A5	8:56:57.4	+48:10:21
17	$\alpha$ Hydrae	2.2	K2	9:25:57.9	- 8:30:53
18	$\alpha$ Leonis (Regulus)	1.3	B8	10:06:37.0	+12:07:45
19	$\beta$ Leonis	2.2	A2	11:47:22.6	+14:45:23
20	$\gamma$ Corvi	2.8	B8	12:14:06.3	-17:21:32
21	$\alpha$ Crucis	1.0	B1	12:24:44.9	-62:54:59
22	$\alpha$ Virginis (Spica)	1.2	B2	13:23:27.1	-10:59:23
23	$\eta$ Ursae Majoris	1.9	B3	13:46:14.5	+49:28:39
24	$\theta$ Centauri	2.3	K0	14:04:44.0	-36:12:30
25	$\alpha$ Bootis (Arcturus)	0.2	gK0	14:14:09.3	+19:21:12
26	$\alpha$ Coronae Borealis	2.3	A0	15:33:17.4	+26:49:29
27	$\alpha$ Scorpii (Antares)	1.2	gK0	16:27:22.8	-26:21:38
28	$\alpha$ Trianguli Austr.	1.9	K2	16:45:09.2	-68:58:11
29	$\alpha$ Ophiuchi	2.1	A5	17:33:24.1	+12:34:58
30	$\alpha$ Lyrae (Vega)	0.1	A0	18:35:49.2	+38:45:07
31	$\alpha$ Sagittarii	2.1	B3	18:53:13.1	-26:20:22
32	$\alpha$ Aquilae (Altair)	0.9	A5	19:49:10.3	+ 8:46:48
33	$\beta$ Capricorni	3.2	F8	20:19:09.5	-14:53:13
34	$\alpha$ Pavonis	2.1	B3	20:23:02.8	-56:50:33
35	$\alpha$ Cygni (Deneb)	1.3	A2	20:40:18.3	+45:09:42
36	$\epsilon$ Pegasi	2.5	K0	21:42:33.8	+ 9:43:22
37	$\alpha$ Piscis Austr. (Fomalhaut)	1.3	A3	22:55:49.8	-29:47:51

TABLE 5-XI.- SUMMARY OF GEMINI GROUND SYSTEMS DOWN TIMES  
GEMINI IX, X, XI, AND XII

[Total Flight Time = 361 Hours]

System or function	Down time, percentage of mission support time
Acquisition	3.7
C-band radar	
Range	4.8
Angles	0.23
Timing standard	0.21
Telemetry (downlink)	2.5
Command (uplink)	0.65
Voice (uplink)	2.4
On-site computer (1218)	0.20
NASCOM	
Teletype	0.041
High speed digital data	3.1



5.8 REFERENCES

1. Blucker, J.: Error Model For Apollo Onboard Navigation System. Memorandum No. 67-FM42-107, MSC Houston, Texas, April 6, 1966.
2. Standard Frequencies and Time Services of the National Bureau of Standards. Miscellaneous Publication, United States Department of Commerce, 1966.
3. Kinney, W. R.: "ETR Time Synchronization", paper presented at the Fourth Space Congress, Cocoa Beach, Florida, April 3-6, 1967.
4. Pan American Airways, Inc., AFETR Instrumentation Handbook, p. 135-142, August 1965.
5. Blucker, J.: Onboard Navigation Additions to ANWG Document No. AN-1.1. Memorandum No. 66-FM42-296, Manned Spacecraft Center, Houston, Texas, November 15, 1966.
6. "Goddard Directory of Tracking Station Locations," No. X-554-67-54, Goddard Space Flight Center, Greenbelt, Maryland, as updated through February 1967.
7. Donegan, J. J.; Head - Data Operations Branch - Manned Flight Operations Division: "Table 5-1a of ANWG Technical Report AN-1.2". Memorandum to Dr. B. Kruger, Mission Analysis Office, GSFC, June 1, 1967.
8. "AIS Error Analysis," Volume 1, Report R-65-047, General Dynamics, Electronics Division - San Diego Operations, September 1965.
9. NASA: Apollo - Saturn V Program Support Requirements. As updated through June 12, 1967.
10. NASA: Apollo - Saturn IB Program Support Requirements. As updated through May 24, 1967.
11. Schmid, P. E.: Apollo C-Band Radar Tracking Capability. GSFC X-551-67-503, September 15, 1967.
12. RCA: Range Instrumentation Systems and Equipment. Defense Electronics Products, Missile and Surface Radar Division, Moorestown, N. J., updated through December 1966.
13. "Support Requirements Reference Handbook for the Apollo Saturn IB/ Saturn V Programs," National Aeronautics and Space Administration, July 1966.

14. Rosenbaum, B.; Mission Analysis Office (MAO): Masking Diagrams for USBS Sites. Memorandum to P. Schmid, MAO, GSFC, June 8, 1967.
15. "Project Apollo Coordinate System Standards," SE 008-001-1, Office of Manned Space Flight - Apollo Program, National Aeronautics and Space Administration, Washington, D. C., June 1965.
16. Domangue, H.: Manned Space Flight Network System Test ST-12 for USB Receiver - Exciter - Ranging. GSFC, June 1, 1967.
17. Collins Technical Manual MH-1058, Unified S-Band 30-Foot Antenna System, April 1, 1966.
18. Collins Technical Manual MH-1075, (Preliminary), Unified S-Band 85-Foot Antenna System, May 1967.
19. Motsch, R. L.: Ha-Dec Tracking Data Corrections. JPL SPS No. 37-39, Volume III, p. 16-17, May 31, 1966.
20. Kruger, B.: The Doppler Equation in Range and Range Rate Measurement. Report No. X-507-65-385, Goddard Space Flight Center, Greenbelt, Maryland, October 8, 1965.
21. "Goddard Space Flight Center, Proceedings of the Apollo Unified S-Band Technical Conference," NASA SP-87, National Aeronautics and Space Administration, July 14-15, 1965.
22. Engel, H.: The Effects of Doppler Radar Errors. Apollo Note No. 393, Bissett-Berman Corporation, Santa Monica, California, December 22, 1965.
23. Curkendall, D. W.: The Influence of Oscillator Instability on Orbit Accuracy. Technical Memorandum 312-624, Jet Propulsion Laboratory, Pasadena, California, December 7, 1965.
24. Kruger, B.: Random Walk Phase Noise. ANWG Memorandum, Goddard Space Flight Center, Greenbelt, Maryland, October 6, 1966.
25. "AS-504 and Subsequent Missions Joint Preliminary Reference Constraints," Trajectory Document No. 66-FMP-13, Marshall Space Flight Center, Huntsville, Alabama and Manned Spacecraft Center, Houston, Texas, July 28, 1966.
26. Apollo Mission Planning Task Force: Design Reference Mission. Report No. LED-540-12, Volume I - Mission Description, October 30, 1964.

27. McCaffery, R. J.: Apollo Ships Project Data Systems Development Plan. Office of Instrumentation Ships, Code 506, NASA, Goddard Space Flight Center, Greenbelt, Maryland, April 22, 1966.
28. Schmid, P. E.: Atmospheric Tracking Errors at S- and C-Band Frequencies. NASA TN D-3470, August 1966.
29. "Performance/Design and Product Configuration Requirements." Part I. MEI No. 2015000, June 21, 1965, MIT (C).
30. "Primary Guidance, Navigation, and Control Systems for LEM," Part I. MEI No. 6015000, October 15, 1965, MIT (C).
31. "Design Control Specification for Navigation and Guidance Subsystem R.R./Transponder and Landing Radar," (U). LSP-370-2C, Grumman Aircraft Corporation, Bethpage, L.I., New York.
32. Blucker, J.: IMU and Engine Error Model for the Apollo Onboard Navigation System. Memorandum No. 67-FM42-15, MSC, Houston, Texas, January 25, 1967. (C).
33. "Apollo Mission Data Specification D- Apollo Saturn 204A and 204B, TRW Systems, Redondo Beach, California, Report No. 2131-H004-R8-000, updated (C).
34. "Saturn V AS-503 Launch Vehicle Guidance and Navigation Error Analysis." Boeing Company, Seattle, Washington, Report No. D5-15428-3, September 26, 1966. (C).
35. Detally, W. A.: Error Model for Mission 205/208 and 503. TRW Systems Interoffice Correspondence - Note 7222.6-94, January 19, 1967.
36. "Apollo Mission Data Specification B- Apollo Saturn 504." TRW Systems, Redondo Beach, California, Report No. 2131-H002-T8-000, March 1, 1966. (C).
37. "Selenodetic Control for NASA Project Apollo." (FA 2.1-1) NASA Defense Purchase Request No. T-21657 (G), by Department of the Army, Corps of Engineers, Army Map Service, Washington, D. C. 20315, June 1966.
38. Roberts, T.: Manned Flight Operations Division, Communication Procedures. GSFC, March 1, 1966.
39. "Data System Development Plan - NASCOM." GSFC, July 6, 1966.

40. Kalil, F.: Ground Tracking Reliability - A Summary From Gemini Flights GTA 9, 10, 11, and 12. GSFC X-507-67-197, May 1967.
41. "Technical Manual, Unified S-Band 30-Foot Antenna System (Ships)."  
By Reeves Instrument Co., Garden City, Long Island, New York,  
for NASA/GSFC, Greenbelt, Maryland, Contract No. NAS 5-9760,  
Report No. MH-1040, December 15, 1966.

27. McCaffery, R. J.: Apollo Ships Project Data Systems Development Plan. Office of Instrumentation Ships, Code 506, NASA, Goddard Space Flight Center, Greenbelt, Maryland, April 22, 1966.
28. Schmid, P. E.: Atmospheric Tracking Errors at S- and C-Band Frequencies. NASA TN D-3470, August 1966.
29. Gardiner, R. A.: Apollo Onboard Navigation System Error Model for ANWG Technical Report. MSC memorandum EG21-M-112-68-816, July 24, 1968.
30. VHF Ranging Program Technical Interchange Meeting, MSC, Houston. September 10, 1968.
31. GAEC: PGNCS Performance and Interface Specifications. GAEC, LSP-370-3, February 17, 1966 (C).
32. CSM/LM Spacecraft Operational Data Book, Volume I, Revision 2, Amendment 3, CSM Data Book, SNA-8-D-027(1), MSC, Sept. 24, 1969.
33. CSM/LM Spacecraft Operational Data Book, Volume II, Revision 2, Amendment 3, LM Data Book, SNA-8-D-027, MSC, Sept. 24, 1969.
34. GAEC: AGS Performance and Interface Specifications. GAEC, LSP-500-1, August 14, 1968 (C).
35. Nolley, Joe W. Revision 1 to Error Source Data for Dispersion Analyses. MSC IN 69-FM-160, June 9, 1969.
36. TRW Systems: Apollo Mission Data Specification B- Apollo Saturn 504. TRW Systems, Redondo Beach, California, Report No. 2131-H002-T8-000, March 1, 1966 (C).
37. Selenodetic Control for NASA Project Apollo. (FA 2.1-1) NASA Defense Purchase Request No. T-21657 (G), by Department of the Army, Corps of Engineers, Army Map Service, Washington, D. C. 20315, June 1966.
38. Roberts, T.: Manned Flight Operations Division, Communication Procedures. GSFC, March 1, 1966.
39. GSFC: Data System Development Plan - NASCOM. GSFC, July 6, 1966.

## 6.0 NAVIGATION SOFTWARE CAPABILITIES

### 6.1 INTRODUCTION

This chapter describes those aspects of Apollo navigation software which influence navigation capability studies. The information is included because the sophistication of the programs and techniques used and the procedures for data processing influence the accuracy and speed with which the orbit may be determined.

The Apollo navigation software system includes the following programs:

1. The RTCC, ground-based, orbit determination program.
2. The CM, LM, and S-IVB onboard orbit determination programs.
3. Apollo ships tracking and acquisition program.

The RTCC navigation program will be able to use values of vehicle position and velocity computed by the CM, LM, or S-IVB onboard programs from accelerometer data taken during a maneuver. CM and LM vectors computed onboard from optical observation or rendezvous radar data may also be used. The onboard systems will be able to use vectors generated by the RTCC program and based on ground tracking data. The use of telemetered vectors is the primary method for combining ground and onboard observations.

### 6.2 RTCC, GROUND-BASED NAVIGATION PROGRAM

The capabilities of the RTCC ground-based navigation program are given in the following sections; additional details can be obtained from reference 1.

#### 6.2.1 TWO-VEHICLE CAPABILITY

The main part of the real-time ground navigation program will determine the orbit of a single vehicle. The program will be called twice when it is necessary to determine the orbits of two vehicles during the same phase of the mission. The supervisory part of the program will keep track of all constants and data peculiar to each vehicle.

## 6.2.2 COMPUTATIONAL METHOD

The program employs a typical, weighted least-squares method in which a weight is given to the previously computed estimate of the vehicle's position and velocity and to the observational data.

The updated state,  $X_{i+1}$  is given by

$$X_{i+1} = X_i + \left( P_o^{-1} + \sum A_j^T W A_j \right)^{-1} \left( P_o^{-1} (X_1 - X_i) + \sum A_j^T W \Delta \gamma_j \right)$$

where

$X_i$  = the previous estimate of the state

$X_1$  = the initial estimate of the state

$A$  = partials of the observations with respect to the state

$W$  = observation weighting matrix

$P_o$  = covariance matrix of the state

$\Delta \gamma$  = observation residuals

The vehicle position and velocity vectors to be corrected will be in the reference body system associated with the anchor (or start) vector. The anchor vector will be at the time of the first observation in the batch of data to be processed. The program will be constructed so that it will not be necessary to have the observations equally spaced chronologically. The effect of significant forces (see chapter 4) in the vicinity of the earth-moon system are considered. Position and velocity will be computed with the current powered-flight polynomial fit program during launch and, when necessary, for earth orbit burns.

The observation weights will be adjusted empirically. The weight given to USBS three-way Doppler and range will depend on whether or not a bias has been solved for. All USBS Doppler weights will vary with the Doppler sampling interval used.

Mean conic (analytic) partials are used in the computation of the  $A$  matrix to relate position and velocity deviations at two different times along the orbit during free flight. The conic is about the reference body in whose sphere of influence the vehicle is located.

During reentry, deviations in position and velocity at two times are related by analytic partials for propagating the state covariance matrix instead of numerical or "secant" partials. Secant drag partials are used, as in the orbit phase, to relate deviations in position and velocity after a time interval to a deviation in atmospheric drag. Deviations in the observations are related to deviations in the anchor vector by means of analytic partials, as in the orbit phase.

### 6.2.3 OBSERVABLES PROCESSED

The real-time ground navigation program must handle S- and C-band tracking data. S-band data types are range, nondestruct two- and three-way Doppler, X angle, Y angle, hour angle, and declination. C-band data consists of range, azimuth, and elevation. LM rendezvous radar data will be processed to compute LM position on the moon, and CM optical data will be processed to determine landing site position.

### 6.2.4 DATA BATCH PROCESSING

The program will process batches of data sequentially. A set of batches may also be processed at once in a single differential correction calculation using from 6 to about 2400 data frames of range, azimuth, and elevation for C-band data and range, X angle, Y angle, and Doppler for S-band data. Except for the maximum number of batches (30) nothing limits the number of tracking stations whose data can be processed at once.

### 6.2.5 STATE ELEMENTS IN THE SOLUTION

The program solves for 6, 7, 8, or 9 elements as controlled by input. The 6-element solution vector consists of position and velocity corrections and is the normal mode. The 7-, 8-, and 9-element solution vectors consist of position and velocity corrections and 1, 2, or 3 measurement biases.

The measurement biases to be included and solved for are the USBS range bias and two- and three-way Doppler biases. Once the values of the biases are known, they are used later to compute residuals.



## 6.2.6 MODEL BIASES

The uncertainties in drag and in the gravitational parameter,  $\mu$ , will be used in propagating the state covariance matrix. (Tracking data is not used to estimate the values of drag and  $\mu$ .) The uncertainty in  $\mu$  is always used, but drag is used only in earth orbit and reentry. It is intended that the variance on these elements partially represent unknown model errors.

6.3 CM AND LM ONBOARD PROGRAMS

The CM and LM onboard programs contain both powered-flight and free-flight trajectory determination schemes. The powered-flight program uses accelerometer readings to estimate the trajectory during thrusting. The free-flight program uses the Kalman filter to process optical (CM) or rendezvous radar (LM) observations.

The Kalman filter used in the CM and LM onboard programs is defined by the two equations below; see references 2 and 3 for additional details of the Kalman filter.

$$\Delta X = K \Delta \gamma$$

and

$$K = WZ \frac{1}{Z^2 + \alpha^2} = Eb \left( b^T E b + \alpha^2 \right)^{-1}$$

where

K = Kalman filter

$\Delta X$  = correction to the state

$\Delta \gamma$  = observation residuals

W = square root of E found by Banachiewicz and Dwyer method

Z =  $W^T b$

E =  $W W^T$  = state error covariance matrix

b = partials of observation with respect to the state

$\alpha^2$  = a priori mean-squared measurement error.

The LM rendezvous radar range, range-rate and two angles, and CM optical data are serially processed by the filter.

### 6.3.1 ONBOARD TRAJECTORY PREDICTION MODEL

#### 6.3.1.1 Earth Orbit Phase

The earth orbit, free-flight model consists of the acceleration due to the central body ( $\mu_E$ ) and the  $J_2$ ,  $J_3$ , and  $J_4$  gravitational coefficients. The earth orbit, powered-flight model consists of the central body ( $\mu_E$ ) and the  $J_2$  gravitational coefficient (see ref. 2).

#### 6.3.1.2 Lunar Orbit Phase

The lunar orbit, free-flight model consists of the acceleration due to the central body ( $\mu_m$ ) and the  $J_2$ ,  $J_3$ ,  $J_4$ , and  $J_{22}$  gravitational coefficients. The lunar orbit, powered-flight gravitational model consists of the central body ( $\mu_m$ ) (see ref. 3).

#### 6.3.1.3 Translunar and Transearth Phases

The translunar and transearth model for free-flight consists of the sun, the secondary body (earth or moon), and the relevant earth or lunar harmonics. The powered-flight model is the same as for earth or lunar orbit depending on the central body.

### 6.3.2 CM ONBOARD NAVIGATION PROGRAM

#### 6.3.2.1 CM Orbit in Translunar and Transearth Phases

The CM onboard program can update the CM orbit in the translunar and transearth phases using the sextant to make

- a. star/earth-landmark observations
- b. star/earth-horizon observations
- c. star/lunar-landmark observations
- d. star/lunar-horizon observations.

#### 6.3.2.2 CM Orbit in Lunar Phase

The CM onboard program can update the CM orbit in lunar phase using data obtained from lunar landmark tracking with the scanning telescope.

#### 6.3.2.3 CM Landing Site Determination

The CM has the ability to determine the landing site using scanning telescope data.

#### 6.3.2.4 CM Rendezvous Navigation

The CM can perform vehicle-to-vehicle tracking using the sextant as a telescope to obtain data to update the LM or CM orbit. An alternate data source, the docking reticle, may be used to update the CM or LM state; however, due to the less accurate data, the reticle should only be used if the sextant fails or the pilot cannot return to the lower equipment bay for sextant sightings.

### 6.3.3 LM ONBOARD NAVIGATION PROGRAM

The LM rendezvous radar can be used to track the CM in the following cases:

- a. While the LM is on the moon in order to check LM position or the CM orbit.
- b. During rendezvous in order to compute LM or CM position and velocity.

## 6.4 S-IVB ONBOARD PROGRAM

### 6.4.1 FREE-FLIGHT NAVIGATION

The orbital navigation scheme provides inertial position and velocity by real-time integration of the equations of motion. Mathematical models are used to predict gravitational, atmospheric drag, and  $LH_2$  venting accelerations. Atmosphere and venting effects are predicted rather than computed during earth parking orbit as these accelerations are currently thought to be less than the accelerometer bias.

The parking orbit navigation scheme uses a fixed step, Runge-Kutta technique requiring three evaluations of the derivatives to update the position and velocity every 8 seconds.

The parking orbit gravitational model retains four zonal harmonics.

The [Q] matrix relates the vehicle-fixed coordinate system to the plumbline system and is computed for each 8-second integration cycle from the processed platform gimbal angle information for use in atmospheric drag and venting acceleration calculations.

The atmospheric density, defined by the 1963 revised Patrick reference atmosphere, (see chapter 4, section 4.4), is represented by a fifth-degree polynomial in altitude. The drag coefficient is computed as a polynomial in angle of attack to account for increased drag effects during parking orbit attitude maneuvers.

The S-IVB stage  $LH_2$  vent thrust magnitude is predicted as a function of time in orbit and is based on the design heating rate. A table look-up consisting of five linear functions in time is used to represent the thrust magnitude of the venting profile. The venting acceleration is resolved into vehicle coordinates and transformed to the space-fixed system using the [Q] matrix.

The translunar coast navigation procedure is a simplified form of the parking orbit navigation procedure, discussed above. Atmospheric drag and the third and fourth gravitational harmonics are deleted. Equations are included to account for venting effects during the coast period after the second S-IVB burn. Numerical integration of the translunar coast navigation equations is performed using the three-pass Runge-Kutta method. An 8-second integration interval is also used for this phase.

#### 6.4.2 POWERED-FLIGHT NAVIGATION

The navigation system provides position, velocity, and acceleration in an earth-centered, space-fixed coordinate system which is parallel to the stabilized inertial platform axes.

Platform accelerometers provide the time integral of thrust and atmospheric drag accelerations for the launch and translunar powered-flight phases. Thrust and drag displacements are obtained by integration of the accelerometer output; gravitational displacement is computed as a second-order, Taylor series expansion using past values of

gravitational velocity and acceleration. Inertial position is obtained by adding these displacements to the past value of position plus the initial velocity multiplied by the computation cycle time.

Gravitational accelerations are computed from the space-fixed position information. The third and fourth zonal harmonic terms are deleted from the reference model for the powered-flight modes. The gravitational velocity is derived by trapezoidal integration of the gravitational acceleration components. Space-fixed velocities are provided by summing the gravitational velocity, platform-measured velocity, and initial velocity.

The position and velocity are updated once every integration cycle time (about 1 second).

#### 6.5 APOLLO SHIP TRACKING AND ACQUISITION PROGRAM

The Apollo ship's tracking and acquisition program processes ship's C-band and S-band radar data, ship's flexure data, attitude data, and ship's position and velocity data using a Kalman filter during free flight and least squares filters during powered flight to yield an estimate of the position and velocity of a vehicle. The primary navigation function of the insertion ship (AGM 19) is to monitor the vehicle during the terminal phase of launch and the hold phase prior to insertion into earth parking orbit. The computations will be prime for the go - no-go decision prior to insertion. The ship is capable of transmitting high and low-speed telemetry and position and velocity vectors updated by both radar sources to the RTCC.

6.6 REFERENCES

1. Schiesser, E. R.; Savely, R. T.; deVezin, H. G.; and Oles, M. J.:  
Basic Equations and Logic for the Real-Time Ground Navigation  
Program for the Apollo Lunar Landing Mission, MSC IN No. 67-FM-51,  
May 31, 1967.
2. CMC Guidance and Navigation Equations, Lunar Landing Mission GSOP  
Preliminary Vol. I, Sec. 5, MIT, June 1967.
3. LGC Guidance and Navigation Equations, Lunar Landing Mission GSOP  
Preliminary Vol. II, Sec. 5, MIT, June 1967.
4. Saturn V Launch Vehicle Guidance and Navigation Equations, SA-504,  
D5-15429-4, October 12, 1966.